



Universidad Nacional Autónoma de México

PROGRAMA DE MAESTRÍA Y DOCTORADO EN CIENCIAS
MATEMÁTICAS Y DE LA ESPECIALIZACIÓN EN
ESTADÍSTICA APLICADA

INSTITUTO DE INVESTIGACIONES EN MATEMÁTICAS
APLICADAS Y EN SISTEMAS (IIMAS UNAM) - INSTITUTO
DE MATEMÁTICAS JURQUILLA (IMATE UNAM)

Gas-liquid flows in pipes with general cross sections

T E S I S

que para optar por el grado de
Maestro en Ciencias Matemáticas

PRESENTA:
José Alfonso Cabrera Sánchez

Director:
Dr. Gerardo Hernández Dueñas (IMATE Juriquilla, UNAM)

CIUDAD DE MÉXICO, 18 de Mayo de 2023

“No hay rama de la matemática, por abstracta que sea, que no pueda aplicarse algún día a los fenómenos del mundo real.”

Nikolai Ivanovich Lobachevski

“La esencia de las matemáticas no es hacer las cosas simples complicadas, sino hacer las cosas complicadas simples.”

Stan Gudder

Acknowledgements

Agradezco y dedico esta tesis a mi padre, José Manuel Cabrera Hernández, por creer y confiar en mi, por toda la ayuda que me brindaste y por ser mi guía en todo el proceso de la maestría, sé que desde el cielo me iluminas siempre y me motivas en mi día a día para continuar y culminar más proyectos como este.

A mi madre, Nadia Guadalupe Sánchez Coello, por tu enseñanza y motivación a la superación académica, por ser mi ejemplo a seguir y por siempre incentivar me a mejorar.

A mi hermano, Manuel Salvador, por creer en mi y por ayudarme a iniciar y culminar este gran proyecto en mi vida, y por motivarme a siempre superarme.

A Mení Castillo, sin su ayuda no habría podido iniciar esta maestría, y por su apoyo, atención y cariño durante el trayecto de la misma.

Al Dr. Gerardo Hernández, por motivarme durante la maestría a escoger mi tema de tesis, y por acompañarme en el desarrollo de este increíble trabajo, sin usted esto no habría sido posible.

Al Dr. Renato Calleja, por aceptarme como su tutorado y guiarme cada semestre con las materias y la maestría.

Al Posgrado en Ciencias Matemáticas, a la UNAM y a todos los Maestros-Doctores con quienes tomé curso en esta increíble casa de estudios.

Al apoyo otorgado por UNAM-DGAPA-PAPIIT IN112222 y Conahcyt A1-S-17634.

A mis amigos, a Los Catanes, a Rubén, Esteban, Luis, Victor, Diego, Gabriel, Julián y Sebastian, por estar siempre al pendiente de mi y de este proyecto.

A mis tíos Jorge y Susana por su interés, cariño y apoyo durante todo mi trayecto académico.

A mis dos abuelas, tíos y primos, por sus constantes preguntas y atención a mi desempeño en mis clases y tesis.

Al equipo de Banorte, por su apoyo a la culminación de esta tesis y maestría.

A todas las personas que aportaron algo para el resultado plasmado en este trabajo, de corazón, **gracias**.

Contents

Acknowledgements	v
Contents	vi
0.1 Introduction	1
1 The Model	5
1.1 Parametrization of the pipe's geometry	5
1.2 The Reynold's transport theorem	9
1.2.1 Cylindrical coordinates	13
1.3 Divergence	17
1.4 Euler isentropic equations	22
1.4.1 Equations of motion in cylindrical coordinates	23
1.4.2 Euler Equations	29
1.5 Cross section averages	30
1.6 Mass conservation equation	31
1.7 Momentum conservation equation	33
1.7.1 Integration of gravity term	34
1.7.2 Hydrostatic Pressure	35
1.7.2.1 Pressure integration for the conservation form	38
1.7.2.2 Pressure integration for the quasi-lineal form	39
1.7.2.3 Interface evolution	44
1.7.3 The final model	45
2 Model properties	47
2.1 Quasi-linear formulation	48
2.2 Hyperbolic properties	54
3 Numerical results	57
3.1 Convenient cross sections' descriptions and corresponding averages	58
3.2 Explicit expressions of flux and source terms	60
3.3 Pipe's discretization	64
3.4 Numerical scheme	65
3.4.1 Semi-discrete central-upwind scheme	66
3.4.2 Non-oscillatory reconstruction	67

3.4.3	Steady state at rest	68
3.4.4	Well-balanced property: Flux and source terms discretizations	69
3.4.5	Evolution in time	72
3.5	Numerical results	73
3.5.1	Steady state at rest	74
3.5.2	Perturbation to a steady state at rest	75
3.5.3	Hydraulic jump 1	78
3.5.4	Hydraulic jump 2	78
4	Conclusions	81
4.1	Conclusions	81
Bibliography		83

Introduction

0.1 Introduction

Leonhard Euler (1707-1783) was a Swiss mathematician who made numerous contributions to mathematics, physics, and engineering. He is considered one of the greatest mathematicians of all time, and his work has had a profound impact on many areas of science and technology.

Throughout his life, Euler made important contributions to many areas of mathematics, including calculus, geometry, number theory, and mechanics. In the field of fluid dynamics, he is best known for his work on the Euler equations, which he derived as a set of differential equations that govern the motion of an inviscid fluid. The equations are based on the principles of mass conservation, momentum conservation, and energy conservation and describe the motion of a fluid in terms of its velocity, pressure, and density.

The Euler equations consist of a fundamental set of equations in fluid dynamics that describe their motion. Despite the fact that the Euler equations describe the motion of an inviscid fluid, they have important applications in many areas of physics, including aerodynamics, hydrodynamics, and astrophysics. Because of their complexity, the Euler equations are notoriously difficult to solve analytically and many numerical methods have been developed to approximate their solutions.

Over the centuries, the Euler equations have been the subject of extensive research, and many researchers have made important contributions to the field of fluid dynamics by working on the equations. Today, the Euler equations remain an active area of study

in modern mathematics and physics, and they continue to play a central role in our understanding of fluid dynamics.

One of the most common applications of the Euler's equations is the calculation of the velocity and pressure of a flow at different points along a duct. The Euler's equations allow us to describe how the pressure and velocity of this change as air moves through the duct. This is especially important in situations where it is necessary to control the speed and pressure of the flow, such as in heating, ventilation, and air conditioning systems.

Another important aspect of using the Euler's equations of motion for describe the gas and air flows through ducts is the ability to predict the occurrence of turbulence. Turbulence can cause a decrease in flow velocity and pressure loss, which can negatively impact system performance. With the Euler's equations, it is possible to calculate the probability of turbulence occurring in different parts of the duct and take measures to minimize its impact. It is also possible to use the Euler's equations of motion to model the behavior of gas and air flow in extreme situations, such as in ventilation systems in fire conditions. In these cases, it is important to understand how the airflow affects the spread of fire and how ducts can be used to minimize its impact.

The use of numerical methods for solving the Euler equations has had a profound impact on the field of fluid dynamics. Numerical simulations have enabled researchers to study fluid flow problems that were previously intractable, such as the formation of shock waves and turbulent flow. They have also been used to design and optimize engineering systems such as aircraft and automobiles. The earliest numerical methods for solving differential equations were finite difference methods, which involved discretizing the equations on a grid and approximating the derivatives using finite differences. In the 1960s, finite element methods were developed, which allowed for more flexible discretization of the equations. In the 1970s, spectral methods were developed, which used a basis of orthogonal functions to approximate the solution. Some of the most important numerical methods used for approximating solutions to the Euler equations also include finite volume, spectral, and discontinuous Galerkin methods. These methods have been used in a wide range of applications, from simulating the flow of blood in arteries to predicting the behavior of atmospheric winds.

Despite the tremendous advances in numerical methods for solving the Euler equations, challenges still remain. The complexity and computational cost of these methods can be high, and researchers continue to develop new techniques to improve their accuracy and efficiency. Nevertheless, the development of numerical methods for solving the Euler equations has revolutionized the study of fluid dynamics and has led to many important discoveries and technological advancements.

The present work is focused in develop a model for Gas-liquid flow in pipes, starting from Euler equations and making a generalization for the pipe; usually for this kind of models it is usually assumed that the pipe is completely horizontal with a circular cross section, for simplicity. In contrasts with that, here we are going to work with a non-circular pipe with some $\alpha(s)$ inclination, giving us a more realistic model but certain more complicated, mathematically speaking.

The model that was derived in this thesis falls within the category of hyperbolic balance laws. Such class has been studied extensively over the last few decades. See for instance [1–4] and references therein. The theory behind hyperbolic balance laws has grown a lot recently. We know for instance that the information travels through characteristic curves at finite speed. Shockwaves can arise in finite time, even if the initial conditions are smooth. This has important implications as discontinuities require the development of a theory for weak solutions. From the numerical point of view, special care must be taken in the presence of jump discontinuities. Otherwise, strong spurious oscillations can arise near shockwaves. This is because monotone numerical methods are at most first order accurate. See theorem 15.6 in [3]. A standard technique is the construction of numerical schemes that are high order accurate in smooth regions, while reducing to a first order accuracy near jump discontinuities. This is done in practice with the use of flux or slope limiters. Such constructions are known as high resolution numerical schemes. In this thesis, we do not focus on the details of hyperbolic conservation laws in general. Instead, the reader is directed to the aforementioned references. We focus on the derivation of the model for the gas-liquid flow in pipes, and use a central-upwind numerical scheme that is known to be robust for this type of PDEs. Although we explain the central-upwind scheme in Section 3.4, more details can be found in [5].

In the Chapter 1, we describe all the pipe's geometry, the operators and coordinates to use and the develop of the model starting off the Euler equations and using cylindrical coordinates. In Chapter 2 we obtain the quasi lineal form of the model with the hyperbolic properties. Finally in Chapter 3 we present a central-upwind numerical scheme to approximate the solutions, showing the discretization of the domain and corresponding approximations, and analyze a variety of numerical examples to exhibit the merits of the model and numerical scheme.

Chapter 1

The Model

We start this chapter by proving details of the model for the two-layer fluid, consisting of liquid in the bottom layer and gas in the top part of the pipe. The derivation of the model is based on the work [6], extending it to general cross sections. That is, the pipe can have any shape, not just circular (axi-symmetric) or having constant width (rectangular). Furthermore, we also assume the pipe be tilted, having gravity playing an important role.

1.1 Parametrization of the pipe's geometry

Our goal in this thesis is to model the fluid's evolution within a pipe, where a liquid phase is transported below gas. Two-layer or multi-layer shallow water systems have been extensively analyzed. See for instance [7] and references therein. However, such flows involve liquid phases with distinct densities only, having heavier fluid sitting at the bottom. Here, our goal is to assume that the top layer's phase is gas. As a result, one can assume ideal gas laws on the top layer, and a hydrostatic pressure assumption at the bottom one. Furthermore, the two-layer fluid is transported in a closed pipe which a general geometry (arbitrary cross section). This way, the top layer can be expanded or compressed according to such laws, exchanging momentum with the bottom liquid phase. See Figure 1.1 for an schematic.

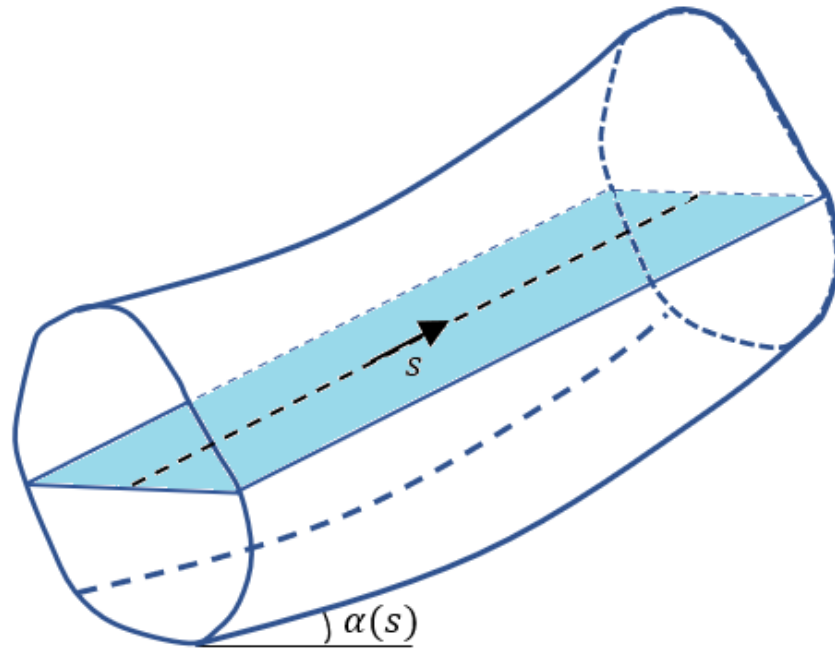


FIGURE 1.1: Pipe's geometry. The axial position is denoted by s . The angle formed with the horizontal axis is denoted by $\alpha(s)$.

The fluid's domain consists of a pipe that extends along a curve in the $x - z$ plane. That is, a curve passes through the center of the pipe and determines the pipe's axial direction. We assume that such curve is known, and can be parametrized by arclength, given by

$$\mathbf{r}(s) = (x_o(s), y = 0, z_o(s)),$$

with s being the arclength position. That means that the parametrization satisfies

$$\left\| \frac{d}{ds} \mathbf{r}(s) \right\| = \left\| \frac{d}{ds} (x_o(s), 0, z_o(s)) \right\| = \sqrt{x_o'(s)^2 + z_o'(s)^2} = 1.$$

Let $\alpha = \alpha(s)$ be the angle between the pipe's center and the horizontal axis. Therefore:

$$(x_o'(s), z_o'(s)) = (\cos(\alpha(s)), \sin(\alpha(s))).$$

On the other hand, let us denote by C_s the cross section, which passes through the center $(x_o(s), 0, z_o(s))$ and is perpendicular to the tangential direction $(\cos(\alpha(s)), \sin(\alpha(s)))$. Let also (x, y, z) be any point in the cross section C_s .

We would like to derive a parametrization of the cross section in polar-like coordinates. We denote by θ the angle between the displacement $(x, y, z) - (x_o(s), 0, z_o(s))$ and the reference vector $(-\sin(\alpha(s)), 0, \cos(\alpha(s)))$, which is perpendicular to the axial direction.

Since the displacement $(x, y, z) - (x_o(s), 0, z_o(s))$ is perpendicular to the axial direction, it satisfies:

$$(x - x_o, y, z - z_o) = (-Z \sin(\alpha(s)), Y, Z \cos(\alpha(s))).$$

for some scalars Y and Z . Let us denote by r the radius (displacement's norm). The vector (Y, Z) can be obtained by rotating the vertical position by θ degree:

$$r \begin{pmatrix} 0 \\ 1 \end{pmatrix} \mapsto r \begin{pmatrix} \cos(\theta) & -\sin(\theta) \\ \sin(\theta) & \cos(\theta) \end{pmatrix} \begin{pmatrix} 0 \\ 1 \end{pmatrix} = \begin{pmatrix} -\sin(\theta)r \\ \cos(\theta)r \end{pmatrix} = \begin{pmatrix} Y \\ Z \end{pmatrix}.$$

Substituting the above relations, one obtains the cylindrical coordinates in terms of $(r, \theta; s)$:

$$\begin{aligned} x &= x(r, \theta; s) = -r \sin(\alpha(s)) \cos(\theta) + x_o(s), \\ y &= y(r, \theta; s) = -r \sin(\theta), \\ z &= z(r, \theta; s) = r \cos(\alpha(s)) \cos(\theta) + z_o(s), \end{aligned} \tag{1.1}$$

with $0 \leq \theta \leq 2\pi$ and $0 < r \leq R(\theta; s)$, where $r = R(\theta; s)$ describes the pipe's wall.

The Jacobian of this transformation must have no null determinant. For that, we need

$$\begin{aligned}
|J| &= \begin{vmatrix} \frac{\partial x}{\partial r} & \frac{\partial x}{\partial \theta} & \frac{\partial x}{\partial s} \\ \frac{\partial y}{\partial r} & \frac{\partial y}{\partial \theta} & \frac{\partial y}{\partial s} \\ \frac{\partial z}{\partial r} & \frac{\partial z}{\partial \theta} & \frac{\partial z}{\partial s} \end{vmatrix} = \begin{vmatrix} -\sin(\alpha) \cos \theta & r \sin \alpha \sin \theta & -r \cos(\alpha) \alpha'(s) \cos \theta + x'_0 \\ -\sin \theta & -r \cos \theta & 0 \\ \cos \alpha \cos \theta & -r \cos \alpha \sin \theta & -r \sin(\alpha) \alpha'(s) \cos \theta + z'_0 \end{vmatrix} \\
&= -\sin \alpha \cos \theta (-r \cos \theta) (-r \sin(\alpha) \alpha'(s) \cos \theta + z'_0(s)) \\
&\quad + r \sin(\alpha) \sin(\theta) \sin(\theta) (-r \sin(\alpha) \alpha' \cos(\theta) + z'_0(s)) \\
&\quad + (-r \cos(\alpha) \alpha'(s) \cos \theta + x'_0(s)) (r \cos(\alpha) \sin^2 \theta + r \cos(\alpha) \cos^2(\theta)) \\
&= r \sin(\alpha) [-r \sin(\alpha) \alpha' \cos(\theta) + z'_0(s)] + r \cos(\alpha) [-r \cos(\alpha) \alpha' \cos(\theta) x'_0(s)] \\
&= r - r^2 \alpha'(s) \cos(\theta) = r(1 - r \alpha'(s) \cos \theta) \neq 0.
\end{aligned}$$

That is, for the parametrization be 1-1 we need that $1 - r \alpha'(s) \cos(\theta)$ be strictly positive, which is satisfied if:

$$1 - R|\alpha'(s)| > 0 \Leftrightarrow R(\theta; s) < \frac{1}{|\alpha'(s)|} = \mathcal{R}(s)$$

where $\mathcal{R}(s)$ is the radius of curvature of the pipe's axis.

Let us now define the vector $\mathbf{r}_p(r, \theta; s)$ that parameterized our pipe's cross sections (for a fixed arclength position s):

$$\mathbf{r}_p(r, \theta; s) = (-r \sin \alpha \cos \theta + x_0(s), -r \sin \theta, r \cos \alpha \cos \theta + z_0(s)).$$

One could compute normal vectors, which it will be relevant later on when we derive our reduced model. For that end, it is easy see that:

$$\begin{aligned}
\partial_r \mathbf{r}_p &= (-\sin \alpha \cos \theta, -\sin \theta, \cos \alpha \cos \theta), \\
\partial_\theta \mathbf{r}_p &= (r \sin \alpha \sin \theta, -r \cos \theta, -r \cos \alpha \sin \theta),
\end{aligned} \tag{1.2}$$

with cross product given by

$$\begin{aligned}
\partial_r \mathbf{r}_p \times \partial_\theta \mathbf{r}_p &= \begin{pmatrix} i & j & k \\ -\sin \alpha \cos \theta & -\sin \theta & \cos \alpha \cos \theta \\ r \sin \alpha \sin \theta & -r \cos \theta & -r \cos \alpha \sin \theta \end{pmatrix}, \\
&= \mathbf{i} (r \cos \alpha \sin^2 \theta + r \cos \alpha \cos^2 \theta) \\
&\quad - \mathbf{j} (r \sin \alpha \cos \alpha \cos \theta \sin \theta - r \sin \alpha \cos \alpha \cos \theta \sin \theta) \\
&\quad + \mathbf{k} (r \sin \alpha \cos^2 \theta + r \sin \alpha \sin^2 \theta), \\
&= (r \cos \alpha, 0, r \sin \alpha).
\end{aligned}$$

We can conclude that:

$$\therefore \|\partial_r \mathbf{r}_p \times \partial_\theta \mathbf{r}_p\| = r. \quad (1.3)$$

This results will be relevant for “The Reynold’s transport theorem”, which will seen on the next section.

1.2 The Reynold’s transport theorem

Theorem 1.1. *The Reynold’s transport theorem (named after Osborne Reynolds) is a three-dimensional generalization of the Leibniz integral rule for time and space; it estipulates that:*

$$\begin{aligned}
\partial_t \left(\int_{\Omega_k} f \, dA \right) &= \int_{\Omega_k} \partial_t f \, dA + \int_{\partial\Omega_k} \left(f|_{r=R_I} \partial_t \mathbf{r}_{p|_{r=R_I}} \right) \cdot \mathbf{n}_k \, dl, \\
\partial_s \left(\int_{\Omega_k} f \, dA \right) &= \int_{\Omega_k} \partial_s f \, dA + \int_{\partial\Omega_k} \left(f|_{r=R_I} \partial_s \mathbf{r}_{p|_{r=R_I}} \right) \cdot \mathbf{n}_k \, dl,
\end{aligned} \quad (1.4)$$

Furthermore, for both time and space and taking $k = 1, 2$ for liquid and gas on Ω_k , the last term can be written as follows:

$$\int_{\partial\Omega_k} \left(f|_{r=R_I} \partial_t \mathbf{r}|_{r=R_I} \right) \cdot \mathbf{n}_k \, dl = \int_{-\pi}^{\pi} f|_{r=R_I} R_I \partial_t R_I \, d\theta$$

$$\int_{\partial\Omega_k} \left(f|_{r=R_I} \partial_s \mathbf{r}|_{r=R_I} \right) \cdot \mathbf{n}_k \, dl = \int_{-\pi}^{\pi} f|_{r=R_I} R_I \partial_s R_I \, d\theta$$
(1.5)

Proof. First, we recall that a generalization of the fundamental theorem of calculus says that

$$\frac{d}{dx} \left(\int_{a(x)}^{b(x)} f(x, y) \, dy \right) = \int_{a(x)}^{b(x)} \frac{\partial f(x, y)}{\partial x} \, dy + f|_{y=b(x)} \frac{db}{dx} - f|_{y=a(x)} \frac{da}{dx},$$
(1.6)

$$\frac{d}{dt} \left(\int_{a(t)}^{b(t)} f(t, y) \, dy \right) = \int_{a(t)}^{b(t)} \frac{\partial f(t, y)}{\partial t} \, dy + f|_{y=b(t)} \frac{db}{dt} - f|_{y=a(t)} \frac{da}{dt},$$

and we define the radius for the gas phase ($k = 2$):

$$R_I = \begin{cases} R(\theta; s), & \text{if } -\theta_I \leq \theta \leq \theta_I \\ \frac{\eta_I - x_0(s) \sin \alpha(s) + z_0(s) \cos \alpha(s)}{\cos \theta}, & \text{if } |\theta| > \theta_I \end{cases}$$

and for the liquid phase ($k = 1$):

$$R_I = \begin{cases} \frac{\eta_I - x_0(s) \sin \alpha(s) + z_0(s) \cos \alpha(s)}{\cos \theta}, & \text{if } -\theta_I \leq \theta \leq \theta_I, \\ R(\theta; s) - \frac{\eta_I - x_0(s) \sin \alpha(s) + z_0(s) \cos \alpha(s)}{\cos \theta}, & \text{if } |\theta| > \theta_I. \end{cases}$$

Without loss of generality, we take $\partial_t \left(\int_{\Omega_k} f \, dA \right)$ and using (1.6) and (1.3) with polar coordinates, we get:

$$\begin{aligned}
\partial_t \left(\int_{\Omega_k} f \, dA \right) &= \partial_t \left(\int_{-\pi}^{\pi} \int_0^{R_I(\theta,t;s)} f \, r \, dr \, d\theta \right), \\
&= \int_{-\pi}^{\pi} \partial_t \left(\int_0^{R_I(\theta,t;s)} f \, r \, dr \right) \, d\theta, \\
&= \int_{-\pi}^{\pi} \int_0^{R_I(\theta,t;s)} \partial_t f \, r \, dr \, d\theta + \int_{-\pi}^{\pi} [(f \, r)|_{r=R_I} \partial_t R_I - f \, r|_{r=0} \partial_t 0] \, d\theta, \\
&= \int_{\Omega_k} \partial_t f \, dA + \int_{-\pi}^{\pi} f|_{r=R_I} R_I \partial_t R_I \, d\theta.
\end{aligned}$$

On the other hand, we are now going to compute the normal vector \mathbf{n}_k . For that end, we need to find a vector $\mathbf{\Gamma}$ perpendicular to the pipe's axis and to $\partial_t \mathbf{r}_p|_{r=R_I, s=s, \theta=\theta}$. Taking the parametrization over the boundary as

$$\mathbf{r}_p|_{r=R_I, s=s, \theta=\theta} = (-R_I \sin \alpha \cos \theta + x_0(s), -R_I \sin \theta, R_I \cos \alpha \cos \theta + z_0(s)), \tag{1.7}$$

$$\implies \partial_\theta \mathbf{r}_p|_{r=R_I, s=s, \theta=\theta} = (-\sin \alpha \partial_\theta (R_I \cos \theta), \partial_\theta (-R_I \sin \theta), \cos \alpha \partial_\theta (R_I \cos \theta + z_0(s))). \tag{1.8}$$

Assuming that $\mathbf{\Gamma} = (a, b, c)$, it must be satisfied that

$$\mathbf{\Gamma} \cdot (\cos \alpha(s), 0, \sin \alpha(s)) = 0, \implies a = -\beta \sin \alpha(s), c = \beta \cos \alpha(s), \text{ with } \beta \in \mathbb{R}.$$

For the sake of simplicity, we take $\beta = 1$. Now we just need to obtain an expression for b . So, notice that

$$\begin{aligned}
\mathbf{\Gamma} \cdot \partial_\theta \mathbf{r}_p|_{r=R_I, s=s, \theta=\theta} &= 0, \\
\iff \sin^2 \alpha(s) \partial_\theta (R_I \cos \theta) + b \partial_\theta (-R_I \sin \theta) + \cos^2 \alpha(s) \partial_\theta (R_I \cos \theta) &= 0, \\
\iff b &= \frac{\partial_\theta (R_I \cos \theta)}{\partial_\theta (R_I \sin \theta)}.
\end{aligned}$$

Finally, we can write $\mathbf{\Gamma}$ as:

$$\mathbf{\Gamma} = \left(-\sin \alpha(s), \frac{\partial_{\theta} (R_I \cos \theta)}{\partial_{\theta} (R_I \sin \theta)}, \cos \alpha(s) \right),$$

or:

$$\mathbf{\Gamma} = (-\sin \alpha(s) \partial_{\theta} (R_I \sin \theta), \partial_{\theta} (R_I \cos \theta), \cos \alpha(s) \partial_{\theta} (R_I \sin \theta)),$$

and

$$\begin{aligned} \|\mathbf{\Gamma}\| &= \sqrt{\partial_{\theta} (\cos \theta R_I)^2 + \partial_{\theta} (\sin \theta R_I)^2} \\ &= \sqrt{R_I^2 + (\partial_{\theta} R_I)^2}. \end{aligned}$$

After normalizing, we get the following expression for \mathbf{n}_k :

$$\mathbf{n}_k = \frac{\mathbf{\Gamma}}{\|\mathbf{\Gamma}\|} = \left(-\frac{\sin \alpha(s) \partial_{\theta} (R_I \sin \theta)}{\sqrt{R_I^2 + (\partial_{\theta} R_I)^2}}, \frac{\partial_{\theta} (R_I \cos \theta)}{\sqrt{R_I^2 + (\partial_{\theta} R_I)^2}}, \frac{\cos \alpha(s) \partial_{\theta} (R_I \sin \theta)}{\sqrt{R_I^2 + (\partial_{\theta} R_I)^2}} \right). \quad (1.9)$$

Using (1.2), we see that:

$$\partial_t \left(\mathbf{r}_p|_{r=R_I} \right) = (-\sin \alpha \cos \theta \partial_t R_I, -\sin \theta \partial_t R_I, \cos \alpha \cos \theta \partial_t R_I),$$

$$\begin{aligned} \|\partial_{\theta} \mathbf{r}_p|_{r=R_I}\| &= \sqrt{(\partial_{\theta} (\cos \theta R_I))^2 + (\partial_{\theta} (\sin \theta R_I))^2} \\ &= \sqrt{R_I^2 + (\partial_{\theta} R_I)^2}, \end{aligned}$$

and then:

$$\begin{aligned}
\partial_t \left(\mathbf{r}_p|_{r=R_I} \right) \cdot \mathbf{n}_k &= \frac{\cos \theta \partial_t R_I \partial_\theta (R_I \sin \theta) - \sin \theta \partial_t R_I \partial_\theta (R_I \cos \theta)}{\sqrt{R_I^2 + (\partial_\theta R_I)^2}} \\
&= \frac{\partial_t R_I (\cos \theta (\cos \theta R_I + \sin \theta \partial_\theta R_I) - \sin \theta (-\sin \theta R_I + \cos \theta \partial_\theta R_I))}{\sqrt{R_I^2 + (\partial_\theta R_I)^2}} \\
&= \frac{R_I \partial_t R_I}{\sqrt{R_I^2 + (\partial_\theta R_I)^2}}.
\end{aligned}$$

Finally:

$$\begin{aligned}
\int_{\partial\Omega_k} \left(f|_{r=R_I} \partial_t \mathbf{r}_p|_{r=R_I} \right) \cdot \mathbf{n}_k \, dl &= \int_{-\pi}^{\pi} f|_{r=R_I} \frac{R_I \partial_t R_I}{\sqrt{R_I^2 + (\partial_\theta R_I)^2}} \|\partial_\theta \mathbf{r}_p|_{r=R_I}\| \, d\theta \\
&= \int_{-\pi}^{\pi} f|_{r=R_I} R_I \partial_t R_I \, d\theta,
\end{aligned}$$

as desired. □

1.2.1 Cylindrical coordinates

The first step in the model's derivation is to write the system in cylindrical coordinates $(r, \theta; s)$. Using the transformation in (1.1), we define

$$f(x, y, z; t) = f(-r \sin(\alpha) \cos(\theta) + x_0(s), -r \sin(\theta), r \cos(\alpha) \cos(\theta) + z_0(s), t) =: \tilde{f}(r, \theta, s; t),$$

where \tilde{f} denotes the function expressed in the new coordinates. The gradient after the change of coordinates is expressed in the following proposition.

Proposition 1.2. *The gradient operators both in Cartesian and cylindrical coordinates satisfy the following relations*

$$\begin{aligned}\partial_r &= -\sin(\alpha)\cos(\theta)\partial_x - \sin(\theta)\partial_y + \cos(\alpha)\cos(\theta)\partial_z, \\ \partial_\theta &= r\sin(\alpha)\sin(\theta)\partial_x - r\cos(\theta)\partial_y - r\cos(\alpha)\sin(\theta)\partial_z, \\ \partial_s &= \cos(\alpha)[1 - r\alpha'(s)\cos(\theta)]\partial_x + \sin(\alpha)[1 - r\alpha'(s)\cos(\theta)]\partial_z.\end{aligned}\tag{1.10}$$

Proof. Applying the chain rule to \tilde{f} , we get:

$$\begin{aligned}\partial_r \tilde{f} &= \partial_r [f(r, \theta, s; t)] = -\partial_x f \sin(\alpha)\cos\theta - \partial_y f \sin(\theta) + \partial_z f \cos(\alpha)\cos(\theta), \\ \partial_\theta \tilde{f} &= \partial_x f r \sin(\alpha)\sin(\theta) - \partial_y f r \cos(\theta) - \partial_z f r \cos(\alpha)\sin(\theta), \\ \partial_s \tilde{f} &= \partial_x f [-r\cos(\alpha)\alpha'(s)\cos(\theta) + \cos(\alpha)] + \partial_z f [-r\sin(\alpha)\alpha'(s)\cos(\theta) + \sin(\alpha)],\end{aligned}$$

which concludes the proof. \square

Proposition 1.3. *The inverted relations are computed as*

$$\begin{aligned}\partial_x &= -\cos(\theta)\sin(\alpha)\partial_r + \sin(\theta)\sin(\alpha)\frac{1}{r}\partial_\theta + \frac{\cos(\alpha)}{1 - r\alpha'(s)\cos(\theta)}\partial_s, \\ \partial_y &= -\sin(\theta) - \cos(\theta)\frac{1}{r}\partial_\theta, \\ \partial_z &= \cos(\theta)\cos(\alpha)\partial_r - \sin(\theta)\cos(\alpha)\frac{1}{r}\partial_\theta + \frac{\sin(\alpha)}{1 - r\alpha'(s)\cos(\theta)}\partial_s.\end{aligned}\tag{1.11}$$

Proof. We are going to invert the operators to get $\nabla_{(x,y,z)}$ in terms of $\nabla_{(r,\theta,s)}$; we can note:

$$\begin{aligned}r\sin\theta\partial_r + \cos\theta\partial_\theta &= -r\sin\alpha\sin\theta\cos\theta\partial_x + r\sin\alpha\cos\theta\sin\theta\partial_x + 0 - r\sin^2\theta\partial_y - r\cos^2\theta\partial_y \\ &= -r\partial_y,\end{aligned}$$

giving

$$\partial_y = -\sin\theta\partial_r - \cos\theta\frac{1}{r}\partial_\theta.$$

On the other hand,

$$\begin{aligned} r \cos \theta \partial_r - \sin \theta \partial_\theta &= -r \sin \alpha \cos^2 \theta \partial_x - r \cos \theta \sin \theta \partial_y + r \cos \alpha \cos^2 \theta \partial_z \\ &\quad - r \sin \alpha \sin^2 \theta \partial_x + r \cos \theta \sin \theta \partial_y + r \cos \alpha \sin^2 \theta \partial_z \\ &= -r \sin \alpha \partial_x + r \cos \alpha \partial_z. \end{aligned}$$

$$\Rightarrow r \cos \theta \partial_r - \sin \theta \partial_\theta = -r \sin \alpha \partial_x + r \cos \alpha \partial_z, \quad (1.12)$$

However,

$$\partial_s = \cos(\alpha)(1 - r\alpha'(s) \cos \theta) \partial_x + \sin(\alpha)(1 - r\alpha'(s) \cos \theta) \partial_z, \quad (1.13)$$

and taking

$$\text{eq.(1.12)} [\sin(\alpha)(1 - r\alpha'(s) \cos \theta)] - \text{eq.(1.13)} [r \cos(\alpha)],$$

we obtain

$$\begin{aligned} r \cos \theta \sin(\alpha)(1 - r\alpha'(s) \cos \theta) \partial_r - \sin \theta \sin \alpha(1 - r\alpha'(s) \cos \theta) \partial_\theta - r \cos \alpha \partial_s \\ = -r \sin^2(\alpha)(1 - r\alpha'(s) \cos \theta) \partial_x - r \cos^2(\alpha)(1 - r\alpha'(s) \cos \theta) \partial_x. \end{aligned}$$

Therefore

$$-r(1 - r\alpha'(s) \cos \theta) \partial_x = r \cos \theta \sin \alpha(1 - r\alpha'(s) \cos \theta) \partial_r - \sin \theta \sin \alpha(1 - r\alpha'(s) \cos \theta) \partial_\theta - r \cos \alpha \partial_s.$$

As a result,

$$\partial_x = -\cos \theta \sin \alpha \partial_r + \sin \theta \sin \alpha \frac{1}{r} \partial_\theta + \frac{\cos \alpha}{1 - r\alpha'(s) \cos \theta} \partial_s.$$

Now, taking:

$$\begin{aligned} r \cos \alpha \partial_z &= r \cos \theta \partial_r - \sin \theta \partial_\theta + r \sin \alpha \partial_x \\ &= r \cos \theta \partial_r - \sin \theta \partial_\theta - r \cos \theta \sin^2 \alpha \partial_r + \sin \theta \sin^2 \alpha \partial_\theta + \frac{r \cos \alpha \sin \alpha}{1 - r\alpha'(s) \cos \theta} \partial_s \\ &= r \cos \theta \cos^2 \alpha \partial_r - \sin \theta \cos^2 \alpha \partial_\theta + \frac{r \cos \alpha \sin \alpha}{1 - r\alpha'(s) \cos \theta} \partial_s, \end{aligned}$$

we get

$$\partial_z = \cos \theta \cos \alpha \partial_r - \sin \theta \cos \alpha \frac{1}{r} \partial_\theta + \frac{\sin \alpha}{1 - r\alpha'(s) \cos \theta} \partial_s.$$

Finally, we get

$$\begin{aligned} \partial_x &= -\cos \theta \sin \alpha \partial_r + \sin \theta \sin \alpha \frac{1}{r} \partial_\theta + \frac{\cos \alpha}{1 - r\alpha'(s) \cos \theta} \partial_s \\ \partial_y &= -\sin \theta \partial_r - \cos \theta \frac{1}{r} \partial_\theta \\ \partial_z &= \cos \theta \cos \alpha \partial_r - \sin \theta \cos \alpha \frac{1}{r} \partial_\theta + \frac{\sin \alpha}{1 - r\alpha'(s) \cos \theta} \partial_s, \end{aligned} \tag{1.14}$$

which concludes the proof. \square

Remark: We note that, if $\alpha = 0$ then

$$\partial_s = \partial_x, \quad \partial_y = -\sin \theta \partial_r - \cos \theta \frac{1}{r} \partial_\theta, \quad \partial_z = \cos \theta \partial_r - \sin \theta \frac{1}{r} \partial_\theta,$$

corresponding to the case of a horizontal pipe.

In the new coordinate system it is necessary to write the radial, angular and axial velocities instead of the usual zonal, meridional and vertical ones. Furthermore, one also needs to derive the relations between the velocities in each coordinate system. For that end, we consider Lagrangian coordinates where a fluid particle moves around the domain with position described by a curves $(x(t), y(t), z(t))$ as a function of time, or equivalently, as $(r(t), \theta(t); s(t))$ in the cylindrical coordinates.

Definition 1.4. In Lagrangian coordinates, we define:

$$u = \frac{dx}{dt}, v = \frac{dy}{dt}, w = \frac{dz}{dt}, \tag{1.15}$$

$$V_r = \frac{dr}{dt}, V_\theta = \frac{d\theta}{dt}, V_s = \frac{ds}{dt}$$

as the velocities both in Cartesian and cylindrical coordinates.

The relation between velocities in each coordinate system is given in the following proposition.

Proposition 1.5. *The fluid's velocity can be transformed from Cartesian to cylindrical coordinates via the following relations*

$$\begin{aligned} V_r &= -\sin(\alpha)\cos(\theta)u - \sin(\theta)v + \cos(\alpha)\cos(\theta)w, \\ V_\theta &= \frac{1}{r}\sin(\alpha)\sin(\theta)u - \frac{\cos(\theta)}{r}v - \frac{1}{r}\cos(\alpha)\sin(\theta)w, \\ V_s &= \frac{1}{1 - r\alpha'(s)\cos(\theta)} [\cos(\alpha)u + \sin(\alpha)w]. \end{aligned} \quad (1.16)$$

Proof. Substituting the parametrization (1.1) into the definition (1.15), we obtain:

$$\begin{aligned} u &= \frac{d}{dt}(x) = \frac{d}{dt}[-r\sin(\alpha)\cos(\theta) + x_0(s)], \\ &= -\frac{dr}{dt}\sin(\alpha)\cos(\theta) - r\cos(\alpha)\alpha'(s)\frac{ds}{dt}\cos(\theta) + r\sin(\alpha)\sin(\theta)\frac{d\theta}{dt} + x_0'(s)\frac{ds}{dt}, \\ &= -\sin(\alpha)\cos(\theta)V_r + r\sin(\alpha)\sin(\theta)V_\theta + (1 - r\alpha'(s)\cos(\theta))\cos(\alpha)V_s. \end{aligned} \quad (1.17)$$

Similarly,

$$v = -\sin(\theta)V_r - r\cos(\theta)V_\theta, \quad (1.18)$$

$$w = \cos(\alpha)\cos(\theta)V_r - r\cos(\alpha)\sin(\theta)V_\theta + [1 - r\alpha'(s)\cos(\theta)]\sin(\alpha)V_s, \quad (1.19)$$

and using equations (1.17), (1.18) & (1.19) we can solve for V_r, V_θ & V_s to get equation (1.16).

□

1.3 Divergence

One also needs to transform important operators that we will need to rewrite the equations in the new coordinate system. One such operator is the divergence, which is described in the new coordinate system as follows.

Theorem 1.6. *The divergence in cylindrical coordinates can be written as:*

$$|J|\nabla_{(x,y,z)} \cdot (F_1, F_2, F_3) = \nabla_{(r,\theta,s)} \cdot (\hat{F}_1, \hat{F}_2, \hat{F}_3),$$

where

$$\hat{F}_1 = |J| \left(-\cos \theta \sin \alpha \tilde{F}_1 - \sin \theta \tilde{F}_2 + \cos \theta \cos \alpha \tilde{F}_3 \right),$$

$$\hat{F}_2 = \frac{1}{r} |J| \left(\sin \theta \sin \alpha \tilde{F}_1 - \cos \theta \tilde{F}_2 - \sin \theta \cos \alpha \tilde{F}_3 \right),$$

$$\hat{F}_3 = r \left(\cos \alpha(s) \tilde{F}_1 + \sin \alpha(s) \tilde{F}_3 \right).$$

Proof. We take a vector function:

$$\vec{F} = (F_1(x, y, z), F_2(x, y, z), F_3(x, y, z)) = \left(\tilde{F}_1(r, \theta; s), \tilde{F}_2(r, \theta; s), \tilde{F}_3(r, \theta; s) \right).$$

Using the operators (1.10), we obtain the divergence as:

$$\begin{aligned} \nabla \cdot (F_1, F_2, F_3) &= \partial_x F_1 + \partial_y F_2 + \partial_z F_3 \\ &= -\cos \theta \sin \alpha \partial_r \tilde{F}_1 + \sin \theta \sin \alpha \frac{1}{r} \partial_\theta \tilde{F}_1 + \frac{\cos \alpha}{1 - r\alpha'(s) \cos \theta} \partial_s \tilde{F}_1 \\ &\quad - \sin \theta \partial_r \tilde{F}_2 - \cos \theta \frac{1}{r} \partial_\theta \tilde{F}_2 \\ &\quad + \cos \theta \cos \alpha \partial_r \tilde{F}_3 - \sin \theta \cos \alpha \frac{1}{r} \partial_\theta \tilde{F}_3 + \frac{\sin \alpha}{1 - r\alpha'(s) \cos \theta} \partial_s \tilde{F}_3, \end{aligned}$$

and recalling that $|J| = r(1 - r\alpha'(s) \cos \theta)$, we write

$$|J| \nabla \cdot (F_1, F_2, F_3) = |J| \partial_x F_1 + |J| \partial_y F_2 + |J| \partial_z F_3$$

$$= -|J| \cos \theta \sin \alpha \partial_r \tilde{F}_1 + |J| \sin \theta \sin \alpha \frac{1}{r} \partial_\theta \tilde{F}_1 + r \cos \alpha \partial_s \tilde{F}_1 \quad (1.20)$$

$$- |J| \sin \theta \partial_r \tilde{F}_2 - |J| \cos \theta \frac{1}{r} \partial_\theta \tilde{F}_2 \quad (1.21)$$

$$+ |J| \cos \theta \cos \alpha \partial_r \tilde{F}_3 - |J| \sin \theta \cos \alpha \frac{1}{r} \partial_\theta \tilde{F}_3 + r \sin \alpha \partial_s \tilde{F}_3. \quad (1.22)$$

First we work on the terms in equation (1.20). Using the chain rule, we get

$$\begin{aligned}
|J|\partial_x F_1 &= -|J|\cos\theta\sin\alpha\partial_r\tilde{F}_1 + |J|\sin\theta\sin\alpha\frac{1}{r}\partial_\theta\tilde{F}_1 + r\cos\alpha\partial_s\tilde{F}_1 \\
&= \partial_r\left(-|J|\cos\theta\sin\alpha(s)\tilde{F}_1\right) + (1 - 2r\alpha'(s)\cos(\theta))\sin(\theta)\sin(\alpha(s))\frac{1}{r}\partial_t\tilde{F}_1 \\
&\quad + \partial_\theta\left(|J|\sin(\theta)\sin(\alpha(s))\frac{1}{r}\tilde{F}_1\right) - \partial_\theta[(1 - r\alpha'(s)\cos(\theta))\sin(\theta)\sin(\alpha(s))]\tilde{F}_1 \\
&\quad + \partial_s\left(r\cos(\alpha(s))\tilde{F}_1\right) - r(-\sin(\alpha(s)))\alpha'(s)\tilde{F}_1 \\
&= \partial_r\left(-|J|\cos\theta\sin\alpha(s)\tilde{F}_1\right) + \partial_\theta\left(|J|\sin(\theta)\sin(\alpha(s))\tilde{F}_1\right) + \partial_s\left(r\cos(\alpha(s))\tilde{F}_1\right) \\
&\quad + (1 - 2r\alpha'(s)\cos(\theta))\sin(\theta)\sin(\alpha(s))\frac{1}{r}\partial_t\tilde{F}_1 \\
&\quad - r\alpha'(s)\sin^2(\alpha(s))\tilde{F}_1 - (1 - r\alpha'(s)\cos(\theta))\cos(\theta)\sin(\alpha(s))\tilde{F}_1 \\
&\quad + r\sin(\alpha(s))\alpha'(s)\tilde{F}_1 \\
&= \partial_r\left(-|J|\cos\theta\sin\alpha(s)\tilde{F}_1\right) + \partial_\theta\left(|J|\sin(\theta)\sin(\alpha(s))\frac{1}{r}\tilde{F}_1\right) + \partial_s\left(r\cos(\alpha(s))\tilde{F}_1\right).
\end{aligned}$$

Now taking equation (1.21), we see that:

$$\begin{aligned}
|J|\partial_y F_2 &= -r(1 - r\alpha'(s)\cos\theta)\sin\theta\partial_r\tilde{F}_2 - r(1 - r\alpha'(s)\cos\theta)\cos\theta\frac{1}{r}\partial_\theta\tilde{F}_2 \\
&= \partial_r(-r(1 - r\alpha'(s)\cos\theta)\sin\theta\tilde{F}_2) + (1 - 2r\alpha'(s)\cos\theta)\sin\theta\tilde{F}_2 \\
&\quad \partial_\theta(-|J|\cos\theta\frac{1}{r}\tilde{F}_2) - \sin\theta\tilde{F}_2 + 2r\alpha'(s)\sin\theta\cos\theta\tilde{F}_2 \\
&= \partial_r(-|J|\sin\theta\tilde{F}_2) + \partial_\theta(-|J|\cos\theta\frac{1}{r}\tilde{F}_2),
\end{aligned}$$

and finally equation (1.22) to get

$$\begin{aligned}
|J|\partial_z F_3 &= \partial_r(-|J|\sin\theta\cos\alpha\frac{1}{r}\tilde{F}_3) + (r\alpha'(s)\sin\theta)\sin\theta\cos\alpha\tilde{F}_3 - (1-r\alpha'(s)\cos\theta)\cos\theta\cos\alpha\tilde{F}_3 \\
&\quad + \partial_s(r\sin\alpha\tilde{F}_3) - r\cos\alpha\alpha'(s)\tilde{F}_3 \\
&= \partial_r(|J|\cos\theta\cos\alpha\tilde{F}_3) + \partial_\theta(-|J|\sin\theta\cos\alpha\frac{1}{r}\tilde{F}_3) + \partial_s(r\sin\alpha\tilde{F}_3) \\
&\quad - \cos\theta\cos\alpha\tilde{F}_3 + 2r\alpha'(s)\cos^2\theta\cos\alpha\tilde{F}_3 + r\alpha'(s)\sin^2\theta\cos\alpha\tilde{F}_3 \\
&\quad + \cos\theta\cos\alpha\tilde{F}_3 - r\alpha'(s)\cos^2\theta\cos\alpha\tilde{F}_3 - r\cos(\alpha)\alpha'(s)\tilde{F}_3 \\
&= \partial_r(-|J|\cos\theta\cos\alpha\tilde{F}_3) + \partial_\theta(-|J|\sin\theta\cos\alpha\frac{1}{r}\tilde{F}_3) + \partial_s(r\sin\alpha\tilde{F}_3).
\end{aligned}$$

$$\begin{aligned}
\therefore \quad &|J|\nabla \cdot (F_1, F_2, F_3) \\
&= \partial_r(-|J|\cos\theta\sin\alpha\tilde{F}_1) + \partial_\theta(|J|\sin\theta\sin\alpha\frac{1}{r}\tilde{F}_1) + \partial_s(r\cos\alpha(s)\tilde{F}_1) + \partial_r(-|J|\sin\theta\tilde{F}_2) \\
&\quad + \partial_\theta(-|J|\cos\theta\frac{1}{r}\tilde{F}_2) + \partial_r(-|J|\cos\theta\cos\alpha\tilde{F}_3) + \partial_\theta(-|J|\sin\theta\cos\alpha\frac{1}{r}\tilde{F}_3) + \partial_s(r\sin\alpha\tilde{F}_3) \\
&= \partial_r\left[-|J|\left(\cos\theta\sin\alpha\tilde{F}_1 + \sin\theta\tilde{F}_2 - \cos\theta\cos\alpha\tilde{F}_3\right)\right] \\
&\quad + \partial_\theta\left[-|J|\frac{1}{r}\left(-\sin\theta\sin\alpha\tilde{F}_1 + \cos\theta\tilde{F}_2 + \sin\theta\cos\alpha\tilde{F}_3\right)\right] \\
&\quad + \partial_s\left[r\left(\cos\alpha(s)\tilde{F}_1 + \sin\alpha(s)\tilde{F}_3\right)\right] \\
&= \nabla_{(r,\theta,s)}\left(\hat{F}_1, \hat{F}_2, \hat{F}_3\right),
\end{aligned}$$

where

$$\begin{aligned}
\hat{F}_1 &= |J|\left(-\cos\theta\sin\alpha\tilde{F}_1 - \sin\theta\tilde{F}_2 + \cos\theta\cos\alpha\tilde{F}_3\right) \\
\hat{F}_2 &= \frac{1}{r}|J|\left(\sin\theta\sin\alpha\tilde{F}_1 - \cos\theta\tilde{F}_2 - \sin\theta\cos\alpha\tilde{F}_3\right) \\
\hat{F}_3 &= r\left(\cos\alpha(s)\tilde{F}_1 + \sin\alpha(s)\tilde{F}_3\right)
\end{aligned}$$

□

The following theorem will be useful in writing the equations of motion in conservation form in the new coordintaes.

Theorem 1.7. *Let $\vec{u} = (u, v, w)$ be the velocity field. Then*

$$|J|\nabla \cdot (f\vec{u}) = \nabla_{(r,\theta,s)} \cdot (|J|f(V_r, V_\theta, V_s)).$$

Furthermore, the material derivative in conservation form can be written as

$$|J|(\partial_t f + \nabla \cdot (\vec{u}f)) = \partial_t (|J|f) + \nabla \cdot (f(V_r, V_\theta, V_s)).$$

Proof. If we expand the term $f|J|\nabla \cdot (\mathbf{u}f)$, we get

$$\begin{aligned} |J|\nabla \cdot (\mathbf{u}f) &= \partial_r (|J|(-\cos\theta \sin\alpha uf + \sin\theta vf + \cos\theta \cos\alpha wf)) \\ &\quad + \frac{1}{r}\partial_\theta (|J|(\sin\theta \sin\alpha uf + \cos\theta vf - \sin\theta \cos\alpha wf)) \\ &\quad + \partial_s (-r(\cos\alpha uf + \sin\alpha wf)) \\ &= \partial_r (|J|(-\cos\theta \sin\alpha f[-\sin\alpha \cos\theta V_{k,r} + r \sin\alpha \sin\theta V_{k,\theta} - \frac{|J|}{r} \cos\alpha V_{k,s}] \\ &\quad + \sin\theta f[\sin\theta V_{k,r} + r \cos\theta V_{k,\theta}] \\ &\quad + \cos\theta \cos\alpha f[\cos\alpha \cos\theta V_{k,r} - r \cos\alpha \sin\theta V_{k,\theta} - \frac{|J|}{r} \sin\alpha V_{k,s}])) \\ &\quad + \frac{1}{r}\partial_\theta (|J|[\sin\theta \sin\alpha f[-\sin\alpha \cos\theta V_{k,r} + r \sin\alpha \sin\theta V_{k,\theta} - \frac{|J|}{r} \cos\alpha V_{k,s}] \\ &\quad + \cos\theta f[\sin\theta V_{k,r} + r \cos\theta V_{k,\theta}] \\ &\quad - \sin\theta \cos\alpha f[\cos\alpha \cos\theta V_{k,r} - r \cos\alpha \sin\theta V_{k,\theta} - \frac{|J|}{r} \sin\alpha V_{k,s}])) \\ &\quad + \partial_s (-r \cos\alpha f[-\sin\alpha \cos\theta V_{k,\theta} + r \sin\alpha \sin\theta V_{k,\theta} - \frac{|J|}{r} \cos\alpha V_{k,s}] \\ &\quad - r \sin\alpha f[\cos\alpha \cos\theta V_{k,r} - r \cos\alpha \sin\theta V_{k,\theta} - \frac{|J|}{r} \sin\alpha V_{k,s}])) \\ &= \partial_r (|J|V_{k,r} f) + \frac{1}{r}\partial_\theta (|J|rV_{k,\theta} f) + \partial_s (|J|V_{k,s} f). \end{aligned}$$

$$\therefore |J|\nabla \cdot (f\mathbf{u}) = \nabla_{(r,\theta;s)} \cdot (|J|f(V_{k,r}, V_{k,\theta}, V_{k,s})).$$

We know that:

$$|J|\nabla \cdot (f\mathbf{u}) = |J|\partial_x(fu) + |J|\partial_y(fv) + |J|\partial_z(fw),$$

and

$$(|J|f(V_{k,r}, V_{k,\theta}, V_{k,s})) = \partial_r(|J|fV_{k,r}) + \partial_\theta(|J|fV_{k,\theta}) + \partial_s(|J|fV_{k,s}),$$

which implies

$$|J|(\partial_t f + \nabla \cdot (\mathbf{u}f)) = \partial_t(|J|f) + \nabla \cdot (f(V_{k,r}, V_{k,\theta}, V_{k,s})).$$

□

1.4 Euler isentropic equations

Definition 1.8. For a vector $\mathbf{u} = (u_k, v_k, w_k)$ and a density ρ , the Euler isentropic equations can be written as:

$$\partial_t \rho_k + \nabla \cdot (\mathbf{u}\rho) = M_k$$

$$\partial_t (\rho_k u_k) + \nabla \cdot (\mathbf{u}\rho_k u_k) = -\partial_x (P_k(\rho_k)) + D_{1,k}$$

$$\partial_t (\rho_k v_k) + \nabla \cdot (\mathbf{u}\rho_k v_k) = -\partial_y (P_k(\rho_k)) + D_{2,k}$$

$$\partial_t (\rho_k w_k) + \nabla \cdot (\mathbf{u}\rho_k w_k) = -\partial_z (P_k(\rho_k)) - \rho g + D_{3,k},$$

or in extended form as

$$\partial_t \rho_k + \partial_x (\rho_k u_k) + \partial_y (\rho_k v_k) + \partial_z (\rho_k w_k) = M_k$$

$$\partial_t (\rho_k u_k) + \partial_x (\rho_k u_k^2) + \partial_y (\rho_k u_k v_k) + \partial_z (\rho_k u_k w_k) = -\partial_x (P_k(\rho_k)) + D_{1,k}$$

$$\partial_t (\rho_k v_k) + \partial_x (\rho_k u_k v_k) + \partial_y (\rho_k v_k^2) + \partial_z (\rho_k v_k w_k) = -\partial_y (P_k(\rho_k)) + D_{2,k}$$

$$\partial_t (\rho_k w_k) + \partial_x (\rho_k u_k w_k) + \partial_y (\rho_k v_k w_k) + \partial_z (\rho_k w_k^2) = -\partial_z (P_k(\rho_k)) - \rho g + D_{3,k},$$

where M_k is the mass interchange term, g is the gravity and $D_{1,K}, D_{2,K}$ and $D_{3,k}$ are momentum exchange source terms.

1.4.1 Equations of motion in cylindrical coordinates

Now that we have the velocity in the new coordinates, the next step is to write the equations for balance of momentum in the radial, angular and axial directions.

In our assumptions to derive the model, we assume that both the axial and angular velocities are small. As a result, we do not write the equations of motion for those variables. All the equations are described in the following proposition, where bottom layer (liquid phase) is associated to $k = 1$ while the top (gas phase) corresponds to $k = 2$.

Proposition 1.9. *The isentropic Euler equations in cylindrical coordinates imply the following equations for conservation of mass and balance of momentum in the axial, radial and angular directions.*

$$\partial_t (|J|\rho_k) + \nabla_c \cdot (|J|\rho_k \mathbf{V}) = M_k,$$

$$\begin{aligned} \partial_t (\rho_k V_{k,r} |J|) + \nabla_c \cdot (|J|\rho_k V_{k,r} \mathbf{V}) &= -|J|\partial_r (P_k(\rho_k)) + |J|\rho_k r V_{k,\theta}^2 \\ &\quad - |J|\rho_k V_{k,s} \cos \theta \alpha'(s) (1 - r\alpha'(s) \cos \theta) V_{k,s} + |J|D_{r,k} \end{aligned}$$

$$\begin{aligned} \partial_t (\rho_k V_{k,\theta} |J|) + \nabla_c \cdot (|J|\rho_k V_{k,\theta} \mathbf{V}) &= -2 \frac{|J|}{r} \rho_k V_{k,r} V_{k,\theta} + \frac{|J|}{r} \rho_k \alpha'(s) \sin \theta (1 - r\alpha'(s) \cos \theta) V_{k,s}^2 \\ &\quad - \frac{|J|}{r^2} \partial_\theta P_k + \frac{|J|}{r} \cos(\alpha(s)) \sin(\theta) \rho_k g + |J|D_{k,\theta} \end{aligned}$$

$$\begin{aligned} \partial_t (\rho V_{k,s} |J|) + \nabla_c \cdot (|J|\rho V_{k,s} \mathbf{V}) &= -\frac{r^2}{|J|} \partial_s P - \frac{r^2}{|J|} D_s + \rho r^2 V_s^2 \alpha''(s) \cos(\theta) \\ &\quad + 2r\alpha'(s) \rho V_s (\cos(\theta) V_r - \sin(\theta) r V_\theta) - g \rho \sin(\alpha(s)), \end{aligned}$$

where $\mathbf{V} = (V_{r,k}, V_{\theta,k}, V_{s,k})$, $\nabla_c = (\partial_r, \partial_\theta, \partial_s)$, and $P_k = P_k(\rho_k)$.

Proof. Expanding the derivatives and using the theorem 1.7 and the definition 1.8, we get:

$$\begin{aligned}\partial_t (|J|\rho_k) &= |J|\partial_t \rho_k = -|J|\nabla \cdot (\rho_k \mathbf{u}_k) = -\nabla_c \cdot (|J|\rho_k (V_r, V_\theta, V_s)) + M_k. \\ \therefore \partial_t (|J|\rho_k) + \nabla_c \cdot (|J|\rho_k (V_r, V_\theta, V_s)) &= M_k\end{aligned}$$

Now, for the angular, radial and axial momentum equation, we use the velocities from 1.16 to define

$$\begin{aligned}V_{k,r} &= -\sin(\alpha) \cos(\theta)u_k - \sin(\theta)v_k + \cos(\alpha) \cos(\theta)w_k, \\ V_{k,\theta} &= \frac{1}{r} \sin(\alpha) \sin(\theta)u_k - \frac{\cos(\theta)}{r}v_k - \frac{1}{r} \cos(\alpha) \sin(\theta)w_k, \\ V_{k,s} &= \frac{1}{1 - r\alpha'(s) \cos(\theta)} [\cos(\alpha)u_k + \sin(\alpha)w_k].\end{aligned}$$

Another expansion gives

$$\begin{aligned}\partial_t (\rho_k V_{k,r} |J|) &= -\sin \alpha \cos \theta \partial_t (\rho_k u_k |J|) - \sin \theta \partial_t (\rho_k v_k |J|) + \cos \alpha \cos \theta \partial_t (\rho_k w_k |J|) \\ &= -\sin \alpha \cos \theta |J| (-\nabla \cdot (\rho_k u_k \mathbf{u}) - \partial_x P_k + D_{1,k}) \\ &\quad - \sin \theta |J| (-\nabla \cdot (\rho_k v_k \mathbf{u}) - \partial_y P_k + D_{2,k}) \\ &\quad + \cos \alpha \cos \theta |J| (-\nabla \cdot (\rho_k w_k \mathbf{u}) - \partial_z P_k + D_{3,k}) \\ &= \sin \alpha \cos \theta \nabla_c \cdot (|J|\rho_k u_k \mathbf{V}) + \sin \theta \nabla_c \cdot (|J|\rho_k v_k \mathbf{V}) - \cos \alpha \cos \theta \nabla_c \cdot (|J|\rho_k w_k \mathbf{V}) \\ &\quad + \sin \alpha \cos \theta |J| \left(-\cos \theta \sin \alpha \partial_r P_k + \sin \theta \sin \alpha \frac{1}{r} \partial_\theta P_k \right. \\ &\quad \left. + \frac{\cos \alpha}{1 - r\alpha'(s) \cos \theta} \partial_s P_k \right) \\ &\quad + \sin \theta |J| \left(-\sin \theta \partial_r P_k(\rho_k) - \cos \theta \frac{1}{r} \partial_\theta P_k(\rho_k) \right) \\ &\quad + \cos \alpha \cos \theta |J| \left(-\cos \theta \cos \alpha \partial_r P_k(\rho_k) + \sin \theta \cos \alpha \frac{1}{r} \partial_\theta P_k \right. \\ &\quad \left. - \frac{\sin \alpha}{1 - r\alpha'(s) \cos \theta} \partial_s P_k(\rho_k) \right) \\ &\quad - \sin \alpha \cos \theta |J| D_{1,k} - \sin \theta |J| D_{2,k} + \cos \alpha \cos \theta |J| D_{3,k}.\end{aligned}\tag{1.23}$$

Here

$$|J|D_{k,r} = -\sin \alpha \cos \theta |J|D_{1,k} - \sin \theta |J|D_{2,k} + \cos \alpha \cos \theta |J|D_{3,k},$$

Now, we reduce the expression for $\partial_t(\rho_k V_{k,r}|J|)$ by making the next calculations

$$\begin{aligned} \sin \alpha \cos \theta \nabla_c \cdot (|J|\rho_k u_k \mathbf{V}) &= \sin \alpha \cos \theta \left(\partial_r (|J|\rho_k u_k V_{k,r}) + \partial_\theta (|J|\rho_k u_k V_{k,\theta}) + \partial_s (|J|\rho_k u_k V_{k,s}) \right) \\ &= \partial_r (|J|\rho_k \sin \alpha \cos \theta u_k V_{k,r}) + \partial_\theta (|J|\sin \alpha \cos \theta u_k V_{k,\theta}) \\ &\quad + \partial_s (|J|\rho_k \sin \alpha \cos \theta u_k V_{k,s}) \\ &\quad + \sin \alpha \sin \theta |J|\rho_k u_k V_{k,\theta} - \cos \alpha \alpha'(s) \cos \theta |J|\rho_k u_k V_{k,s} \\ &= \nabla_c \cdot (|J|\rho_k u_k \sin \alpha \cos \theta \mathbf{V}) \\ &\quad + \sin \alpha \sin \theta |J|\rho_k u_k V_{k,\theta} - \cos \alpha \alpha'(s) \cos \theta |J|\rho_k u_k V_{k,s}. \end{aligned} \tag{1.24}$$

Analogously:

$$\sin(\theta) \nabla_c \cdot (|J|\rho_k v_k \mathbf{V}) = \nabla_c \cdot (|J|\sin \theta \rho_k v_k \mathbf{V}) - \cos \theta |J|\rho_k v_k V_{k,\theta}, \tag{1.25}$$

and finally:

$$\begin{aligned} -\cos \alpha \cos \theta \cdot (|J|\rho_k w_k \mathbf{V}) &= -\nabla_c \cdot (|J|\cos \alpha \cos \theta \rho_k w_k \mathbf{V}) \\ &\quad + \cos \alpha (-\sin \theta) |J|\rho_k w_k V_{k,\theta} \\ &\quad + (-\sin \alpha) \alpha'(s) \cos \theta |J|\rho_k w_k V_{k,s}. \end{aligned} \tag{1.26}$$

Substituting the relations (1.24), (1.25) and (1.26) in (1.23) we obtain

$$\begin{aligned}
\partial_t(\rho V_{k,r}|J|) &= \nabla_c \cdot \left(|J| \rho_k u_k \sin \alpha \cos \theta \mathbf{V} \right) \\
&\quad + \sin \alpha \sin \theta |J| \rho_k u_k V_{k,\theta} - \cos \alpha \alpha'(s) \cos \theta |J| \rho_k u_k V_{k,s} \\
&\quad \nabla_c \cdot \left(\sin \theta \rho_k |J| v_k \mathbf{V} \right) - \cos \theta |J| \rho_k v_k V_{k,\theta} \\
&\quad - \nabla_c \cdot \left(\cos \alpha \cos \theta |J| \rho_k w_k \mathbf{V} \right) + \cos \alpha (-\sin \theta) |J| \rho_k w_k V_{k,\theta} \\
&\quad + (-\sin \alpha \alpha'(s)) |J| \cos \theta \rho_k w_k V_{k,s} \\
&\quad - |J| \partial_r P_k(\rho_k) + |J| D_{r,k} \\
&= -\nabla_c \cdot \left(|J| \rho_k V_{k,r} \mathbf{V} \right) + \rho_k V_{k,\theta} |J| [\sin \alpha \sin \theta - \cos \theta v_k - \cos \alpha \sin \theta w_k] \\
&\quad - \rho_k V_{k,s} |J| \cos \theta \alpha'(s) (\cos \alpha u_k + \sin \alpha w_k) - \partial_r P_k(\rho_k) + |J| D_{r,k}.
\end{aligned}$$

So, we get

$$\begin{aligned}
\partial_t(\rho_k V_{k,r}|J|) + \nabla_c \cdot \left(|J| \rho_k V_{k,r} \mathbf{V} \right) &= - |J| \partial_r (P_k(\rho_k)) + |J| \rho_k r V_{k,\theta}^2 \\
&\quad - |J| \rho_k V_{k,s} \cos \theta \alpha'(s) (1 - r \alpha'(s) \cos \theta) V_{k,s} + |J| D_{r,k}.
\end{aligned}$$

Expanding again we get

$$\begin{aligned}
\partial_t(\rho_k V_{k,\theta}|J|) &= |J|\partial_t \left(\frac{1}{r} \sin \alpha \sin \theta \rho_k u_k - \frac{\cos \theta}{r} \rho_k v_k - \frac{1}{r} \cos \alpha \sin \theta \rho_k w_k \right) \\
&= \frac{|J|}{r} \sin \alpha \sin \theta (-\nabla \cdot (u_k \rho_k \mathbf{u}) - \partial_x P_k + D_1) \\
&\quad - \frac{|J|}{r} \cos \theta (-\nabla \cdot (v_k \rho_k \mathbf{u}) - \partial_y P_k + D_2) \\
&\quad - \frac{|J|}{r} \cos \alpha \sin \theta (-\nabla \cdot (w_k \rho_k \mathbf{u}) - \partial_z P_k - \rho_k g + D_3) \\
&= -\frac{1}{r} \sin \alpha \sin \theta \nabla_c (|J| u_k \rho_k \mathbf{V}) + \frac{\cos \theta}{r} \nabla_c \cdot (|J| v_k \rho_k \mathbf{V}) \\
&\quad + \frac{1}{r} \cos \alpha \sin \theta \nabla_c \cdot (|J| w_k \rho_k \mathbf{V}) \\
&\quad - \frac{|J|}{r^2} \partial_\theta P_k + \frac{|J|}{r} \cos(\alpha(s)) \sin(\theta) \rho_k g + |J| D_\theta \\
&= -\nabla_c \cdot \left(|J| \frac{1}{r} \sin \alpha \sin \theta u_k \rho_k \mathbf{V} \right) - \nabla_c \cdot \left(-|J| \left(\frac{\cos \theta}{r} v_k \right) \rho_k \mathbf{V} \right) \\
&\quad - \nabla_c \cdot \left(-|J| \frac{1}{r} \cos \alpha \sin \theta w_k \rho_k \mathbf{V} \right) + |J| u_k \rho_k V_{k,r} \left(-\frac{1}{r^2} \sin \alpha \sin \theta \right) \\
&\quad - |J| v_k \rho_k V_{k,r} \left(-\frac{1}{r^2} \cos \theta \right) - |J| w_k \rho_k V_{k,r} \left(-\frac{1}{r^2} \cos \alpha \sin \theta \right) \\
&\quad + |J| u_k \rho_k V_{k,\theta} \left(\frac{1}{r} \sin \alpha \cos \theta \right) - |J| v_k \rho_k V_{k,\theta} \left(-\frac{\sin \theta}{r} \right) \\
&\quad - |J| w_k \rho_k V_{k,\theta} \left(\frac{1}{r} \cos \alpha \cos \theta \right) \\
&\quad + |J| u_k \rho_k V_{k,s} \left(\frac{1}{r} \cos \alpha + \alpha'(s) \sin \theta \right) - |J| w_k \rho_k V_{k,s} \left(-\frac{1}{r} \sin \alpha \alpha'(s) \sin \theta \right) \\
&\quad - \frac{|J|}{r^2} \partial_\theta P_k + \frac{|J|}{r} \cos(\alpha(s)) \sin(\theta) \rho_k g + |J| D_\theta \\
&= -\nabla_c \cdot (|J| \rho_k V_{k,\theta} \mathbf{V}) - 2 \frac{|J|}{r} \rho_k V_{k,r} V_{k,\theta} + \frac{|J|}{r} \rho_k \alpha'(s) \sin \theta (1 - r \alpha'(s) \cos \theta) V_{k,s}^2 \\
&\quad - \frac{|J|}{r^2} \partial_\theta P_k + \frac{|J|}{r} \cos(\alpha(s)) \sin(\theta) \rho_k g + |J| D_{k,\theta}.
\end{aligned}$$

Thus

$$\begin{aligned}
\partial_t(\rho_k V_{k,\theta}|J|) + \nabla_c \cdot (|J| \rho_k V_{k,\theta} \mathbf{V}) &= -2 \frac{|J|}{r} \rho_k V_{k,r} V_{k,\theta} + \frac{|J|}{r} \rho_k \alpha'(s) \sin \theta (1 - r \alpha'(s) \cos \theta) V_{k,s}^2 \\
&\quad - \frac{|J|}{r^2} \partial_\theta P_k + \frac{|J|}{r} \cos(\alpha(s)) \sin(\theta) \rho_k g + |J| D_{k,\theta},
\end{aligned}$$

where:

$$|J|D_{k,\theta} = \frac{|J|}{r} \sin \alpha \sin \theta D_1 - \frac{|J|}{r} \cos \theta D_2 - \frac{|J|}{r} \cos \alpha \sin \theta D_3.$$

Now we expand once more and obtain

$$\begin{aligned} \partial_t(\rho V_{k,s}|J|) &= \frac{-r \cos \alpha}{|J|} \nabla_c \cdot (|J|\rho u \mathbf{V}) - \frac{r \sin \alpha}{|J|} \nabla_c \cdot (|J|\rho w \mathbf{V}) \\ &\quad - \frac{r^2}{|J|} \partial_s P - \frac{r^2}{|J|} D_s - r \sin(\alpha(s)) \rho g \\ &= -\nabla_c \cdot (r \cos \alpha \rho u \mathbf{V}) - \nabla_c \cdot (r \sin \alpha \rho w \mathbf{V}) \\ &\quad + |J|\rho u V_{k,r} \partial_r \left(\frac{\cos \alpha}{1 - r\alpha'(s) \cos \theta} \right) + |J|\rho u V_{k,\theta} \partial_\theta \left(\frac{\cos \alpha}{1 - r\alpha'(s) \cos \theta} \right) \\ &\quad + |J|\rho u V_{k,s} \partial_s \left(\frac{\cos \alpha}{1 - r\alpha'(s) \cos \theta} \right) \\ &\quad + |J|\rho w V_{k,r} \partial_r \left(\frac{\sin \alpha}{1 - r\alpha'(s) \cos \theta} \right) + |J|\rho w V_{k,\theta} \partial_\theta \left(\frac{\sin \alpha}{1 - r\alpha'(s) \cos \theta} \right) \\ &\quad + |J|\rho w V_{k,s} \partial_s \left(\frac{\sin \alpha}{1 - r\alpha'(s) \cos \theta} \right) \\ &\quad - \frac{r^2}{|J|} \partial_s P - \frac{r^2}{|J|} D_s \end{aligned}$$

Furthermore, direct computations gives us

$$\begin{aligned} \partial_r \left(\frac{\cos \alpha}{1 - r\alpha'(s) \cos \theta} \right) &= \frac{\cos \alpha}{(1 - r\alpha'(s) \cos \theta)^2} \alpha'(s) \cos \theta, \\ \partial_\theta \left(\frac{\cos \alpha}{1 - r\alpha'(s) \cos \theta} \right) &= \frac{\cos \alpha}{(1 - r\alpha'(s) \cos \theta)^2} r\alpha'(s) \sin \theta, \\ \partial_s \left(\frac{\cos \alpha}{1 - r\alpha'(s) \cos \theta} \right) &= -\frac{\sin \alpha \alpha'(s)}{1 - r\alpha'(s) \cos \theta} + \frac{\cos \alpha}{(1 - r\alpha'(s) \cos \theta)^2} r\alpha''(s) \cos \theta, \\ \partial_r \left(\frac{\sin \alpha}{1 - r\alpha'(s) \cos \theta} \right) &= \frac{\sin \alpha}{(1 - r\alpha'(s) \cos \theta)^2} \alpha'(s) \cos \theta, \\ \partial_\theta \left(\frac{\sin \alpha}{1 - r\alpha'(s) \cos \theta} \right) &= \frac{-\sin \alpha}{(1 - r\alpha'(s) \cos \theta)^2} r\alpha'(s) \sin \theta, \\ \partial_s \left(\frac{\sin \alpha}{1 - r\alpha'(s) \cos \theta} \right) &= \frac{\cos \alpha \alpha'(s)}{1 - r\alpha'(s) \cos \theta} + \frac{\sin \alpha}{(1 - r\alpha'(s) \cos \theta)^2} r\alpha''(s) \cos \theta. \end{aligned}$$

So the equation of motion for the axial momentum is then computed as

$$\begin{aligned}
\partial_t(\rho V_{k,s}|J|) &= -\nabla_c \cdot (r\rho(1 - r\alpha'(s)\cos\theta)V_{k,s}\mathbf{V}) - \frac{r^2}{|J|}\partial_s P - \frac{r^2}{|J|}D_s \\
&\quad + |J|\rho V_{k,r}\frac{\alpha'(s)\cos\theta}{1 - r\alpha'(s)\cos\theta}V_{k,s} + |J|\rho V_{k,\theta}\frac{-r\alpha'(s)\sin\theta}{1 - r\alpha'(s)\cos\theta}V_{k,s} \\
&\quad + |J|\rho V_{k,s}\frac{\alpha'(s)}{1 - r\alpha'(s)\cos\theta}(-\sin\alpha u + \cos\theta w) \\
&\quad + |J|\rho V_{k,s}\frac{r\alpha''(s)\cos\theta}{1 - r\alpha'(s)\cos\theta}V_{k,s} \\
&= -\nabla_c \cdot (|J|\rho V_{k,s}\mathbf{V}) - \frac{r^2}{|J|}\partial_s P - \frac{r^2}{|J|}D_s \\
&\quad + r\rho V_{k,r}\alpha'(s)\cos\theta V_{k,s} + r\rho V_{k,\theta}(-r\alpha'(s)\sin\theta)V_{k,s} \\
&\quad + r\rho V_{k,s}\alpha'(s)(-\sin\alpha u + \cos\theta w) + r\rho V_{k,s}(r\alpha''(s)\cos\theta)V_{k,s} \\
&= -\nabla_c \cdot (|J|\rho V_{k,s}\mathbf{V}) - \frac{r^2}{|J|}\partial_s P - \frac{r^2}{|J|}D_s + \rho r^2 V_s^2 \alpha''(s)\cos(\theta) \\
&\quad + 2r\alpha'(s)\rho V_s(\cos(\theta)V_r - \sin(\theta)rV_\theta) - g\rho\sin(\alpha(s)),
\end{aligned}$$

giving us

$$\begin{aligned}
\partial_t(\rho V_{k,s}|J|) + \nabla_c \cdot (|J|\rho V_{k,s}\mathbf{V}) &= -\frac{r^2}{|J|}\partial_s P - \frac{r^2}{|J|}D_s + \rho r^2 V_s^2 \alpha''(s)\cos(\theta) \\
&\quad + 2r\alpha'(s)\rho V_s(\cos(\theta)V_r - \sin(\theta)rV_\theta) - g\rho\sin(\alpha(s)).
\end{aligned}$$

□

1.4.2 Euler Equations

The reduced model is obtained by cross averaging the isentropic Euler equations in each cross section C_s , both in the angular and radial directions. Therefore, the angular and radial velocities will not appear in the reduced model, as they are assumed to be small. The relevant equations are then the equations for conservation of mass and balance of momentum in the axial directions. In each layer, such equations are given respectively

by

$$\begin{aligned} \partial_t (|J|\rho_k) + \nabla_c \cdot (|J|\rho_k \mathbf{V}) &= M_k, \\ \partial_t (|J|\rho_k V_{s,k}) + \nabla_c \cdot (|J|\rho_k V_s \mathbf{V}) &= -\frac{r^2}{|J|} \partial_s P_k - \frac{r^2}{|J|} D_s + \rho r^2 V_s^2 \alpha''(s) \cos(\theta) \\ &\quad + 2r \alpha'(s) \rho V_s (\cos(\theta) V_r - \sin(\theta) r V_\theta) - g \rho \sin(\alpha(s)), \end{aligned} \tag{1.27}$$

for pipe's layer k (1 for the liquid and 2 for the gas), ρ_k is the density, P_k is the pressure and $D_{s,k}$ is the momentum exchange.

For the derivation of the model, we assume that the radial and angular velocities are much smaller compared to the axial velocity

$$\mathbf{V}_\theta, \mathbf{V}_r \ll \mathbf{V}_s.$$

As a result, the leading order contributions from equations (1.27) satisfy

$$\Rightarrow \begin{cases} \partial_t (|J|\rho_k) + \partial_s (|J|\rho_k V_{k,s}) = M_k, \\ \partial_t (|J|\rho_k V_{s,k}) + \partial_s (|J|\rho_k V_{k,s}^2) = -\frac{r^2}{|J|} \partial_s P - \frac{r^2}{|J|} D_s + \rho r^2 V_{k,s}^2 \alpha''(s) \cos \theta - g \rho \sin(\alpha(s)). \end{cases} \tag{1.28}$$

1.5 Cross section averages

Once the leading order terms are obtained, the next step in the derivation is the cross sectional averaging process. For that end, we need to determine the cross-sectional average of any quantity.

Definition 1.10. For the bottom layer, the cross-sectional integrated Jacobian is defined as

$$A_1 = \int_{\theta_{I,1}}^{2\pi - \theta_{I,1}} \int_{R_{0,1}}^{R_{e,1}} |J| dr d\theta. \tag{1.29}$$

On the other hand, for any given a function $f(r, \theta; s, t)$, we defined the cross sectional average as

$$\bar{f}_1(s, t) = \frac{1}{A_1} \int_{\theta_{I,1}}^{2\pi - \theta_{I,1}} \int_{R_{0,1}}^{R_{e,1}} f(r, \theta; s, t) |J| dr d\theta = \frac{1}{A_1} \int_{\Omega_1} \frac{f|J|}{r} dA. \quad (1.30)$$

Note: In the case of a straight pipe ($\alpha = \text{constant}$, $J/r = 1$ and the cross-sectional average is given in terms of the regular integral.

Analogously, for the top layer the integrated Jacobian is:

$$A_2 = \int_{-\theta_{I,2}}^{\theta_{I,2}} \int_{R_{0,2}}^{R_{e,2}} |J| dr d\theta, \quad (1.31)$$

and the average for the top layer (denoted with double over lines) are

$$\bar{\bar{f}}_2(s, t) = \frac{1}{A_2} \int_{-\theta_{I,2}}^{\theta_{I,2}} \int_{R_{0,2}}^{R_{e,2}} f(r, \theta; s, t) |J| dr d\theta = \frac{1}{A_2} \int_{\Omega_2} \frac{f|J|}{r} dA. \quad (1.32)$$

1.6 Mass conservation equation

Now, we are going to integrate the equations in each layer. For that, the Reynold's theorem 1.4 will be very useful. In this section, we state it and include some special cases in its proof for illustration.

For the mass conservation equation (1.28) (over the top layer), we have:

$$\begin{aligned}
A_2 \bar{M}_2 &= \int_{-\theta_{I,2}}^{\theta_{I,2}} \int_{R_{0,2}}^{R_{e,2}} M_2 |J| dr d\theta \\
&= \int_{-\theta_{I,2}}^{\theta_{I,2}} \int_{R_{0,2}}^{R_{e,2}} [\partial_t (|J| \rho_1) + \partial_s (|J| \rho_1 V_{s,1})] dr d\theta \\
&= \int_{-\theta_{I,2}}^{\theta_{I,2}} \left[\partial_t \left(\int_{R_{0,2}}^{R_{I,2}} |J| \rho_1 dr \right) - |J| \rho_1 \Big|_{r=R_e} \frac{dR_e}{dt} + |J| \rho_1 \Big|_{r=R_0} \frac{dR_0}{dt} \right] d\theta \\
&\quad + \int_{-\theta_{I,2}}^{\theta_{I,2}} \left[\partial_s \left(\int_{R_{0,2}}^{R_{I,2}} |J| \rho_1 V_s dr \right) - |J| \rho_1 V_s \Big|_{r=R_e} \frac{dR_e}{ds} + |J| \rho_1 V_s \Big|_{r=R_0} \frac{dR_0}{ds} \right] d\theta \\
&= \partial_t \left(\int_{-\theta_I}^{\theta_I} \int_{R_0}^{R_e} |J| \rho_1 dr d\theta \right) - \int_{R_0}^{R_e} |J| \rho_1 dr \Big|_{\theta=\theta_I} \frac{d\theta_I}{dt} + \int_{R_0}^{R_e} |J| \rho_1 dr \Big|_{\theta=-\theta_I} \frac{-d\theta_I}{dt} \\
&\quad + \int_{-\theta_{I,2}}^{\theta_{I,2}} \left(-|J| \rho_1 \Big|_{r=R_e} \frac{dR_e}{dt} + |J| \rho_1 \Big|_{r=R_0} \frac{dR_0}{dt} \right) d\theta + \partial_s \left(\int_{-\theta_I}^{\theta_I} \int_{R_0}^{R_e} |J| \rho_1 V_s dr d\theta \right) \\
&\quad + \int_{-\theta_I}^{\theta_I} \left(-|J| \rho_1 V_s \Big|_{r=R_e} \frac{dR_e}{ds} + |J| \rho_1 V_s \Big|_{r=R_0} \frac{dR_0}{ds} \right) d\theta \\
&= \partial_t \left(\int_{-\theta_I}^{\theta_I} \int_{R_0}^{R_e} |J| \rho_1 dr d\theta \right) + \partial_s \left(\int_{-\theta_I}^{\theta_I} \int_{R_0}^{R_e} |J| \rho_1 V_s dr d\theta \right) \\
&\quad - \int_{R_0}^{R_e} \left(|J| \rho_1 \Big|_{\theta=\theta_I} \left(\frac{d\theta_I}{dt} + V_s \Big|_{\theta=\theta_I} \frac{d\theta_I}{ds} \right) \right) dr + \int_{R_0}^{R_e} \left(|J| \rho_1 \Big|_{\theta=-\theta_I} \left(\frac{d\theta_I}{dt} + V_s \Big|_{\theta=-\theta_I} \frac{d\theta_I}{ds} \right) \right) dr \\
&\quad - \int_{-\theta_I}^{\theta_I} |J| \rho_1 \Big|_{r=R_e} \left(\frac{dR_e}{dt} + V_s \Big|_{r=R_e} \frac{dR_e}{ds} \right) d\theta + \int_{-\theta_I}^{\theta_I} |J| \rho_1 \Big|_{r=R_0} \left(\frac{dR_0}{dt} + V_s \Big|_{r=R_0} \frac{dR_0}{ds} \right) d\theta.
\end{aligned}$$

We can proceed in an analogous way for the bottom layer. Finally, we get the motion equations for the top and bottom layers:

$$\partial_t (A_1 \bar{\rho}_1) + \partial_s (A_1 \bar{\rho}_1 \bar{V}_{s,1}) = A_1 \bar{M}_1, \tag{1.33}$$

$$\partial_t (A_2 \bar{\rho}_2) + \partial_s (A_2 \bar{\rho}_2 \bar{V}_{s,2}) = A_2 \bar{M}_2,$$

where the total mass exchange $A_1 \bar{M}_1 + A_2 \bar{M}_2 = 0$ vanishes.

1.7 Momentum conservation equation

As the Jacobian was integrated to obtain conservation of mass, we are also going to integrate the left side from the momentum conservation equation (1.28):

$$\partial_t(|J|\rho_k V_{s,k}) + \partial_s(|J|\rho_k V_{k,s}^2) = -\frac{r^2}{|J|}\partial_s P - \frac{r^2}{|J|}D_s + \rho r^2 V_{k,s}^2 \alpha''(s) \cos \theta - g\rho \sin(\alpha(s)),$$

for the bottom and top layer. Without loss of generality, we will only proceed for the bottom layer. The integration of the right side will be seen on next sections, and also in the next chapters with the quasi-linear and conservative form. So, integrating the left side for $k = 2$ we get:

$$\begin{aligned} & \int_{-\theta_I,1}^{\theta_I,1} \int_{R_{e,1}}^{R_{e,1}} \left[\partial_t(|J|\rho_1 V_{s,1}) + \partial_s(|J|\rho_1 V_s^2) \right] dr d\theta \\ &= \int_{-\theta_I}^{\theta_I} \left[\partial_t \int_{R_0}^{R_e} |J|\rho_1 V_{k,s} dr - |J|\rho_1 V_{k,s} \Big|_{r=R_e} \frac{dR_e}{dt} + |J|\rho_1 V_{k,s} \Big|_{r=R_0} \frac{dR_0}{dt} \right] d\theta \\ & \quad + \int_{-\theta_I}^{\theta_I} \left[\partial_s \int_{R_0}^{R_e} |J|\rho_1 V_{k,s}^2 dr - |J|\rho_1 V_{k,s}^2 \Big|_{r=R_e} \frac{dR_e}{ds} + |J|\rho_1 V_{k,s}^2 \Big|_{r=R_0} \frac{dR_0}{ds} \right] d\theta \\ &= \partial_t \left(\int_{-\theta_I}^{\theta_I} \int_{R_0}^{R_e} |J|\rho_1 V_{k,s} dr d\theta \right) - \underbrace{\int_{R_0}^{R_e} |J|\rho_1 V_{k,s} dr \Big|_{\theta=\theta_I} \frac{d\theta_I}{dt}}_{(1)} + \underbrace{\int_{R_0}^{R_e} |J|\rho_1 V_{k,s} dr \Big|_{\theta=-\theta_I} \frac{-d\theta_I}{dt}}_{(2)} \\ & \quad + \int_{-\theta_I}^{\theta_I} \left[\underbrace{-|J|\rho_1 V_{k,s} \Big|_{r=R_e} \frac{dR_e}{dt}}_{(3)} + \underbrace{|J|\rho_1 V_{k,s} \Big|_{r=R_0} \frac{dR_0}{dt}}_{(4)} \right] d\theta \\ & \quad + \partial_s \left(\int_{-\theta_I}^{\theta_I} \int_{R_0}^{R_e} |J|\rho_1 V_{k,s}^2 dr \right) - \underbrace{\int_{R_0}^{R_e} |J|\rho_1 V_{k,s}^2 dr \Big|_{\theta=\theta_I} \frac{d\theta_I}{ds}}_{(1)} + \underbrace{\int_{R_0}^{R_e} |J|\rho_1 V_{k,s}^2 dr \Big|_{\theta=-\theta_I} \frac{-d\theta_I}{ds}}_{(1)} \\ & \quad + \int_{-\theta_I}^{\theta_I} \left[\underbrace{-|J|\rho_1 V_{k,s}^2 \Big|_{r=R_e} \frac{dR_e}{ds}}_{(3)} + \underbrace{|J|\rho_1 V_{k,s}^2 \Big|_{r=R_0} \frac{dR_0}{ds}}_{(4)} \right] d\theta. \end{aligned}$$

If we factor out (1), (2), (3) y (4), we get the “**streamline condition**”, which is:

$$\int_{R_0}^{R_e} |J| \rho_1 V_{k,s} dr \Big|_{\theta=\theta_I} \frac{d\theta_I}{dt} + \int_{R_0}^{R_e} |J| \rho_1 V_{k,s}^2 dr \Big|_{\theta=\theta_I} \frac{d\theta_I}{ds} = \int_{R_0}^{R_e} |J| \rho_1 V_{k,s} \left(\frac{d\theta_I}{dt} + V_{k,s} \frac{d\theta_I}{ds} \right) \Big|_{\theta=\theta_I} dr = 0$$

so we finally get:

$$\int_{-\theta_{I,1}}^{\theta_{I,1}} \int_{R_{e,1}}^{R_{e,1}} \left[\partial_t (|J| \rho_1 V_{s,1}) + \partial_s (|J| \rho_1 V_s^2) \right] dr d\theta = \partial_t (A_1 \bar{\rho}_1 \bar{V}_s) + \partial_s (A_1 \bar{\rho}_1 \bar{V}_s^2)$$

The above is after assuming that $\overline{\rho_1 V_s} \approx \bar{\rho}_1 \bar{V}_s$ and $\overline{\rho_1 V_s^2} \approx \bar{\rho}_1 \bar{V}_s^2$. We left the integral of the right side in its general expression (explicit expressions to be described in the next chapter). So

$$\partial_t (\rho_2 A_2 V_{s,2}) + \partial_s (\rho_2 A_2 V_{s,2}^2) = - \overline{\frac{r^2}{|J|} \partial_s P} - \overline{\frac{r^2}{|J|} D_s} + \overline{\rho r^2 V_{k,s}^2 \alpha''(s) \cos \theta} - \overline{g \rho \sin(\alpha(s))}. \quad (1.34)$$

Analogously for the bottom layer:

$$\partial_t (\rho_1 A_1 V_{s,1}) + \partial_s (\rho_1 A_1 V_{s,1}^2) = - \overline{\frac{r^2}{|J|} \partial_s P} - \overline{\frac{r^2}{|J|} D_s} + \overline{\rho r^2 V_{k,s}^2 \alpha''(s) \cos \theta} - \overline{g \rho \sin(\alpha(s))}. \quad (1.35)$$

1.7.1 Integration of gravity term

Proposition 1.11. *For the integration of the gravity term on the momentum equation, one gets:*

$$\overline{g \rho \sin(\alpha(s))} \approx \sin(\alpha(s)) g A_k \rho_k \left(\overline{\frac{r}{|J|}} \right).$$

Proof. Expanding out the expressions we get

$$\begin{aligned}
\overline{g\rho \sin(\alpha(s))} &= \int_{\Omega_k} r \sin(\alpha(s)) \rho_k g \, dA \\
&= \int_{\Omega_k} \frac{r}{|J|} \sin(\alpha(s)) \rho_k g |J| \, dA \\
&\approx \sin(\alpha(s)) g A_k \rho_k \overline{\left(\frac{r}{|J|}\right)}.
\end{aligned} \tag{1.36}$$

□

1.7.2 Hydrostatic Pressure

Definition 1.12. The hydrostatic pressure is defined as:

$$\nabla P = -g\rho\hat{z},$$

where \hat{z} is the canonical vector $(0, 0, 1)$, g is the gravity, P is the pressure and ρ is the density. For our model, we have two pressures, one for the liquid phase ($k = 1$) and the other for the gas phase ($k = 2$). Each one is given by:

$$\begin{aligned}
\tilde{P}_2 &= P_{2,ref} \left(\frac{\rho_2}{\rho_{2,ref}} \right)^{\gamma_2} = P_I = P_I(\rho_2), \\
P_1 &= P_I - g\rho\hat{z}.
\end{aligned}$$

We are going to project over the direction $\theta = \pi$. So

$$\begin{aligned}
&(-r \sin(\alpha) \cos \theta + x_0(s), -r \sin \theta, r \cos(\alpha) \cos \theta + z_0(s)) - (x_0(s), 0, z_0(s)) \\
&= (r \sin \alpha, 0, -r \cos \alpha) \sim (\sin \alpha, 0, -\cos \alpha) \perp (\cos \alpha, 0, \sin \alpha).
\end{aligned}$$

We take the dot product and see that:

$$\nabla P \cdot (\sin \alpha, 0, -\cos \alpha) = (P_I - g\rho\hat{z}) \cdot (\sin \alpha, 0, -\cos \alpha) = P_I + g\rho \cos \alpha,$$

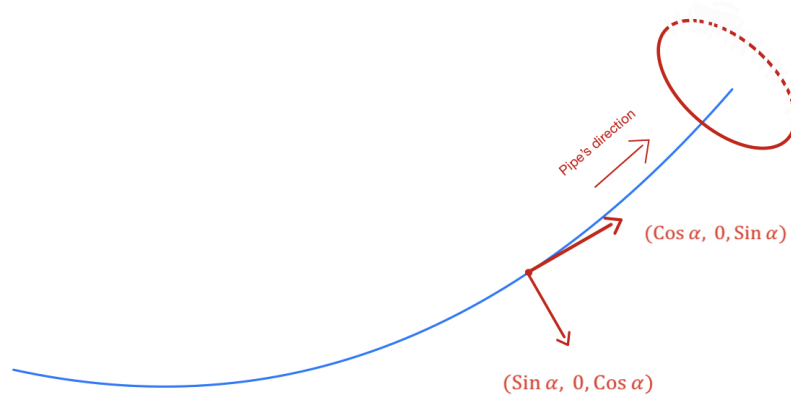


FIGURE 1.2: Pressure's projection

but also

$$\nabla P \cdot (\sin \alpha, 0, -\cos \alpha) = \sin \alpha \partial_x - \cos \alpha \partial_z = \frac{\partial P}{\partial \mathbf{n}},$$

where

$$\mathbf{n} = (\sin \alpha, 0, -\cos \alpha).$$

Therefore, the hydrostatic pressure in the liquid phase depends only in the projection:

$$\begin{aligned} (-r \sin \alpha \cos \theta, -r \sin \theta, r \cos \alpha \cos \theta) \cdot (\sin \alpha, 0, -\cos \alpha) &= -r \sin^2 \alpha \cos \theta - r \cos^2 \alpha \cos \theta \\ &= -r \cos \theta. \end{aligned}$$

Therefore, the pressure over the projection is:

$$P = \tilde{P}(r \cos \theta).$$

Now we remember from (1.14) that

$$\partial_x = -\cos \theta \sin \alpha \partial_r + \sin \theta \sin \alpha \frac{1}{r} \partial_\theta + \frac{\cos \alpha}{1 - r \alpha'(s) \cos \theta} \partial_s,$$

$$\partial_y = -\sin \theta \partial_r - \cos \theta \frac{1}{r} \partial_\theta,$$

$$\partial_z = \cos \theta \cos \alpha \partial_r - \sin \theta \cos \alpha \frac{1}{r} \partial_\theta + \frac{\sin \alpha}{1 - r \alpha'(s) \cos \theta} \partial_s.$$

So

$$\begin{aligned}
\frac{\partial P}{\partial \mathbf{n}} &= \sin \alpha \partial_x(\tilde{P}(r \cos \theta)) - \cos \alpha \partial_z(\tilde{P}(r \cos \theta)) \\
&= \sin \alpha(-\cos \theta \sin \alpha \tilde{P}' \cos \theta + \sin \theta \sin \alpha \frac{1}{r} \tilde{P}'(-r \sin \theta)) \\
&\quad - \cos \alpha(\cos \theta \cos \alpha \tilde{P}' \cos \theta - \sin \theta \cos \alpha \frac{1}{r} \tilde{P}'(-r \sin \theta)) \\
&= \sin \alpha(-\sin \alpha \tilde{P}') - \cos \alpha \cos \alpha \tilde{P}' \\
&= -\tilde{P}'.
\end{aligned}$$

$$\Rightarrow -\tilde{P}' = g\rho \cos \alpha.$$

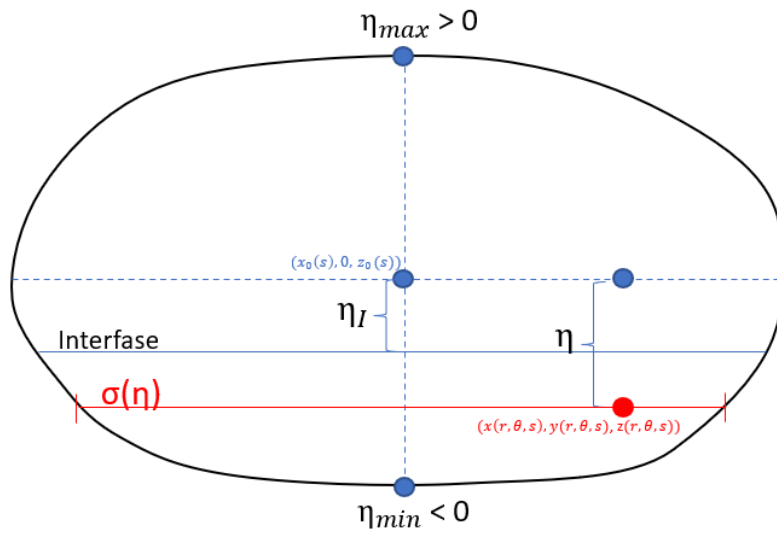


FIGURE 1.3: Pipe's geometry described in terms of displacement from the center (η) and width ($\sigma(\eta)$)

Most integrals can be better expressed in terms of the displacements from the center. On the one hand, let η be the distance from the center line $(x_o(s), 0, z_o(s))$ and any point under (or above) the interface line in layers 1 (or 2) at $(x(r, \theta; s), y(r, \theta; s), z(r, \theta; s))$. Geometrically, a constant η corresponds to a layer parallel to the pipe's axis. On one other hand, η_I is the distance between the center of the pipe to the interface. See Figure 1.3 for more details.

In absolute value, the distance from the axis to the point in the cross section is given by

$$\sqrt{(x_0(s) - x)^2 + (z_0(s) - z)^2} = \sqrt{r^2 \sin^2 \alpha \cos^2 \theta + r^2 \cos^2 \alpha \cos^2 \theta} = r |\cos \theta|,$$

and taking the sign into consideration, η is positive/negative above/below the axis. So, we get

$$\eta = r \cos(\theta). \quad (1.37)$$

Therefore, since

$$\eta = r \cos \theta \quad \Rightarrow \quad \tilde{P}(\eta) = -g\rho(\eta) \cos \alpha.$$

We assume that $\rho \approx \bar{\rho}$, which is the liquid phase average, so

$$\begin{aligned} \tilde{P} &= P_I + \bar{\rho}g(\eta_I - \eta) \cos \alpha \\ \therefore \tilde{P}_1 &= P_I + g \cos \alpha \bar{\rho}(\eta_I - \eta). \end{aligned}$$

1.7.2.1 Pressure integration for the conservation form

For the Pressure integration we need to prove the next proposition.

Proposition 1.13. *The Pressure term of the momentum equation can be expressed as*

$$\overline{-\frac{r^2}{|J|} \partial_s \tilde{P}_k} = \int_{\partial\Omega_k} \frac{r}{|J|} \tilde{P}_k \Big|_{r=R} \partial_s (\vec{r}_{P|r=R}) \cdot \mathbf{n}_k + \int_{\Omega_k} \partial_s \left(\frac{r}{|J|} \right) \tilde{P}_k dA_k - \partial_s (A_k \bar{P}_k)$$

Proof. It's easy to see that:

$$\begin{aligned} \overline{\frac{r^2}{|J|} \partial_s P_k} &= \int_{\Omega_k} \frac{r}{|J|} \partial_s \tilde{P}_k dA_k = \int_{\Omega_k} \left[\partial_s \left(\frac{r}{|J|} \tilde{P}_k \right) - \partial_s \left(\frac{r}{|J|} \right) \tilde{P}_k \right] dA_k \\ &= \int_{\Omega_k} \partial_s \left(\frac{r}{|J|} \tilde{P}_k \right) dA_k - \int_{\Omega_k} \partial_s \left(\frac{r}{|J|} \right) \tilde{P}_k dA_k. \end{aligned} \quad (1.38)$$

Using the Reynold's Theorem 1.4 we note:

$$\partial_s \left(\int_{\Omega_k} \frac{r}{|J|} \tilde{P}_k dA_k \right) = \int_{\Omega_k} \partial_s \left(\frac{r}{|J|} \tilde{P}_k \right) dA_k + \int_{\partial\Omega_k} \frac{r}{|J|} \tilde{P}_k \Big|_{r=R} \partial_s (\mathbf{r}_{P|r=R}) \cdot \mathbf{n}_k,$$

so

$$\begin{aligned} \int_{\Omega_k} \partial_s \left(\frac{r}{|J|} \tilde{P}_k \right) dA_k &= \partial_s \left(\int_{\Omega_k} \frac{r}{|J|} \tilde{P}_k dA_k \right) - \int_{\partial\Omega_1} \frac{r}{|J|} \tilde{P}_k \Big|_{r=R} \partial_s (\mathbf{r}_{P|r=R}) \cdot \mathbf{n}_k, \\ &= \partial_s (A_k \overline{P_k}) - \int_{\partial\Omega_k} \frac{r}{|J|} \tilde{P}_k \Big|_{r=R} \partial_s (\mathbf{r}_{P|r=R}) \cdot \mathbf{n}_k, \end{aligned} \quad (1.39)$$

substituting (1.39) in (1.38)

$$\overline{\frac{r^2}{|J|} \partial_s \tilde{P}_k} = \partial_s (A_k \overline{P_k}) - \int_{\partial\Omega_k} \frac{r}{|J|} \tilde{P}_k \Big|_{r=R} \partial_s (\vec{r}_{P|r=R}) \cdot \mathbf{n}_k - \int_{\Omega_k} \partial_s \left(\frac{r}{|J|} \right) \tilde{P}_k dA_k,$$

therefore

$$-\overline{\frac{r^2}{|J|} \partial_s \tilde{P}_k} = \int_{\partial\Omega_k} \frac{r}{|J|} \tilde{P}_k \Big|_{r=R} \partial_s (\mathbf{r}_{P|r=R}) \cdot \mathbf{n}_k + \int_{\Omega_k} \partial_s \left(\frac{r}{|J|} \right) \tilde{P}_k dA_k - \partial_s (A_k \overline{P_k})$$

□

If we substituted this last relation with the gravity term integration in the momentum conservation equations (1.35), (1.34) we obtain the final expression for the momentum conservation equations

$$\begin{aligned} \partial_t (\rho_k A_k V_{s,k}) + \partial_s (\rho_k A_k V_{s,k}^2 + A_k \tilde{P}_k) &= \int_{\partial\Omega_k} \frac{r}{|J|} \tilde{P}_k \Big|_{r=R} \partial_s (\mathbf{r}_{P|r=R}) \cdot \mathbf{n}_k - \overline{\frac{r^2}{|J|} D_{k,s}} \\ &+ \int_{\Omega_k} \partial_s \left(\frac{r}{|J|} \right) \tilde{P}_k dA_k + \overline{\rho r^2 V_{k,s}^2 \alpha''(s) \cos \theta} \\ &- \sin(\alpha(s)) g A_k \rho_k \overline{\left(\frac{r}{|J|} \right)}. \end{aligned} \quad (1.40)$$

1.7.2.2 Pressure integration for the quasi-lineal form

We now proceed to compute the pressure integration coming from the momentum equation. For this end, we first need to prove the next proposition.

Proposition 1.14. *The area of each layer can be re-written as:*

$$A_1 = \int_{\eta_{min}}^{\eta_I} (1 - \alpha'(s)\eta) \sigma(\eta), d\eta$$

$$A_2 = \int_{\eta_I}^{\eta_{max}} (1 - \alpha'(s)\eta) \sigma(\eta) d\eta.$$

Moreover, the function average can be re-written as

$$\bar{f}_1 = \int_{\eta_{min}}^{\eta_I} \sigma(\eta) f_1(\eta; s, t), d\eta$$

$$\bar{f}_2 = \int_{\eta_I}^{\eta_{max}} \sigma(\eta) f_2(\eta; s, t) d\eta.$$

Proof. Without loss of generality, we prove the result for phase 1. Recalling definition 1.10, we get

$$A_1 = \int_{\theta_{I,1}}^{2\pi - \theta_{I,1}} \int_{R_{0,1}}^{R_{e,1}} |J| dr d\theta.$$

We also note that

$$|J| = r(1 - r\alpha'(s)\cos(\theta)) \Rightarrow \frac{|J|}{r} = 1 - r\alpha'(s)\cos(\theta) = 1 - \alpha'(s)\eta.$$

So

$$\begin{aligned} \int_{\theta_{I,1}}^{2\pi - \theta_{I,1}} \int_{R_{0,1}}^{R_{e,1}} |J| dr d\theta &= \int_{\Omega_1} \int \frac{|J|}{r} r dr d\theta \\ &= \int_{\Omega_1} (1 - \alpha'(s)\eta) r dA \\ &= \int_{\eta_I}^{\eta_{max}} (1 - \alpha'(s)\eta) \sigma(\eta) d\eta. \end{aligned}$$

On the other hand:

$$\begin{aligned}
\bar{f}_1(s, t) &= \frac{1}{A_1} \int_{\Omega_1} \frac{f|J|}{r} dA \\
&= \frac{1}{A_1} \int_{\Omega_1} f(r, \theta; s, t) (1 - \alpha'(s)\eta) dA \\
&= \frac{1}{A_1} \int_{\eta_{min}}^{\eta_I} (1 - \alpha'(s)\eta) \sigma(\eta) d\eta.
\end{aligned}$$

□

This is an important result. We have not only changed the limits of integration but we have also proved that the integration depends only in the depth of the layer. **In other words, it only depends on η .** Now we can integrate the pressure term of the momentum equation. This is, for phase 1 we obtain

$$\begin{aligned}
\int_{\theta_{I,1}}^{2\pi-\theta_{I,1}} \int_0^{R_s} \frac{r^2}{|J|} \partial_s \tilde{P}_1 dr d\theta &= \int_{\Omega_1} \frac{r}{|J|} \partial_s \tilde{P}_1 dA \\
&= \int_{\eta_m}^{\eta_I} \frac{1}{(1 - \alpha'(s)\eta)} \partial_s \tilde{P}_1 \sigma(\eta) d\eta \\
&= \int_{\eta_m}^{\eta_I} \frac{\sigma(\eta)}{1 - \alpha'(s)\eta} \left[\frac{\partial P_I}{\partial \rho_2} \partial_s \tilde{\rho}_2 + g \partial_s \tilde{\rho}_1 (\eta_I - \eta) \cos(\alpha(s)) \right. \\
&\quad \left. + g \tilde{\rho}_1 \partial_s \eta_I \cos(\alpha(s)) - g \tilde{\rho}_1 (\eta_I - \eta) \sin(\alpha(s)) \alpha'(s) \right] d\eta \\
&= \int_{\eta_m}^{\eta_I} \frac{\sigma(\eta)}{1 - \alpha'(s)\eta} d\eta \left[\frac{\partial P_I}{\partial \rho_2} \partial_s \tilde{\rho}_2 + g \tilde{\rho}_1 \cos(\alpha(s)) \partial_s \eta_I \right] \\
&\quad + g \cos(\alpha(s)) \int_{\eta_m}^{\eta_I} \frac{\sigma(\eta)}{1 - \alpha'(s)\eta} (\eta_I - \eta) d\eta \partial_s \tilde{\rho}_1 \quad (1.41) \\
&\quad - g \sin(\alpha(s)) \alpha'(s) \tilde{\rho}_1 \int_{\eta_m}^{\eta_I} \frac{\sigma(\eta)}{1 - \alpha'(s)\eta} (\eta_I - \eta) d\eta.
\end{aligned}$$

We can calculate the deviating density for the liquid phase as

$$\partial_s \rho_1 = \partial_s \left(\frac{A_1 \rho_1}{A_1} \right) = \frac{\partial_s (A_1, \rho_1) A_1 - A_1 \rho_1 \partial_s A_1}{A_1^2} =$$

$$\frac{1}{A_1} \partial_s(A_1 \rho_1) - \frac{\rho_1}{A_1} \left[(1 - \alpha'(s)\eta_I) \sigma(\eta_I) \partial_s \eta_I + \int_{\eta_m}^{\eta_I} -\alpha''(s) \eta \sigma(\eta) d\eta - (1 - \alpha'(s)\eta_{min}) \sigma(\eta_{min}) \partial_s \eta_{min} \right]. \quad (1.42)$$

Analogously, we get

$$\partial_s \rho_2 = \frac{1}{A_2} \partial_s(A_2 \rho_2) - \frac{\rho_2}{A_2} \partial_s A_2 = \frac{1}{A_2} \partial_s(A_2 \rho_2) - \frac{\rho_2}{A_2} \left[-(1 - \alpha'(s)\eta_I) \sigma(\eta_I) \partial_s \eta_I - \int_{\eta_I}^{\eta_{max}} \alpha''(s) \eta \sigma(\eta) d\eta + (1 - \alpha'(s)\eta_{max}) \sigma(\eta_{max}) \partial_s \eta_{max} \right]. \quad (1.43)$$

Substituting this last expression (1.42) and (1.43) in (1.41), we obtain:

$$\begin{aligned} & \int_{\theta_{I,1}}^{2\pi - \theta_{I,1}} \int_{R_{0,1}}^{R_{e,1}} \frac{r^2}{|J|} \partial_s \tilde{p}_1 dr d\theta \\ &= \int_{\eta_{min}}^{\eta_I} \frac{\sigma(\eta)}{(1 - \alpha'(s)\eta)} d\eta \frac{\partial P_I}{\partial \rho_2} \left[\frac{1}{A_2} \partial_s(A_2 \rho_2) - \frac{\rho_2}{A_2} \left(-(1 - \alpha'(s)\eta_I) \sigma(\eta_I) \partial_s \eta_I \right. \right. \\ & \quad \left. \left. - \int_{\eta_I}^{\eta_{max}} \alpha''(s) \eta \sigma(\eta) d\eta + (1 - \alpha'(s)\eta_{max}) \sigma(\eta_{max}) \partial_s \eta_{max} \right) \right] \\ & \quad + g \tilde{\rho}_1 \cos(\alpha(s)) \int_{\eta_{min}}^{\eta_I} \frac{\sigma(\eta)}{(1 - \alpha'(s)\eta)} d\eta \partial_s \eta_I \\ & \quad + g \cos(\alpha(s)) \int_{\eta_{min}}^{\eta_I} \frac{\sigma(\eta)}{(1 - \alpha'(s)\eta)} (\eta_I - \eta) d\eta \left[\frac{1}{A_1} \partial_s(A_1 \rho_1) \right. \\ & \quad \left. - \left(\frac{\rho_1}{A_1} (1 - \alpha'(s)\eta_I) \sigma(\eta_I) \partial_s \eta_I - \int_{\eta_{min}}^{\eta_I} \alpha''(s) \eta \sigma(\eta) d\eta - (1 - \alpha'(s)\eta_{min}) \sigma(\eta_{min}) \partial_s \eta_{min} \right) \right] \\ & \quad - g \sin(\alpha(s)) \alpha'(s) \tilde{\rho}_1 \int_{\eta_{min}}^{\eta_I} \frac{\sigma(\eta)}{1 - \alpha'(s)\eta} (\eta_I - \eta) d\eta, \end{aligned}$$

and finally:

$$\begin{aligned} & \int_{\eta_{min}}^{\eta_I} \frac{\sigma(\eta)}{1 - \alpha'(s)\eta} d\eta \frac{\partial P_I}{\partial \rho_2} \frac{1}{A_2} \partial_s(A_2 \rho_2) g \cos(\alpha(s)) \int_{\eta_{min}}^{\eta_I} \frac{\sigma(\eta)}{1 - \alpha'(s)\eta} (\eta_I - \eta) d\eta \frac{1}{A_1} \partial_s(A_1 \rho_1) \\ & \quad + \left[\int_{\eta_{min}}^{\eta_I} \frac{\sigma(\eta)}{1 - \alpha'(s)\eta} d\eta \frac{\partial P_I}{\partial \rho_2} \frac{\rho_2}{A_2} (1 - \alpha'(s)\eta_I) \sigma(\eta_I) \right. \\ & \quad \left. + g \tilde{\rho}_1 \cos(\alpha(s)) \int_{\eta_{min}}^{\eta_I} \frac{\sigma(\eta)}{1 - \alpha'(s)\eta} d\eta \right] \partial_s \eta_I + S_{\rho_1}, \end{aligned}$$

where S_{ρ_1} are the source terms:

$$\begin{aligned}
& + \int_{\eta_{min}}^{\eta_I} \frac{\sigma(\eta)}{1 - \alpha'(s)\eta} d\eta \frac{\partial P_I}{\partial \rho_2} \frac{\rho_2}{A_2} \left(- \int_{\eta_{min}}^{\eta_I} \alpha''(s)\eta\sigma(\eta)d\eta + (1 - \alpha'(s)\eta_{max})\sigma(\eta_{max})\partial_s\eta_{max} \right) \\
& + g \cos(\alpha(s)) \int_{\eta_{min}}^{\eta_I} \frac{\sigma(\eta)}{(1 - \alpha'(s)\eta)} (\eta_I - \eta) d\eta + \left(\alpha''(s)\eta\sigma(\eta) d\eta + (1 - \alpha'(s)\eta_{min})\sigma(\eta_{min})\partial_s\eta_{min} \right) \\
& - g \sin(\alpha(s))\alpha'(s)\tilde{\rho}_1 \int_{\eta_{min}}^{\eta_I} \frac{\sigma(\eta)}{1 - \alpha'(s)\eta} (\eta_I - \eta) d\eta.
\end{aligned}$$

Now for the phase 2, we have

$$\int_{-\theta_{I,2}}^{\theta_{I,2}} \int_{R_{0,2}}^{R_{e,2}} \frac{r^2}{|J|} \partial_s \tilde{P}_2 dr d\theta = \int_{\Omega_2} \frac{r}{|J|} \partial_s \tilde{P}_1 dA = \int_{\eta_I}^{\eta_{max}} \frac{\sigma(\eta)}{1 - \alpha'(s)\eta} \partial_s \tilde{P}_2 \sigma(\eta) d\eta,$$

and then

$$\begin{aligned}
& = \int_{\eta_I}^{\eta_{max}} \frac{\sigma(\eta)}{1 - \alpha'(s)\eta} \left[\frac{\partial P_I}{\partial \rho_2} \partial_s \bar{\rho} \right] d\eta = \int_{\eta_I}^{\eta_{max}} \frac{\sigma(\eta)}{1 - \alpha'(s)\eta} d\eta \left[\frac{\partial P_I}{\partial \rho_2} \partial_s \bar{\rho} \right] \\
& = \int_{\eta_I}^{\eta_{max}} \frac{\sigma(\eta)}{1 - \alpha'(s)\eta} d\eta \frac{\partial P_I}{\partial \rho_2} \left[\frac{1}{A_2} \partial_s (A_2 \rho_2) - \frac{\rho_2}{A_2} \left(- (1 - \alpha'(s)\eta_I)\sigma(\eta_I)\partial_s\eta_I \right. \right. \\
& \quad \left. \left. - \int_{\eta_I}^{\eta_{max}} \alpha''(s)\eta\sigma(\eta)d\eta + (1 - \alpha'(s)\eta_{max})\sigma(\eta_{max})\partial_s\eta_{max} \right) \right].
\end{aligned}$$

Substituting the partial derivatives in (1.42) and (1.43) we see that

$$\begin{aligned}
& \int_{\eta_I}^{\eta_{max}} \frac{\sigma(\eta)}{1 - \alpha'(s)\eta} d\eta \frac{\partial P_I}{\partial \rho_2} \left[\frac{1}{A_2} \partial_s (A_2 \rho_2) - \frac{\rho_2}{A_2} \left(- (1 - \alpha'(s)\eta_I)\sigma(\eta_I)\partial_s\eta_I \right. \right. \\
& \quad \left. \left. - \int_{\eta_I}^{\eta_{max}} \alpha''(s)\eta\sigma(\eta)d\eta + (1 - \alpha'(s)\eta_{max})\sigma(\eta_{max})\partial_s\eta_{max} \right) \right] \\
& = \int_{\eta_I}^{\eta_{max}} \frac{\sigma(\eta)}{1 - \alpha'(s)\eta} d\eta \frac{\partial P_I}{\partial \rho_2} \frac{1}{A_2} \partial_s (A_2 \rho_2) \\
& \quad + \int_{\eta_I}^{\eta_{max}} \frac{\sigma(\eta)}{1 - \alpha'(s)\eta} d\eta \frac{\partial P_I}{\partial \rho_2} \frac{\rho_2}{A_2} (1 - \alpha'(s)\eta_I)\sigma(\eta_I)\partial_s\eta_I \\
& \quad + \int_{\eta_I}^{\eta_{max}} \frac{\sigma(\eta)}{1 - \alpha'(s)\eta} d\eta \frac{\partial P_I}{\partial \rho_2} \frac{\rho_2}{A_2} \left(\int_{\eta_I}^{\eta_{max}} \alpha''(s)\eta\sigma(\eta)d\eta - (1 - \alpha'(s)\eta_{max})\sigma(\eta_{max})\partial_s\eta_{max} \right).
\end{aligned}$$

1.7.2.3 Interface evolution

We must now derive the time evolution equation for the interface. In fact, it appears as a boundary condition. For that end, let us parametrize the interface in the new coordinates as

$$(s, \eta(s, t)).$$

The normal vector is proportional to

$$(-\partial_s \eta, 1).$$

The interface propagates with time velocity $(0, \partial_t \eta)$. The boundary condition requires that the velocity $(U_I, W_I - \partial_t \eta)$ is tangent to the interface. That is, the surface is a streamline that offers no resistance to its surroundings. That is, we have

$$0 = (U_I, W_I - \partial_t \eta) \cdot (-\partial_s \eta, 1),$$

which reduces to

$$\partial_t \eta + U_I \partial_s \eta = W_I. \quad (1.44)$$

Furthermore, we assume that the axial velocity of the interface is dominated by the liquid phase, so

$$U_I = V_{s,1}.$$

On the other hand, we also require that η always satisfies

$$\eta_{\min} \leq \eta \leq \eta_{\max}.$$

The above inequalities hold when both $\eta - \eta_{\min}$ and $\eta_{\max} - \eta$ are positive. One can easily see that such quantities satisfy the equations

$$\begin{aligned} \partial_t(\eta - \eta_{\min}) + U_I \partial_s(\eta - \eta_{\min}) &= W_I - U_I \partial_s \eta_{\min}(s), \\ \partial_t(\eta_{\max} - \eta) + U_I \partial_s(\eta_{\max} - \eta) &= U_I \partial_s \eta_{\max}(s) - \eta. \end{aligned}$$

So, the next expression satisfy the above equations:

$$W_I = \begin{cases} \partial_s \eta V_{s,1} & \text{if } V_{s,1} \partial_s \eta_{min} \leq V_{s,1} \partial_s \eta \leq V_{s,1} \partial_s \eta_{max} \\ 0 & \text{otherwise.} \end{cases}$$

1.7.3 The final model

Putting all of the identities from the previous sections, and adding a relaxation term to the interface evolution, the model in its final form is summarized as

$$\partial_t(A_1 \bar{\rho}_1) + \partial_s(A_1 \bar{\rho}_1 \bar{V}_{s,1}) = A_1 \bar{M}_1, \quad (1.45)$$

$$\begin{aligned} \partial_t(\rho_1 A_1 V_{s,1}) + \partial_s(\rho_1 A_1 V_{s,1}^2 + A_1 \tilde{P}_1) &= \int_{\partial\Omega_1} \frac{r}{|J|} \tilde{P}_1 \Big|_{r=R} \partial_s(\mathbf{r}_{P|r=R}) \cdot \mathbf{n}_1 - \overline{\frac{r^2}{|J|} D_{1,s}} \\ &+ \int_{\Omega_1} \partial_s \left(\frac{r}{|J|} \right) \tilde{P}_1 dA_1 + \overline{\rho r^2 V_{1,s}^2 \alpha''(s) \cos \theta} \\ &- \sin(\alpha(s)) g A_1 \rho_1 \overline{\left(\frac{r}{|J|} \right)}, \end{aligned} \quad (1.46)$$

$$\partial_t(A_2 \bar{\rho}_2) + \partial_s(A_2 \bar{\rho}_2 \bar{V}_{s,2}) = A_2 \bar{M}_2, \quad (1.47)$$

$$\begin{aligned} \partial_t(\rho_2 A_2 V_{s,2}) + \partial_s(\rho_2 A_2 V_{s,2}^2 + A_2 \tilde{P}_2) &= \int_{\partial\Omega_2} \frac{r}{|J|} \tilde{P}_2 \Big|_{r=R} \partial_s(\mathbf{r}_{P|r=R}) \cdot \mathbf{n}_2 - \overline{\frac{r^2}{|J|} D_{2,s}} \\ &+ \int_{\Omega_2} \partial_s \left(\frac{r}{|J|} \right) \tilde{P}_2 dA_2 + \overline{\rho r^2 V_{2,s}^2 \alpha''(s) \cos \theta} \\ &- \sin(\alpha(s)) g A_1 \rho_1 \overline{\left(\frac{r}{|J|} \right)}, \end{aligned} \quad (1.48)$$

$$\partial_t \eta + U_I \partial_s \eta = W_I + \mu(\rho_1 - \rho_{1,\text{ref}}) / \rho_{1,\text{ref}}, \quad (1.49)$$

where:

$$A_1 M_1 + A_2 M_2 = 0$$

$$A_1 + A_2 = \text{Total pipe's area}$$

$$\tilde{P}_2 = P_{2,ref} \left(\frac{\rho_2}{\rho_{2,ref}} \right)^{\gamma_2} = P_I = P_I(\rho_2)$$

$$\tilde{P}_1 = P_I + \bar{\rho}_1 g (\eta_I(s, t) - \eta) \cos(\alpha(s))$$

$$U_I = V_{s,1}$$

$$W_I = \begin{cases} \partial_s \eta V_{s,1} & \text{if } V_{s,1} \partial_s \eta_{min} \leq V_{s,1} \partial_s \eta \leq V_{s,1} \partial_s \eta_{max} \\ 0 & \text{otherwise.} \end{cases}$$

Here, $\rho_{1,ref}$ and $\rho_{2,ref}$ are densities reference values, and $P_{2,ref}$ is a pressure reference value, for this work, one can use the perfect gas law.

Chapter 2

Model properties

The model that we present here falls within the class of hyperbolic balance laws. For Partial Differential Equations in that class, there are several theoretical and numerical challenges. One of them is the presence of shockwaves, even when the initial conditions are smooth. Such waves propagate at a finite speed. A theory of weak solutions has been developed in the last decades. See for instance [3] and references therein. Weak solutions admit discontinuities and entropy inequalities have been helpful in choosing physically relevant solutions, achieving uniqueness. Correctly approximating solutions in the presence of shockwaves require a careful analysis of the PDEs' discretizations. There exists a variety of numerical schemes that are robust and precise when approximating such solutions. In particular, here we implement central-upwind schemes, which have several desirable properties, as it will be discussed below. As a first step, in this chapter we show the hyperbolic properties of the model by writing the equations in quasi-linear form and analyzing the coefficient matrix.

2.1 Quasi-linear formulation

Definition 2.1. We define the vector \mathbf{W} as:

$$\mathbf{W} = (W_1, W_2, W_3, W_4, W_5)^T,$$

where

$$W_1 = A_1 \rho_1,$$

$$W_2 = A_1 \rho_1 V_{s,1},$$

$$W_3 = A_2 \rho_2,$$

$$W_4 = A_2 \rho_2 V_{s,2},$$

$$W_5 = \eta.$$

The following theorem rewrites the conservation law in quasi-linear form. The resulting coefficient matrix must have real eigenvalues and a complete set of eigenvectors in order to show that the model is of hyperbolic type.

Theorem 2.2. *The final model can be written in quasi linear form as:*

$$\mathbf{W}_t + M(W)\mathbf{W}_s = \mathbf{S},$$

where

$$M = \begin{pmatrix} 0 & 1 & 0 & 0 & 0 \\ c_1^2 - v_{s,1}^2 & 2v_{s,1} & M_{2,3} & 0 & 0 \\ 0 & 0 & 0 & 1 & 0 \\ 0 & 0 & c_2^2 - v_{s,2}^2 & 2v_{s,2} & M_{4,5} \\ 0 & 0 & 0 & 0 & U_I \end{pmatrix}, S = \begin{bmatrix} A_1 M_1 \\ S_2 \\ A_2 M_2 \\ S_4 \\ W_I \end{bmatrix},$$

and

$$\begin{aligned}
 S_2 = & \int_{\eta_{min}}^{\eta_I} \frac{\sigma(\eta)}{1 - \alpha'(s)\eta} d\eta \frac{\partial P_I}{\partial \rho_2} \frac{\rho_2}{A_2} \left(- \int_{\eta_I}^{\eta_{max}} \alpha''(s)\eta\sigma(\eta)d\eta + (1 - \alpha'(s)\eta_{max})\sigma(\eta_{max})\partial_s\eta_{max} \right) \\
 & + g \cos(\alpha(s)) \int_{\eta_{min}}^{\eta_I} \frac{\sigma(\eta)}{1 - \alpha'(s)\eta} (\eta_I - \eta) d\eta \\
 & + \int_{\eta_{min}}^{\eta_I} \alpha''(s)\eta\sigma(\eta)d\eta + (1 - \alpha'(s)\eta_{min})\sigma(\eta_{min})\partial_s\eta_{min} \\
 & - g \sin(\alpha(s))\alpha'(s)\bar{\rho} \int_{\eta_{min}}^{\eta_I} \frac{\sigma(\eta)}{1 - \alpha'(s)\eta} (\eta_I - \eta) d\eta. \\
 & + A_1 \frac{\bar{r}^2}{|J|^2} D_{s,1} + A_1 \rho_1 \frac{\bar{r}^2}{|J|} V_{s,1}^2 \alpha''(s) \cos \theta - \sin(\alpha(s)) g A_1 \rho_1 \left(\frac{r}{|J|} \right), \\
 \\
 S_4 = & \int_{\eta_I}^{\eta_{max}} \frac{\sigma(\eta)}{1 - \alpha'(s)\eta} d\eta \frac{\partial P_I}{\partial \rho_2} \frac{\rho_2}{A_2} \left(\int_{\eta_I}^{\eta_{max}} \alpha''(s)\eta\sigma(\eta)d\eta - (1 - \alpha'(s)\eta_{max})\sigma(\eta_{max})\partial_s\eta_{max} \right) \\
 & + A_2 \frac{\bar{r}^2}{|J|^2} D_{s,2} + A_1 \rho_2 \frac{\bar{r}^2}{|J|} V_{s,2}^2 \alpha''(s) \cos \theta - \sin(\alpha(s)) g A_2 \rho_2 \left(\frac{r}{|J|} \right).
 \end{aligned}$$

Proof. We have already defined the vector \mathbf{W} for the conserved variables. Let us construct the matrix M . We define the M matrix as:

$$M = \begin{pmatrix} M_{1,1} & M_{1,2} & M_{1,3} & M_{1,4} & M_{1,5} \\ M_{2,1} & M_{2,2} & M_{2,3} & M_{2,4} & M_{2,5} \\ M_{3,1} & M_{3,2} & M_{3,3} & M_{3,4} & M_{3,5} \\ M_{4,1} & M_{4,2} & M_{4,3} & M_{4,4} & M_{4,5} \\ M_{5,1} & M_{5,2} & M_{5,3} & M_{5,4} & M_{5,5} \end{pmatrix} = \begin{pmatrix} M_1 \\ M_2 \\ M_3 \\ M_4 \\ M_5 \end{pmatrix}, \quad (2.1)$$

where $M_{i,j}$ and M_k are the entries and rows of the matrix M respectively, for $i, j, k = 1, 2, \dots, 5$. Now we are going to construct row by row the matrix.

First row M_1 : We need a row $(M_{1,1}, M_{1,2}, M_{1,3}, M_{1,4}, M_{1,5})$ that satisfy:

$$(M_{1,1}, M_{1,2}, M_{1,3}, M_{1,4}, M_{1,5}) \begin{bmatrix} A_1 \rho_1 \\ A_1 \rho_1 V_{s,1} \\ A_2 \rho_2 \\ A_2 \rho_2 V_{s,2} \\ \eta \end{bmatrix}_{\partial_s} = \partial_s (A_1 \rho_1 V_{s,1}).$$

In order for that to happen, the $M_{1,i}$ entries (with $i = 1, 2, \dots, 5$) must be

$$M_{1,1} = 0, M_{1,2} = 1, M_{1,3} = M_{1,4} = M_{1,5} = 0.$$

So, the first row is $M_1 = (0, 1, 0, 0, 0)$.

Second row M_2 : We need a row $(M_{2,1}, M_{2,2}, M_{2,3}, M_{2,4}, M_{2,5})$ to satisfy

$$M_2 \begin{bmatrix} A_1 \rho_1 \\ A_1 \rho_1 V_{s,1} \\ A_2 \rho_2 \\ A_2 \rho_2 V_{s,2} \\ \eta \end{bmatrix}_{\partial_s} = \partial_s(A_1 \rho_1 V_{s,1}^2) + c_1^2 \partial_s(A_1 \rho_1) + \left(\int_{\eta_I}^{\eta_{max}} \frac{\sigma(\eta)}{1 - \alpha'(s)\eta} d\eta \frac{\partial P_I}{\partial \rho_2} \frac{1}{A^2} \right) \partial_s(A_2 \rho_2),$$

where

$$c_1^2 = \frac{g \cos(\alpha(s))}{A_1} \int_{\eta_I}^{\eta_{max}} \frac{\sigma(\eta)}{1 - \alpha'(s)\eta} (\eta_I - \eta) d\eta, \quad (2.2)$$

and c_1 is the speed of sound. Here we note that we need to express $V_{s,1}^2$ in terms of the conservative variables. For that end, notice that

$$\partial_s(A_1 \rho_1 V_{s,1}^2) = \partial_s \left(\frac{(A_1 \rho_1 V_{s,1})^2}{A_1 \rho_1} \right) = -V_{s,1}^2 \partial_s(A_1 \rho_1) + 2V_{s,1} \partial_s(A_1 \rho_2 V_{s,1}).$$

So, we can see now that the entries for the second row must be

$$M_{2,1} = \frac{g \cos(\alpha(s))}{A_1} \int_{\eta_I}^{\eta_{max}} \frac{\sigma(\eta)}{1 - \alpha'(s)\eta} (\eta_I - \eta) d\eta - V_{s,1}^2 = C_1^2 - V_{s,1}^2$$

$$M_{2,2} = 2V_{s,1}$$

$$M_{2,3} = \int_{\eta_I}^{\eta_{max}} \frac{\sigma(\eta)}{1 - \alpha'(s)\eta} d\eta \frac{\partial P_I}{\partial \rho_2} \frac{1}{A^2}$$

$$M_{2,4} = M_{2,5} = 0,$$

giving us

$$M_2 = (C_1^2 - V_{s,1}^2, 2V_{s,1}, M_{2,3}, 0, 0).$$

Third row M_3 : We need a row $(M_{3,1}, M_{3,2}, M_{3,3}, M_{3,4}, M_{3,5})$ that satisfy:

$$(M_{3,1}, M_{3,2}, M_{3,3}, M_{3,4}, M_{3,5}) \begin{bmatrix} A_1 \rho_1 \\ A_1 \rho_1 V_{s,1} \\ A_2 \rho_2 \\ A_2 \rho_2 V_{s,2} \\ \eta \end{bmatrix}_{\partial_s} = \partial_s(A_2 \rho_1 V_{s,2}).$$

In order for that to happen, the $M_{3,i}$ entries (with $i = 1, 2, \dots, 5$) must be

$$M_{3,1} = M_{3,2} = M_{3,3} = 0, M_{3,4} = 1, M_{3,5} = 0.$$

So, the third row is $M_3 = (0, 0, 0, 1, 0)$.

Fourth row M_4 : We need a row $(M_{4,1}, M_{4,2}, M_{4,3}, M_{4,4}, M_{4,5})$ that satisfy:

$$M_4 \begin{bmatrix} A_1 \rho_1 \\ A_1 \rho_1 V_{s,1} \\ A_2 \rho_2 \\ A_2 \rho_2 V_{s,2} \\ \eta \end{bmatrix}_{\partial_s} = \partial_s(A_2 \rho_2 V_{s,2}^2) + c_2^2 \partial_s(A_2 \rho_2) + \left(\int_{\eta_I}^{\eta_{max}} \frac{\sigma(\eta)}{1 - \alpha'(s)\eta} d\eta \frac{\partial P_I}{\partial \rho_2} \frac{\rho_2}{A_2} (1 - \alpha'(s)\eta_I) \sigma(\eta_I) \right) \partial_s(\eta_I),$$

where

$$c_2^2 = \int_{\eta_I}^{\eta_{max}} \frac{\sigma(\eta)}{1 - \alpha'(s)\eta} d\eta \frac{\partial P_I}{\partial \rho_2} \frac{1}{A^2}, \quad (2.3)$$

and c_2 is the speed of sound for the top layer. Once again, we need to express $V_{s,2}^2$ in terms of the conservative variables. We note that

$$\partial_s(A_2 \rho_2 V_{s,2}^2) = \partial_s \left(\frac{(A_2 \rho_2 V_{s,2})^2}{A_2 \rho_2} \right) = -V_{s,2}^2 \partial_s(A_2 \rho_2) + 2V_{s,2} \partial_s(A_2 \rho_2 V_{s,2}).$$

So, we can see now that the entries must be

$$\begin{aligned}
 M_{4,1} &= M_{4,2} = 0 \\
 M_{4,3} &= \int_{\eta_I}^{\eta_{max}} \frac{\sigma(\eta)}{1 - \alpha'(s)\eta} d\eta \frac{\partial P_I}{\partial \rho_2} \frac{1}{A^2} - V_{s,2}^2 = c_2^2 - V_{s,2}^2 \\
 M_{4,4} &= 2V_{s,2} \\
 M_{4,5} &= \int_{\eta_I}^{\eta_{max}} \frac{\sigma(\eta)}{1 - \alpha'(s)\eta} d\eta \frac{\partial P_I}{\partial \rho_2} \frac{\rho_2}{A_2} (1 - \alpha'(s)\eta_I)\sigma(\eta_I).
 \end{aligned}$$

The fourth row is then

$$M_4 = (0, 0, C_2^2 - V_{s,2}^2, 2V_{s,2}, M_{4,5}).$$

Fifth row M_5 : For the last row, we need that $(M_{5,1}, M_{5,2}, M_{5,3}, M_{5,4}, M_{5,5})$ satisfy:

$$(M_{5,1}, M_{5,2}, M_{5,3}, M_{5,4}, M_{5,5}) \begin{bmatrix} A_1\rho_1 \\ A_1\rho_1 V_{s,1} \\ A_2\rho_2 \\ A_2\rho_2 V_{s,2} \\ \eta \end{bmatrix}_{\partial_s} = U_I \partial_s \eta.$$

In order for that to happen, it is easy to see that the $M_{1,i}$ entries (with $i = 1, 2, \dots, 5$) must be:

$$M_{5,1} = M_{5,2} = M_{5,3} = M_{5,4} = 0, M_{5,5} = U_I.$$

So, the fifth and last row is $M_5 = (0, 0, 0, 0, U_I)$. Therefore, the quasilinear system reads

$$\mathbf{W}_t + M(W)\mathbf{W}_s = \mathbf{S},$$

where

$$\mathbf{W} = \begin{bmatrix} A_1\rho_1 \\ A_1\rho_1 V_{s,1} \\ A_2\rho_2 \\ A_2\rho_2 V_{s,2} \\ \eta \end{bmatrix}, \quad \mathbf{W}_t = \begin{bmatrix} \partial_t (A_1\rho_1) \\ \partial_t (A_1\rho_1 V_{s,1}) \\ \partial_t (A_2\rho_2) \\ \partial_t (A_2\rho_2 V_{s,2}) \\ \partial_t (\eta) \end{bmatrix}, \quad \mathbf{W}_s = \begin{bmatrix} \partial_s (A_1\rho_1) \\ \partial_s (A_1\rho_1 V_{s,1}) \\ \partial_s (A_2\rho_2) \\ \partial_s (A_2\rho_2 V_{s,2}) \\ \partial_s (\eta) \end{bmatrix},$$

$$M = \begin{pmatrix} 0 & 1 & 0 & 0 & 0 \\ c_1^2 - v_{s,1}^2 & 2v_{s,1} & M_{2,3} & 0 & 0 \\ 0 & 0 & 0 & 1 & 0 \\ 0 & 0 & c_2^2 - v_{s,2}^2 & 2v_{s,2} & M_{4,5} \\ 0 & 0 & 0 & 0 & U_I \end{pmatrix}, \mathbf{S} = \begin{bmatrix} S_1 \\ S_2 \\ S_3 \\ S_4 \\ S_5 \end{bmatrix}.$$

Here, \mathbf{S} is the vector of source terms, and each entry is

$$S_1 = A_1 M_1.$$

$$\begin{aligned} S_2 = & \int_{\eta_{min}}^{\eta_I} \frac{\sigma(\eta)}{1 - \alpha'(s)\eta} d\eta \frac{\partial P_I}{\partial \rho_2} \frac{\rho_2}{A_2} \left(- \int_{\eta_I}^{\eta_{max}} \alpha''(s)\eta\sigma(\eta)d\eta + (1 - \alpha'(s)\eta_{max})\sigma(\eta_{max})\partial_s\eta_{max} \right) \\ & + g \cos(\alpha(s)) \int_{\eta_{min}}^{\eta_I} \frac{\sigma(\eta)}{1 - \alpha'(s)\eta} (\eta_I - \eta) d\eta \\ & + \int_{\eta_{min}}^{\eta_I} \alpha''(s)\eta\sigma(\eta)d\eta + (1 - \alpha'(s)\eta_{min})\sigma(\eta_{min})\partial_s\eta_{min} \\ & - g \sin(\alpha(s))\alpha'(s)\bar{\rho} \int_{\eta_{min}}^{\eta_I} \frac{\sigma(\eta)}{1 - \alpha'(s)\eta} (\eta_I - \eta) d\eta. \\ & + A_1 \frac{\bar{r}^2}{|J|^2} D_{s,1} + A_1 \rho_1 \frac{\bar{r}^2}{|J|} V_{s,1}^2 \alpha''(s) \cos \theta - \sin(\alpha(s)) g A_1 \rho_1 \left(\frac{r}{|J|} \right). \end{aligned}$$

$$S_3 = A_2 M_2.$$

$$\begin{aligned} S_4 = & \int_{\eta_I}^{\eta_{max}} \frac{\sigma(\eta)}{1 - \alpha'(s)\eta} d\eta \frac{\partial P_I}{\partial \rho_2} \frac{\rho_2}{A_2} \left(\int_{\eta_I}^{\eta_{max}} \alpha''(s)\eta\sigma(\eta)d\eta - (1 - \alpha'(s)\eta_{max})\sigma(\eta_{max})\partial_s\eta_{max} \right) \\ & + A_2 \frac{\bar{r}^2}{|J|^2} D_{s,2} + A_1 \rho_2 \frac{\bar{r}^2}{|J|} V_{s,2}^2 \alpha''(s) \cos \theta - \sin(\alpha(s)) g A_2 \rho_2 \left(\frac{r}{|J|} \right). \end{aligned}$$

$$S_5 = W_I$$

□

2.2 Hyperbolic properties

Once we have the quasi-linear form of the PDE, one can analyze the eigensystem to show the hyperbolic properties of the model, as described in the following theorem.

Theorem 2.3. *The coefficient matrix M associate to the quasi-lineal form has real eigenvalues and a complete set of eigenvectors provided that*

$$c_1 \neq 0, V_{s,2} - V_{s,1} \neq \pm(c_2 \pm c_1), V_{s,1} - U_I \neq \pm c_1, V_{s,2} - U_I \neq \pm c_2. \quad (2.4)$$

As a result, the model (1.45)-(1.49) is conditionally hyperbolic.

We note that condition (2.4) guarantees that the eigenvalues are different, which implies that the eigenvectors form a basis. The (very) special cases where the eigenvalues coincide could still lead to hyperbolicity. A deeper analysis including those special cases will be treated in a future work.

Proof. Let us calculate the characteristic polynomial, as follows.

$$\begin{aligned}
 \det(\lambda I - M) &= \begin{bmatrix} \lambda & -1 & 0 & 0 & 0 \\ -c_1^2 + V_{s,1}^2 & \lambda - 2V_{s,1} & -M_{2,3} & 0 & 0 \\ 0 & 0 & \lambda & -1 & 0 \\ 0 & 0 & -c_2^2 + V_{s,2}^2 & \lambda - 2V_{s,2} & -M_{4,5} \\ 0 & 0 & 0 & 0 & \lambda - U_I \end{bmatrix} \\
 &= \begin{bmatrix} \lambda & -1 & 0 & 0 & 0 \\ 0 & \lambda - 2V_{s,1} + \frac{-c_1^2 + V_{s,1}^2}{\lambda} & -M_{2,3} & 0 & 0 \\ 0 & 0 & \lambda & -1 & 0 \\ 0 & 0 & 0 & \lambda - 2V_{s,2} - \frac{c_2^2 - V_{s,2}^2}{\lambda} & -M_{4,5} \\ 0 & 0 & 0 & 0 & \lambda - U_I \end{bmatrix} \\
 &= (\lambda) \left(\lambda - 2V_{s,1} + \frac{-c_1^2 + V_{s,1}^2}{\lambda} \right) (\lambda) \left(\lambda - 2V_{s,2} - \frac{c_2^2 - V_{s,2}^2}{\lambda} \right) (\lambda - U_I) \\
 &= (\lambda^2 - 2V_{s,1}\lambda + -c_1^2 + V_{s,1}^2) (\lambda^2 - 2V_{s,2}\lambda - c_2^2 - V_{s,2}^2) (\lambda - U_I) \\
 &= (\lambda - c_1 - V_{s,1}) (\lambda - c_1 + V_{s,1}) (\lambda - c_2 - V_{s,2}) (\lambda - c_2 + V_{s,2}) (\lambda - U_I).
 \end{aligned}$$

So the eigenvalues are

$$\lambda_1 = V_{s,1} - c_1, \quad \lambda_2 = V_{s,1} + c_1, \quad \lambda_3 = V_{s,2} - c_2, \quad \lambda_4 = V_{s,2} + c_2, \quad \lambda_5 = U_I. \quad (2.5)$$

□

Chapter 3

Numerical results

We recall that the model can be written in conservation form as

$$\begin{aligned}
\partial_t(A_1\rho_1) + \partial_s(A_1\rho_1V_{s,1}) &= A_1M_1 \\
\partial_t(A_1\rho_1V_{s,1}) + \partial_s(A_1\rho_1V_{s,1}^2 + A_1p_1) &= \int_{\partial\Omega_1} \frac{r}{j} \bar{p}_{1,r=R} \partial_s(\mathbf{r}_p|_{r=R}) \cdot \mathbf{n}_1 d\ell \\
&\quad + \int_{\Omega_1} \partial_s\left(\frac{r}{j}\right) p_1 dA + A_1 \overline{\frac{r^2}{j^2}} D_{s,1} \\
&\quad + A_1 \rho_1 \overline{\frac{r^2}{j^2}} V_{s,1}^2 \alpha''(s) \cos\theta - \sin(\alpha(s)) g A_1 \rho_1 \overline{\frac{r}{j}} \\
\partial_t(A_2\rho_2) + \partial_s(A_2\rho_2V_{s,2}) &= A_2M_2 \\
\partial_t(A_2\rho_2V_{s,2}) + \partial_s(A_2\rho_2V_{s,2}^2 + A_2\bar{p}_2) &= \int_{\partial\Omega_2} \frac{r}{j} p_{2,r=R} \partial_s(\mathbf{r}_p|_{r=R}) \cdot \mathbf{n}_2 d\ell \\
&\quad + \int_{\Omega_2} \partial_s\left(\frac{r}{j}\right) p_2 dA + A_2 \overline{\frac{r^2}{j^2}} D_{s,2} \\
&\quad + A_2 \rho_2 \overline{\frac{r^2}{j^2}} V_{s,2}^2 \alpha''(s) \cos\theta - \sin(\alpha(s)) g A_2 \rho_2 \overline{\frac{r}{j}} \\
\partial_t\eta_I + \partial_s(U_I\eta) &= -\eta\partial_s U_I + W_I + \mu(\rho_1 - \rho_{1,\text{ref}})/\rho_{1,\text{ref}}.
\end{aligned} \tag{3.1}$$

Here A_1, A_2 are the Jacobian integrated in each cross section, which coincides with the cross sectional area in horizontal pipes where Jacobian reduces to the identity. Furthermore, $V_{s,1}, V_{s,2}$ are the corresponding velocities in the axial directions, η is the interface

displacement, U_I and W_I are the axial and vertical velocities at the interface, and p_1, p_2 are the corresponding pressures in each layer. The term $\mu(\rho_1 - \rho_{1,\text{ref}})/\rho_{1,\text{ref}}$ determines the interface displacement due to density deviations from reference values.

We note that the total integral $A_1 + A_2 = A = A(s)$ is known and depends only on the pipe's geometry, that does not change in time. On the other hand, the pressures in each layer are given by

$$\begin{aligned}
 \tilde{p}_1 &= P_I + \rho_1 g(\eta_I - \eta) \cos(\alpha(s)), \\
 p_1 &= \overline{\tilde{p}_1}, \\
 p_1 &= P_{2,\text{ref}} \left(\frac{\rho_2}{\rho_{2,\text{ref}}} \right)^{\gamma_2} = p_I, \\
 p_2 &= \overline{\overline{\tilde{p}_2}}.
 \end{aligned} \tag{3.2}$$

The vertical velocity at the interface is computed as

$$W_I = \begin{cases} V_{s,1} \partial_s \eta_I & \text{if } V_{s,1} \partial_s \eta_{\min} \leq V_{s,1} \partial_s \eta_I \leq V_{s,1} \partial_s \eta_{\max} \\ 0 & \text{otherwise.} \end{cases} \tag{3.3}$$

3.1 Convenient cross sections' descriptions and corresponding averages

We recall that any function f is averaged in each cross section as

$$\begin{aligned}
 \bar{f} &= \frac{1}{A_1} \int_{\Omega_1} \frac{J}{r} f \, dA, \\
 \overline{\overline{f}} &= \frac{1}{A_2} \int_{\Omega_2} \frac{J}{r} f \, dA,
 \end{aligned}$$

which in cylindrical-type or polar coordinates (for a fixed cross section) can also be written as

$$\begin{aligned}
 \bar{f} &= \frac{1}{A_1} \int_{\Omega_1} \frac{J}{r} f \, r \, dr \, d\theta, \\
 \overline{\overline{f}} &= \frac{1}{A_2} \int_{\Omega_2} \frac{J}{r} f \, r \, dr \, d\theta,
 \end{aligned}$$

with the limits in r and θ as specified in previous chapters. This is not always the most practical way of computing averages. A more convenient description of each cross section is through the variables

$$\eta = r \cos(\theta), \quad \eta^\perp = r \sin(\theta), \quad (3.4)$$

where η is the displacement from the point in the cross section to the equator line passing through the center at constant angle $\theta = \pi/2$, and η^\perp is the displacement from the point in the cross section to the line passing through the center from the center at constant angle $\theta = \pi$. This way, η is negative/positive below/above the center, and η^\perp is negative/positive to the left/right of the pipe's center.

The pipe's geometry determines a minimum and maximum displacements $\eta_{\min}(s)$, $\eta_{\max}(s)$ that can vary in the axial direction. At each depth η , one can assume the pipe has a width given by $\sigma(\eta)$. In the case where the pipe is symmetric across the vertical line, the variables η , η^\perp have the following limits

$$\eta_{\min}(s) \leq \eta \leq \eta_{\max}(s), \quad -\frac{\sigma(\eta)}{2} \leq \eta^\perp \leq \frac{\sigma(\eta)}{2}.$$

Using Fubini's theorem, the averages are computed in each layer as

$$\bar{f} = \frac{1}{A_1} \int_{\eta_{\min}(s)}^{\eta_I} \int_{-\frac{\sigma(\eta)}{2}}^{\frac{\sigma(\eta)}{2}} \frac{J}{r} f \, d\eta^\perp d\eta,$$

$$\bar{\bar{f}} = \frac{1}{A_2} \int_{\eta_I}^{\eta_{\max}(s)} \int_{-\frac{\sigma(\eta)}{2}}^{\frac{\sigma(\eta)}{2}} \frac{J}{r} f \, d\eta^\perp d\eta.$$

As we will see below, all of the flux and source terms are functions independent of η^\perp . In that case, the cross section averages are conveniently computed as

$$\bar{f} = \frac{1}{A_1} \int_{\eta_{\min}(s)}^{\eta_I} \sigma(\eta) \frac{J}{r} f \, d\eta, \quad (3.5)$$

$$\bar{\bar{f}} = \frac{1}{A_2} \int_{\eta_I}^{\eta_{\max}(s)} \sigma(\eta) \frac{J}{r} f \, d\eta.$$

3.2 Explicit expressions of flux and source terms

The areas A_1 and A_2 are given by

$$A_1 = \int_{\Omega_1} \frac{J}{r} dA = \int_{\eta_{\min}(s)}^{\eta_I} (1 - \alpha'(s)\eta) \sigma(\eta) d\eta, \text{ and}$$

$$A_2 = \int_{\Omega_2} \frac{J}{r} dA = \int_{\eta_J}^{\eta_{\max}(s)} (1 - \alpha'(s)\eta) \sigma(\eta) d\eta.$$

We recall that the pressures in the two layers before being averaged are given by

$$\begin{aligned} \tilde{p}_2 &= P_{2,\text{ref}} \left(\frac{\rho_2}{\rho_{2,\text{ref}}} \right)^{\gamma_2} = P_I \\ \tilde{P}_1 &= P_I + \rho_1 g (\eta_I(s, t) - \eta) \cos(\alpha(s)), \end{aligned} \tag{3.6}$$

where we are assuming the two densities ρ_1 and ρ_2 are constant. The average pressure in the top layer is written as

$$A_2 \bar{p}_2 = \int_{\Omega_2} \frac{r}{J} p_2 dA = P_{2,\text{ref}} \left(\frac{\rho_2}{\rho_{2,\text{ref}}} \right)^{\gamma_2} \int_{\eta_I}^{\eta_{\max}(s)} \frac{1}{1 - \alpha'(s)\eta} \sigma(\eta) d\eta.$$

The averaged pressure on the bottom layer is given by

$$\begin{aligned} A_1 \bar{p}_1 = \int_{\Omega_1} \frac{r}{J} p_1 dA &= P_{2,\text{ref}} \left(\frac{\rho_2}{\rho_{2,\text{ref}}} \right)^{\gamma_2} \int_{\eta_{\min}(s)}^{\eta_I} \frac{1}{1 - \alpha'(s)\eta} \sigma(\eta) d\eta \\ &+ \rho_1 g \cos(\alpha(s)) \int_{\eta_{\min}(s)}^{\eta_I} \frac{\eta_I(s, t) - \eta}{1 - \alpha'(s)\eta} \sigma(\eta) d\eta. \end{aligned}$$

One of the first source terms is the line integral over the layer's boundaries

$$\int_{\partial\Omega_1} \frac{r}{J} \tilde{p}_1|_{r=R} \partial_s(\mathbf{r}_p|_{r=R}) \cdot \mathbf{n}_1 d\ell.$$

Here \mathbf{r} is the parametrization given by equation (1.7) and \mathbf{n}_1 is the normal vector given by (1.9).

As it was shown in the previous chapter, we have

$$\partial_s(\mathbf{r}_1|_{r=R}) \cdot \mathbf{n}_1 = \frac{1}{R^2 + (\partial_\theta R)^2} R \partial_s R.$$

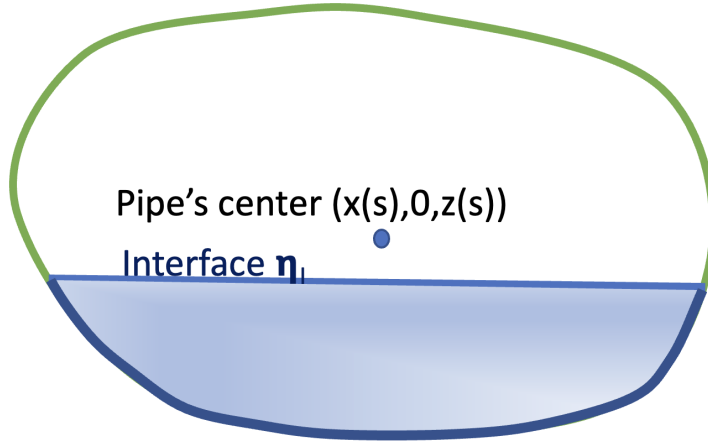


FIGURE 3.1: Schematic of a pipe's cross section and boundary of the bottom layer.

The boundary of each layer consists of the interface plus the section of the wall containing the corresponding layer. See Figure 3.1 for an schematic showing the boundary of the bottom layer. One can compute the line integral both on the wall instead of interface. For that, we notice that

$$d\ell = \|\partial_\theta \mathbf{r}_p|_{r=R}\| d\theta.$$

We also note that

$$\begin{aligned} \|\partial_\theta \mathbf{r}_p\|^2 &= \|(-R_\theta \sin(\alpha) \cos(\theta) - \sin \theta R \sin(\alpha), R_\theta \sin \theta + R \cos \theta, R_\theta \cos(\alpha) \cos \theta - R \cos(\alpha) \sin \theta)\|^2 \\ &= R^2 + R_\theta^2 \end{aligned}$$

Therefore,

$$\partial_s(\mathbf{r}_1|_{r=R}) \cdot \mathbf{n}_1 d\ell = R \partial_s R d\theta.$$

If we parametrize the wall by $\theta \rightarrow \mathbf{r}_p(R(\theta, s), \theta; s)$, the line integral over the wall is computed as

$$\int_{\theta_I}^{2\pi - \theta_I} \frac{1}{1 - \alpha'(s) R(\theta, s) \cos \theta} \tilde{p}_1|_{r=R} R \partial_s R d\theta.$$

Now, over the interface, the parametrization is given by

$$\mathbf{r}_p|_{\eta=\eta_I} = (-\sin(\alpha)\eta_I + x_o(s), \eta_I \tan \theta, \cos(\alpha)\eta_I + z_o(s)),$$

which gives

$$\partial_\theta \mathbf{r}_p|_{\eta=\eta_I} = (0, \eta_I \sec^2 \theta, 0),$$

and the normal vector is therefore

$$\mathbf{n}_1 = (-\sin \alpha, 0, \cos \alpha).$$

Furthermore,

$$||\partial_\theta \mathbf{r}_p|| d\theta = |\eta_I| \sec^2 \theta d\theta = -\eta_I \frac{d}{d\theta}(\tan \theta) d\theta = d(-\eta_I \tan \theta) = dy.$$

On the other hand,

$$\partial_s \mathbf{r}_p|_{\eta=\eta_I} = (-\cos \alpha \alpha'(s)\eta_I - \sin \alpha \partial_s \eta_I + \cos \alpha, \tan \theta \partial_s \eta_I, -\sin \alpha \alpha'(s)\eta_I + \cos \alpha \partial_s \eta_I + \sin \alpha),$$

which implies

$$\begin{aligned} \partial_s \mathbf{r}_p|_{\eta=\eta_I} \cdot \mathbf{n}_1 &= -\cos \alpha \sin \alpha \alpha'(s)\eta_I + \sin^2 \alpha \partial_s \eta_I \\ &\quad - \sin \alpha \cos \alpha \alpha'(s)\eta_I + \cos^2 \alpha \partial_s \eta_I + \sin \alpha \cos \alpha \\ &= \partial_s \eta_I. \end{aligned}$$

The corresponding integral over the interface is then computed as

$$\frac{1}{1 - \alpha'(s)\eta_I} p_I \partial_s \eta_I \sigma_I,$$

where

$$\sigma_I = \sigma(\eta_I) \tag{3.7}$$

is the pipe's width at the interface.

The line integral over the boundary is then computed as

$$\int_{\partial\Omega_1} \frac{r}{J} \tilde{p}_1|_{r=R} \partial_s(\mathbf{r}_p|_{r=R}) \cdot \mathbf{n}_1 d\ell = \int_{\theta_I}^{2\pi-\theta_I} \frac{1}{1-\alpha'(s)R(\theta,s)\cos\theta} \tilde{p}_1|_{r=R} R \partial_s R d\theta + \frac{1}{1-\alpha'(s)\eta_I} p_I \partial_s \eta_I \sigma_I. \quad (3.8)$$

Similarly, the source term associated to the upper layer is given by

$$\int_{\partial\Omega_2} \frac{r}{J} \tilde{p}_2|_{r=R} \partial_s(\mathbf{r}_p|_{r=R}) \cdot \mathbf{n}_2 d\ell = \int_{-\theta_I}^{\theta_I} \frac{1}{1-\alpha'(s)R(\theta,s)\cos\theta} \tilde{p}_2|_{r=R} R \partial_s R d\theta - \frac{1}{1-\alpha'(s)\eta_I} p_I \partial_s \eta_I \sigma_I. \quad (3.9)$$

The source terms associated to the momentum exchange are given by

$$\begin{aligned} A_1 \overline{\frac{r^2}{J^2} D_{s,1}} &= \int_{\Omega_1} \frac{r^2}{J^2} \frac{J}{r} dA D_{s,1} = \int_{\eta_{\min}(s)}^{\eta_I} \frac{\sigma(\eta)}{1-\alpha'(s)\eta} d\eta D_{s,1}, \\ A_2 \overline{\frac{r^2}{J^2} D_{s,2}} &= \int_{\Omega_2} \frac{r^2}{J^2} \frac{J}{r} dA D_{s,2} = \int_{\eta_I}^{\eta_{\max}(s)} \frac{\sigma(\eta)}{1-\alpha'(s)\eta} d\eta D_{s,2}. \end{aligned}$$

The source term associated to gravity effects are given by

$$\begin{aligned} \sin\alpha g \rho_1 A_1 \overline{\frac{r}{J}} &= g \sin\alpha \rho_1 \int_{\Omega_1} \frac{r}{J} \frac{J}{r} dA = g \sin\alpha \rho_1 \int_{\eta_{\min}(s)}^{\eta_I} \sigma(\eta) d\eta, \\ \sin\alpha g \rho_2 A_2 \overline{\frac{r}{J}} &= g \sin\alpha \rho_2 \int_{\Omega_2} \frac{r}{J} \frac{J}{r} dA = g \sin\alpha \rho_2 \int_{\eta_I}^{\eta_{\max}(s)} \sigma(\eta) d\eta. \end{aligned}$$

The last source terms are given by

$$\begin{aligned} A_1 \rho_1 u_1^2 \alpha''(s) \overline{\cos\theta \frac{r^2}{J}} &= \rho_1 \alpha''(s) u_1^2 \int_{\Omega_1} \cos\theta \frac{r^2}{J} \frac{J}{r} dA = \rho_1 \alpha''(s) u_1^2 \int_{\eta_{\min}(s)}^{\eta_I} \eta \sigma(\eta) d\eta, \text{ and} \\ A_2 \rho_2 u_2^2 \alpha''(s) \overline{\cos\theta \frac{r^2}{J}} &= \rho_2 \alpha''(s) u_2^2 \int_{\Omega_2} \cos\theta \frac{r^2}{J} \frac{J}{r} dA = \rho_2 \alpha''(s) u_2^2 \int_{\eta_I}^{\eta_{\max}(s)} \eta \sigma(\eta) d\eta. \end{aligned}$$

It is important to note that all flux and source terms were independent of η^\perp , i.e., are constant on each fixed depth. It allows us to write the cross sectional averages as integrals in the η directions, with weights involving the pipe's width $\sigma(\eta)$. In the next section, we show how we can discretize the cross sections to make it as general as possible, approximated by piecewise trapezoidal reconstructions.

3.3 Pipe's discretization

One of the contributions in this thesis is the generalization of the model found in [6] to pipes with general cross sections. In the cited work, rectangular and circular cross sections are considered. Here, one can handle any cross section with arbitrary shape, as long as they can be well described in cylindrical coordinates, as specified in previous sections.

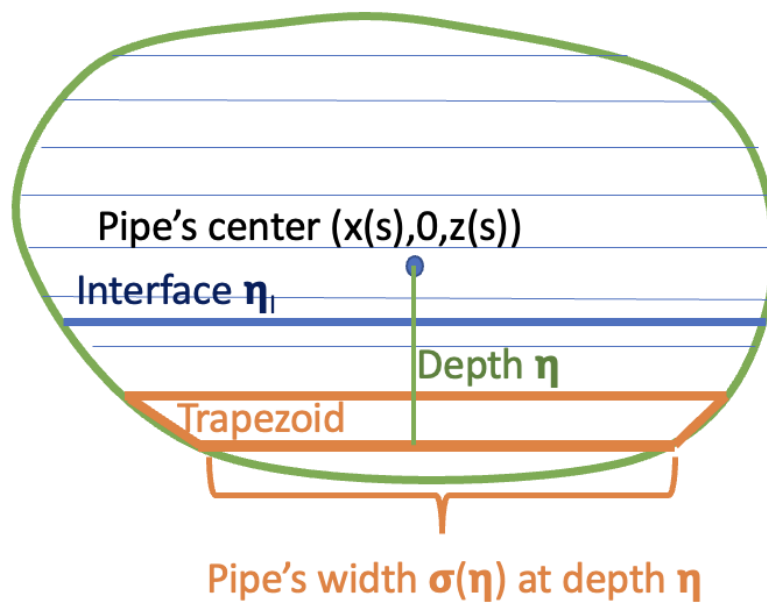


FIGURE 3.2: Pipe's discretization

Let us assume that each cross section consists of M trapezoids with edges at depths and angles

$$\eta_k, \theta_k, k = 1, \dots, M.$$

Even though one can consider arbitrary cross sections, we still need to either compute the involved integrals in an exact form when the geometry of the pipe is given by explicit expressions, or one could discretize it. In any case, in real life applications one usually does not have explicit expressions but only measurements. Having that in mind, we discretize our cross section by assuming that it is piecewise trapezoidal. See Figure 3.2 for a schematic of it.

All the flux and source terms that are written in terms of integrals with respect to η , except for the line integral. When the cross section is piecewise trapezoidal, the integrals with respect to η are replaced by Riemann sums.

Regarding the line integrals, they are approximated by

$$\begin{aligned} \int_{\partial\Omega_1} \frac{r}{J} \tilde{p}_1|_{r=R} \partial_s(\mathbf{r}_p|_{r=R}) \cdot \mathbf{n}_1 d\ell &\approx \sum_{\eta_k \leq \eta_I} \frac{1}{1-\eta_k \alpha'(s)} \tilde{p}_1|_{\eta=\eta_k} R(\theta_k, s) \partial_s R(\theta_k, s) (\theta_{k+1} - \theta_k) \\ &\quad + \frac{1}{1-\alpha'(s)\eta_I} p_I \partial_s \eta_I \sigma_I, \end{aligned}$$

$$\begin{aligned} \int_{\partial\Omega_2} \frac{r}{J} \tilde{p}_2|_{r=R} \partial_s(\mathbf{r}_p|_{r=R}) \cdot \mathbf{n}_2 d\ell &\approx \sum_{\eta_k \geq \eta_I} \frac{1}{1-\eta_k \alpha'(s)} \tilde{p}_2|_{\eta=\eta_k} R(\theta_k, s) \partial_s R(\theta_k, s) (\theta_{k+1} - \theta_k) \\ &\quad - \frac{1}{1-\alpha'(s)\eta_I} p_I \partial_s \eta_I \sigma_I. \end{aligned}$$

3.4 Numerical scheme

In this section, we describe the central-upwind numerical scheme implemented for solving equation (3.1) and the scheme's properties. Let us consider a hyperbolic balance law of the form

$$\mathbf{W}_t + (\mathbf{F}(\mathbf{W}))_s = \mathbf{S}(\mathbf{W}, s), \quad (3.10)$$

where both the flux and source may have terms that depend on the spatial variable s .

We partition the spatial domain into grid cells $I_j := [s_{j-\frac{1}{2}}, s_{j+\frac{1}{2}}]$, where Δs is the spatial scale, $s_{j\pm\frac{1}{2}} = s_j \pm \frac{\Delta s}{2}$, and s_j is the center of the grid cell. Let us denote by $\overline{\mathbf{W}}_j(t)$ the computed cell average of $\mathbf{W}(s, t)$ over the cell I_j , which is defined as

$$\overline{\mathbf{W}}_j(t) = \frac{1}{\Delta s} \int_{s_{j-\frac{1}{2}}}^{s_{j+\frac{1}{2}}} \mathbf{W}(s, t) ds. \quad (3.11)$$

Furthermore, let us consider a semi-discrete formulation of equation (3.10) given by

$$\frac{d}{dt} \overline{\mathbf{W}}_j = -\frac{\mathbf{F}_{j+\frac{1}{2}} - \mathbf{F}_{j-\frac{1}{2}}}{\Delta s} + \overline{\mathbf{S}}_j. \quad (3.12)$$

Following [8], we provide the following definition to be used below.

Our model (3.1) has conservative variables and a flux function given by

$$\mathbf{W} = \begin{pmatrix} A_1 \rho_1 \\ A_1 \rho_1 V_{s,1} \\ A_2 \rho_2 \\ A_2 \rho_2 V_{s,2} \\ \eta_I \end{pmatrix}, \quad \mathbf{F}(\mathbf{W}) = \begin{pmatrix} A_1 \rho_1 V_{s,1} \\ A_1 \rho_1 V_{s,1}^2 + A_1 p_1 \\ A_2 \rho_2 V_{s,2} \\ A_2 \rho_2 V_{s,2}^2 + A_2 p_2 \\ U_I \eta_I \end{pmatrix} \quad (3.13)$$

on the left hand side, and the source term is given by

$$\mathbf{S} = \begin{pmatrix} A_1 M_1 \\ \int_{\partial\Omega_1} \frac{r}{J} p_{1,r=R} \partial_s (\mathbf{r}_p|_{r=R}) \cdot \mathbf{n}_1 dl - \int_{\Omega_1} \partial_s \left(\frac{r}{J} \right) p_1 dA + A_1 \overline{\frac{r^2}{J^2}} D_{s,1} \\ \quad + A_1 \rho_1 \overline{\frac{r^2}{J^2}} u_1^2 \alpha''(s) \cos \theta - \sin(\alpha(s)) g A_1 \rho_1 \overline{\frac{r}{J}} \\ A_1 M_2 \\ \int_{\partial\Omega_2} \frac{r}{J} p_{2,r=R} \partial_s (\mathbf{r}_p|_{r=R}) \cdot \mathbf{n}_2 dl - \int_{\Omega_2} \partial_s \left(\frac{r}{J} \right) p_2 dA + A_2 \overline{\frac{r^2}{J^2}} D_{s,2} \\ \quad + A_2 \rho_2 \overline{\frac{r^2}{J^2}} u_2^2 \alpha''(s) \cos \theta - \sin(\alpha(s)) g A_2 \rho_2 \overline{\frac{r}{J}} \\ W_I - \partial_s U_I \eta_I \end{pmatrix}. \quad (3.14)$$

3.4.1 Semi-discrete central-upwind scheme

The semi-discrete formulation for the cell averages as in (3.11) is obtained after integrating equation (3.10) over each cell I_j , obtaining equation (3.12). The semi-discrete formulation is approximated by

$$\frac{d}{dt} \overline{\mathbf{W}}_j(t) = - \frac{\mathbf{H}_{j+\frac{1}{2}} - \mathbf{H}_{j-\frac{1}{2}}}{\Delta s} + \frac{1}{\Delta s} \int_{s_{j-\frac{1}{2}}}^{s_{j+\frac{1}{2}}} \mathbf{S}(\mathbf{W}, s) ds, \quad (3.15)$$

where $\mathbf{H}_{j\pm\frac{1}{2}}$ is the numerical flux at the cell interface $s_{j\pm\frac{1}{2}}$. Typical semi-discrete central-upwind schemes consider flux values at the interfaces obtained by non-oscillatory polynomial reconstructions. Non-oscillatory behavior is usually achieved by the use of nonlinear

limiters, as described in [9].

The flux at the cell interfaces, $\mathbf{F}(\mathbf{W}(s_{j\pm\frac{1}{2}}), t)$, is approximated by the numerical flux $\mathbf{H}_{j\pm\frac{1}{2}}(t)$ given by

$$\mathbf{H}_{j\pm\frac{1}{2}}(t) = \frac{a_{j\pm\frac{1}{2}}^+ \mathbf{F}(\mathbf{W}_{j\pm\frac{1}{2}}^-(t)) - a_{j\pm\frac{1}{2}}^- \mathbf{F}(\mathbf{W}_{j\pm\frac{1}{2}}^+(t))}{a_{j\pm\frac{1}{2}}^+ - a_{j\pm\frac{1}{2}}^-} + \frac{a_{j\pm\frac{1}{2}}^+ a_{j\pm\frac{1}{2}}^-}{a_{j\pm\frac{1}{2}}^+ - a_{j\pm\frac{1}{2}}^-} (\mathbf{W}_{j\pm\frac{1}{2}}^+(t) - \mathbf{W}_{j\pm\frac{1}{2}}^-(t)). \quad (3.16)$$

The numerical flux is of HLL type, as described in [10]. The interface point-values $\mathbf{W}_{j\pm\frac{1}{2}}^\pm(t)$ are recovered from the cell averages via a non-oscillatory piecewise polynomial reconstruction that is described in the next section. The one-sided local speeds in this scheme are approximated using the eigenvalues of the Jacobian:

$$\begin{aligned} a_{j\pm\frac{1}{2}}^- &= \min \left\{ V_{1,j\pm\frac{1}{2}}^+ - c_{1,j\pm\frac{1}{2}}^+, V_{1,j\pm\frac{1}{2}}^- - c_{1,j\pm\frac{1}{2}}^-, V_{2,j\pm\frac{1}{2}}^+ - c_{2,j\pm\frac{1}{2}}^+, V_{2,j\pm\frac{1}{2}}^- - c_{2,j\pm\frac{1}{2}}^-, 0 \right\}, \\ a_{j\pm\frac{1}{2}}^+ &= \max \left\{ V_{1,j\pm\frac{1}{2}}^+ + c_{1,j\pm\frac{1}{2}}^+, V_{1,j\pm\frac{1}{2}}^- + c_{1,j\pm\frac{1}{2}}^-, V_{2,j\pm\frac{1}{2}}^+ + c_{2,j\pm\frac{1}{2}}^+, V_{2,j\pm\frac{1}{2}}^- + c_{2,j\pm\frac{1}{2}}^-, 0 \right\}. \end{aligned} \quad (3.17)$$

In some cases, we have increased the viscosity to maintain stability. We note that $a_{j\pm\frac{1}{2}}^+ - a_{j\pm\frac{1}{2}}^- > 0$ is always positive unless $c_{k,j\pm\frac{1}{2}}^\pm$ and $u_{k,j\pm\frac{1}{2}}^\pm$, $k = 1, 2$ all vanish in a collapsed state with “no fluid motion”.

3.4.2 Non-oscillatory reconstruction

The construction of a numerical scheme that is second-order accurate in smooth regions is one of the goals in this work. The numerical scheme becomes first-order accurate near shock waves to achieve stability. The interface point values $\mathbf{W}_{j\pm\frac{1}{2}}(t)$ are calculated from the cell averages $\overline{\mathbf{W}}_j(t)$ via piecewise polynomial reconstruction. For that end, the reconstruction implemented here conserves cell averages, is second-order accurate in smooth regions, has a non-oscillatory behaviour, recognizes steady states at rest, and preserves the positivity of the cross-sectional area A . See references [11–14] for details.

A second-order reconstruction of any quantity $q(s, t)$ is chosen from its cell average \bar{q}_j as

$$q_{j-\frac{1}{2}}^+ = \bar{q}_j - \frac{\Delta s}{2} q'_j, \quad q_{j+\frac{1}{2}}^- = \bar{q}_j + \frac{\Delta s}{2} q'_j. \quad (3.18)$$

The *limited* slopes q'_j are calculated according to reference [15] as

$$q'_j = \frac{1}{\Delta_s} \text{minmod} \left(\theta (\bar{q}_j - \bar{q}_{j-1}), \frac{1}{2} (\bar{q}_{j+1} - \bar{q}_{j-1}), \theta (\bar{q}_{j+1} - \bar{q}_j) \right), \quad (3.19)$$

where $1 \leq \theta < 2$, and

$$\text{minmod}(r_1, r_2, r_3, \dots, r_k) = \begin{cases} \min_j(r_j) & \text{if } r_j > 0 \forall j \\ \max_j(r_j) & \text{if } r_j < 0 \forall j \\ 0 & \text{otherwise} \end{cases}.$$

Unless otherwise specified, $\theta = 1.5$, thus for simplicity. We note that this minmod limiter is commonly used in central-upwind schemes. It guarantees the local maximum principle with respect to the cell averages [9].

3.4.3 Steady state at rest

System 3.1 admits steady state solutions when there is a balance between flux gradients and source terms. Such balance can be in complicated conditions when the cross section is complex and gravity and other geometrical effects come into play. From all possibilities, it is easier to identify those steady state that are at rest. We require that the velocity vanishes ($V_{s,1} = V_{s,2} = 0$), the pipe is placed horizontally ($\alpha = \text{constant}$), no mass exchange ($M_1 = M_2 = 0$), and no momentum exchange ($D_{s,1} = D_{s,2} = 0$). The balance between flux gradients and source terms require

$$0 = \partial_s(A_k \bar{p}_k) - \int_{\partial\Omega_1} \frac{r}{J} \bar{p}_{1,r=R} \partial_s(\mathbf{r}_p|_{r=R}) \cdot \mathbf{n}_1 dl = \int_{\Omega_k} \partial_s \left(\frac{r}{J} p_k \right) dA,$$

where the Reynold's transport theorem has been used in the last equality. Since the pipe is horizontal, $J = 1$. Now, we require for the solution to be steady that p_k is constant. For the top layer where ideal gas laws are used, we need the top density to be constant $\rho_2 = \text{const}$. For the bottom layer, the interface pressure coincides with the top one, which

is already constant. A hydrostatic pressure component is considered, which is given by

$$-g\rho_1(\eta - \eta_I(s, t)),$$

provided that ρ_1 is constant. The hydrostatic pressure component is constant provided that η_I is constant along the axial direction. We have then proved the following proposition.

Proposition 3.1. *Let us consider a horizontal pipe ($\alpha = \text{constant}$), and assume that the fluid has no mass exchange ($M_1 = M_2 = 0$), and no momentum exchange ($D_{s,1} = D_{s,2} = 0$). System 3.1 admits steady state solutions at rest, satisfying the following conditions*

$$V_{s,1} = V_{s,2} = 0, \rho_1, \rho_2 \text{ and } \eta_I \text{ are independent of } s. \quad (3.20)$$

Knowing that steady state solutions at rest exists, our goal is to construct a numerical scheme that preserves such states. That is, when a solution satisfies the conditions in equation (3.20) at time t and the pipe meets the description in Proposition 3.1, we expect the numerical solution to remain the same in the next time step $t + \Delta t$. We say that the numerical scheme satisfies the well-balanced property when it respects those states in the above sense. This is important because flows in many situations can consist of small perturbations to steady states, except for situations like hydraulic jumps. The next section explains the correct way for the data reconstruction and the discretization of source terms in order to achieve the well balance property.

3.4.4 Well-balanced property: Flux and source terms discretizations

An important step in achieving the well balance property is in the data reconstruction. We apply the same non-oscillatory reconstruction as in equation (3.18). However, we have different ways of doing it. For instance, one could reconstruct η_I and integrate in the corresponding layers to obtain A_1 and A_2 . However, we could also reconstruct A_1 directly. One could also reconstruct directly the variable $A_1\rho_1$ and divide by the

reconstruction of A_1 to obtain an approximation of ρ_1 . At the continuous limit, the order in which we do it does not matter. However, at the discrete level some ways could inherit more advantages in comparison to others, specially in the well balance property.

Since $V_{s,1} = V_{s,2} = 0$, ρ_1 , ρ_2 and η_I are constant in a steady state of rest, we propose to reconstruct those variables first. Applying the non-oscillatory reconstruction in (3.18), we get

$$V_{1,j\pm\frac{1}{2}}^\pm = V_{2,j\pm\frac{1}{2}}^\pm, \rho_{1,j\pm\frac{1}{2}}^\pm, \rho_{2,j\pm\frac{1}{2}}^\pm \text{ and } \eta_{I,j\pm\frac{1}{2}}^\pm,$$

which are unchanged in steady states of rest.

Once the above variables are reconstructed at the interfaces, we proceed to reconstruct the flux and source terms as follows.

The integrated Jacobians are reconstructed as

$$A_{1,j\pm\frac{1}{2}}^\pm = \sum_{\eta_k \leq \eta_{I,j\pm\frac{1}{2}}^\pm} (1 - \alpha'(s_{j\pm\frac{1}{2}})\eta_k) \sigma(\eta_k) \Delta\eta_k, \text{ and}$$

$$A_{2,j\pm\frac{1}{2}}^\pm = \sum_{\eta_{I,j\pm\frac{1}{2}}^\pm \leq \eta_k} (1 - \alpha'(s_{j\pm\frac{1}{2}})\eta_k) \sigma(\eta_k) \Delta\eta_k.$$

The integrated pressures are given by

$$A_{2,j\pm\frac{1}{2}}^\pm \bar{p}_{2,j\pm\frac{1}{2}}^\pm = P_{2,\text{ref}} \left(\frac{\rho_{2,j\pm\frac{1}{2}}^\pm}{\rho_{2,\text{ref}}} \right)^{\gamma_2} \sum_{\eta_{I,j\pm\frac{1}{2}}^\pm \leq \eta_k} \frac{\sigma(\eta_k)}{1 - \alpha'(s_{j\pm\frac{1}{2}})\eta_k} \Delta\eta_k,$$

and

$$\begin{aligned} A_{1,j\pm\frac{1}{2}}^\pm \bar{p}_{1,j\pm\frac{1}{2}}^\pm &= P_{2,\text{ref}} \left(\frac{\rho_{2,j\pm\frac{1}{2}}^\pm}{\rho_{2,\text{ref}}} \right)^{\gamma_2} \sum_{\eta_k \leq \eta_{I,j\pm\frac{1}{2}}^\pm} \frac{\sigma(\eta_k)}{1 - \alpha'(s_{j\pm\frac{1}{2}})\eta_k} \Delta\eta_k \\ &+ \rho_{1,j\pm\frac{1}{2}}^\pm g \cos(\alpha(s_{j\pm\frac{1}{2}})) \sum_{\eta_k \leq \eta_{I,j\pm\frac{1}{2}}^\pm} \frac{\eta_{I,j\pm\frac{1}{2}}^\pm - \eta_k}{1 - \alpha'(s_{j\pm\frac{1}{2}})\eta_k} \sigma(\eta_k) \Delta\eta_k. \end{aligned}$$

The above expressions give us the reconstructions of all flux terms. We now proceed to handle the source terms. The first term is the line integrals in equations (3.8) and (3.9). Assuming symmetry across the vertical line ($\theta = 0$), those line integrals are approximated

as

$$\begin{aligned} \int_{\partial\Omega_1} \frac{r}{J} \tilde{p}_1|_{r=R} \partial_s(\mathbf{r}_p|_{r=R}) \cdot \mathbf{n}_1 d\ell &\approx 2 \sum \eta_k \leq \eta_{I,j}^\pm \frac{\tilde{p}_1|_{r=R(\theta_k, s_j)} R(\theta_k, s_j) \partial_s R(\theta_k, s_j) \Delta\theta_k}{1 - \alpha'(s_j) R(\theta_k, s_j) \cos \theta_k} \\ &+ \frac{2}{1 - \alpha'(s_j) \eta_{I,j}} p_{I,j} \frac{\Delta\eta_I}{\Delta s} \sigma_{I,j}, \text{ and} \end{aligned} \quad (3.21)$$

$$\begin{aligned} \int_{\partial\Omega_2} \frac{r}{J} \tilde{p}_2|_{r=R} \partial_s(\mathbf{r}_p|_{r=R}) \cdot \mathbf{n}_2 d\ell &\approx 2 \sum_{\eta_{I,j} \leq \eta_k} \frac{\tilde{p}_2|_{r=R(\theta_k, s_j)} R(\theta_k, s_j) \partial_s R(\theta_k, s_j) \Delta\theta_k}{1 - \alpha'(s_j) R(\theta_k, s_j) \cos \theta_k} \\ &- \frac{2}{1 - \alpha'(s_j) \eta_{I,j}} p_{I,j} \frac{\Delta\eta_I}{\Delta s} \sigma_{I,j}. \end{aligned}$$

Here $\Delta\eta_I$ is a central difference in the axial direction, computed with the minmod technique from the previous section, and $\sigma_{I,j}$ is the pipe's width at the interface, located at axial position $s = s_j$.

The other source terms are computed as

$$\begin{aligned} A_{1,j} \overline{\frac{r^2}{J^2}} D_{s,1} &\approx \sum_{\eta_k \leq \eta_{I,j}} \frac{\sigma(\eta_k)}{1 - \alpha'(s_j) \eta_k} \Delta\eta_k D_{s,1}, \\ A_{2,j} \overline{\frac{r^2}{J^2}} D_{s,2} &\approx \sum_{\eta_{I,j} \leq \eta_k} \frac{\sigma(\eta_k)}{1 - \alpha'(s_j) \eta_k} \Delta\eta_k D_{s,2}, \\ \sin(\alpha(s_j)) g \rho_{1,j} A_{1,j} \overline{\frac{r}{J}} &\approx g \sin(\alpha(s_j)) \rho_{1,j} \sum_{\eta_k \leq \eta_{I,j}} \sigma(\eta_k) \Delta\eta_k, \\ \sin(\alpha(s_j)) g \rho_{2,j} A_{2,j} \overline{\frac{r}{J}} &\approx g \sin(\alpha(s_j)) \rho_{2,j} \sum_{\eta_{I,j} \leq \eta_k} \sigma(\eta_k) \Delta\eta_k, \\ A_{1,j} \rho_{1,j} V_{1,j}^2 \alpha''(s_j) \overline{\cos(\theta) \frac{r^2}{J}} &= \rho_{1,j} \alpha''(s_j) u_{1,j}^2 \sum_{\eta_k \leq \eta_{I,j}} \eta_k \sigma(\eta_k) \Delta\eta_k, \text{ and} \\ A_{2,j} \rho_{2,j} V_{2,j}^2 \alpha''(s_j) \overline{\overline{\cos \theta} \frac{r^2}{J}} &= \rho_{2,j} \alpha''(s_j) u_{2,j}^2 \sum_{\eta_{I,j} \leq \eta_k} \eta_k \sigma(\eta_k) \Delta\eta_k. \end{aligned} \quad (3.22)$$

The above discretizations are appropriate in the sense that they are consistent with the Partial Differential Equation, it results in a robust central-upwind scheme, and they can recognize certain steady state at rest as we will see below.

3.4.5 Evolution in time

The time integration of the ODE system (3.15) is done using the second-order strong stability preserving Runge-Kutta scheme [16]

$$\mathbf{W}^{(1)} = \mathbf{W}^{(0)} + \Delta t \mathbf{C}[\mathbf{W}^{(0)}] \quad (3.23a)$$

$$\mathbf{W}^{(2)} = \frac{1}{2} \mathbf{W}^{(0)} + \frac{1}{2} (\mathbf{W}^{(1)} + \Delta t \mathbf{C}[\mathbf{W}^{(1)}]) \quad (3.23b)$$

$$\overline{\mathbf{W}}(t + \Delta t) := \mathbf{W}^{(2)}, \quad (3.23c)$$

with

$$\mathbf{C}[\mathbf{W}(t)] = -\frac{\mathbf{H}_{j+\frac{1}{2}}(\mathbf{W}(t)) - \mathbf{H}_{j-\frac{1}{2}}(\mathbf{W}(t))}{\Delta s} + \overline{\mathbf{S}}_j(t), \quad (3.24)$$

$\mathbf{H}_{j+\frac{1}{2}}(\mathbf{W}(t))$ is the vector of flux term (3.14) discretized according to equation (3.16), reconstructions as in equation (3.18), in the way described in Section 3.4.4. Furthermore, $\overline{\mathbf{S}}_j(t)$ is the vector of source terms (3.14) discretized according to equation (3.21) and (3.22).

The CFL condition that determines the time step Δt is given by

$$\frac{a\Delta t}{\Delta s} \leq \frac{1}{2}, \quad (3.25)$$

where $a = \max_j \max(a_{j\pm\frac{1}{2}}^+, -a_{j\pm\frac{1}{2}}^-)$.

The numerical scheme presented here is based on the central-upwind approximation. This class of numerical scheme has shown to be very robust in many applications where the PDE-based model is hyperbolic. In particular, it has desirable properties as in the following proposition.

Proposition 3.2. *Let us consider a horizontal pipe ($\alpha = 0$) with general cross section but independent of s (uniform in the axial direction). Let us assume that there is no mass or momentum exchange ($D_{s,1} = D_{s,2} = 0$, $M_1 = M_2 = 0$). Furthermore, suppose that the initial conditions consists of a steady state at rest at time t_n . That is, the velocities u_1 and u_2 are zero, ρ_1 and ρ_2 , and η are constant. Then, the solution at time $t_{n+1} = t_n + \Delta t$ computed with the numerical scheme described in Sections 3.4.1, 3.4.2, and 3.4.3 coincides*

with the solution at time t_n . That is, the numerical scheme recognizes the steady states at rest.

Proof. One needs to show a balance between flux gradients and source terms at a discrete level. Most of the terms vanish because the velocities are zero and the densities in each layer are constant. The only terms that are not trivial are those associated to the pressures. The balance occurs thanks to the Reynold's transport theorem and the fact that the pressures (before being integrated in each cross sections) are independent of s for steady states. That always occurs at the continuous limit. In the case where the geometry of the pipe is independent of time, both $A_k p_k$ and the corresponding line integral in the source terms are independent of time. The reconstructions at the interfaces are also independent of s .

One still need to make it sure the viscosity terms $\frac{a_{j\pm\frac{1}{2}}^+ a_{j\pm\frac{1}{2}}^-}{a_{j\pm\frac{1}{2}}^+ - a_{j\pm\frac{1}{2}}^-} \left(\mathbf{W}_{j\pm\frac{1}{2}}^+(t) - \mathbf{W}_{j\pm\frac{1}{2}}^-(t) \right)$ vanish. This happens because each of the terms in the solution vector and the corresponding discretizations are independent of time, so $\mathbf{W}_{j\pm\frac{1}{2}}^+(t) - \mathbf{W}_{j\pm\frac{1}{2}}^-(t) = 0$. \square

3.5 Numerical results

In this section, we present a variety of numerical tests aimed at showing the merits of the scheme in different aspects of the fluid's dynamics. Throughout the numerical tests in this work, we take zero mass and momentum exchange $D_{s,1} = D_{s,2} = 0$, $M_1 = M_2 = 0$. The ratio of gas constants at the top layer will be taken to be $\gamma_2 = 1.4$. The domain is $[0, 5] \ni s$. In all numerical tests, we will use zero Neumann boundary conditions.

In all cases, 200 grid points are used in the axial direction and 100 levels are taken in the vertical direction in each cross section. A CFL number of 0.45 is used in order to guarantee stability.

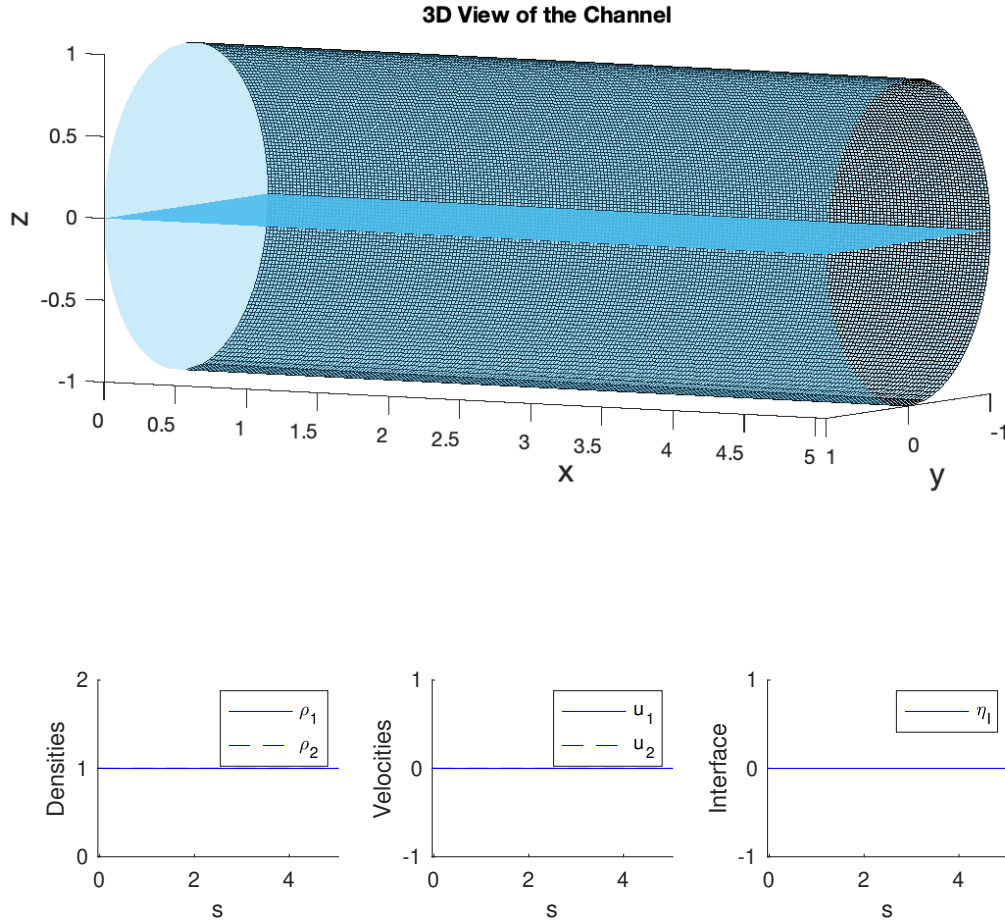


FIGURE 3.3: Solution at time $t = 0.5$ for initial conditions given by equation (3.26). Top panel: 3D view of the pipe, showing the interface in blue. Bottom left: densities of lower (solid line) and upper (dashed lines) layers. Bottom middle: Corresponding velocities. Bottom right: interface.

3.5.1 Steady state at rest

In this numerical test, we consider a steady state at rest in a horizontal pipe ($\alpha = 0$) with circular cross section with constant radius $R(\theta, s) = 1$. The gravity constant is set to $g = 9.81 \text{ ms}^{-2}$. The reference densities and pressures are $\rho_{1,\text{ref}} = \rho_{2,\text{ref}} = 1$ and $P_{2,\text{ref}} = 1$. The vertical velocity at the interface is $W_I = 0$ with no interface displacement ($\mu = 0$).

The initial conditions are given by

$$\rho_1 = \rho_2 = 1, V_{s,1} = V_{s,2} = 0, \eta_I = 0. \quad (3.26)$$

This state corresponds to a steady solution in the absence of mass and momentum exchange and interface displacements. According to Proposition 3.2, the proposed numerical scheme recognizes those states, and the numerical solution remains independent of time. This is confirmed by the numerical solution shown in Figure 3.3. The 3D view of the pipe is displayed in the top panel. As we can see, the interface remains flat with no numerical errors. The steady solution is then recognized exactly. This is corroborated in the bottom panels. The densities and velocities are plotted in the bottom left and bottom middle panels. The quantities associated to the first layer is identified with solid lines, while the ones associated with the second layer uses dashed lines.

3.5.2 Perturbation to a steady state at rest

In this numerical test, we now introduce a perturbation to a steady state for a horizontal pipe ($\alpha = 0$) with circular cross sections with radius that grow linearly with respect to the axial position

$$R(\theta, s) = 1 + 0.1s.$$

A coefficient $\mu = 10$ generates an interface displacement when density variations occur.

The initial conditions are given by

$$\rho_1 = \rho_2 = 1, V_{s,1} = V_{s,2} = 0, \eta_I = \begin{cases} \epsilon & \text{if } 3 \leq s \leq 3.5 \\ 0 & \text{otherwise,} \end{cases} \quad (3.27)$$

with $\epsilon = 10^{-2}$.

The top panel shows the 3D view of the pipe at time $T = 0.5$. The rest of the panels show the profiles at times $t = 0, 0.25, 0.5$ in descending order. The densities, velocities and interface are shown from left to right. As in the previous test, the bottom layer is

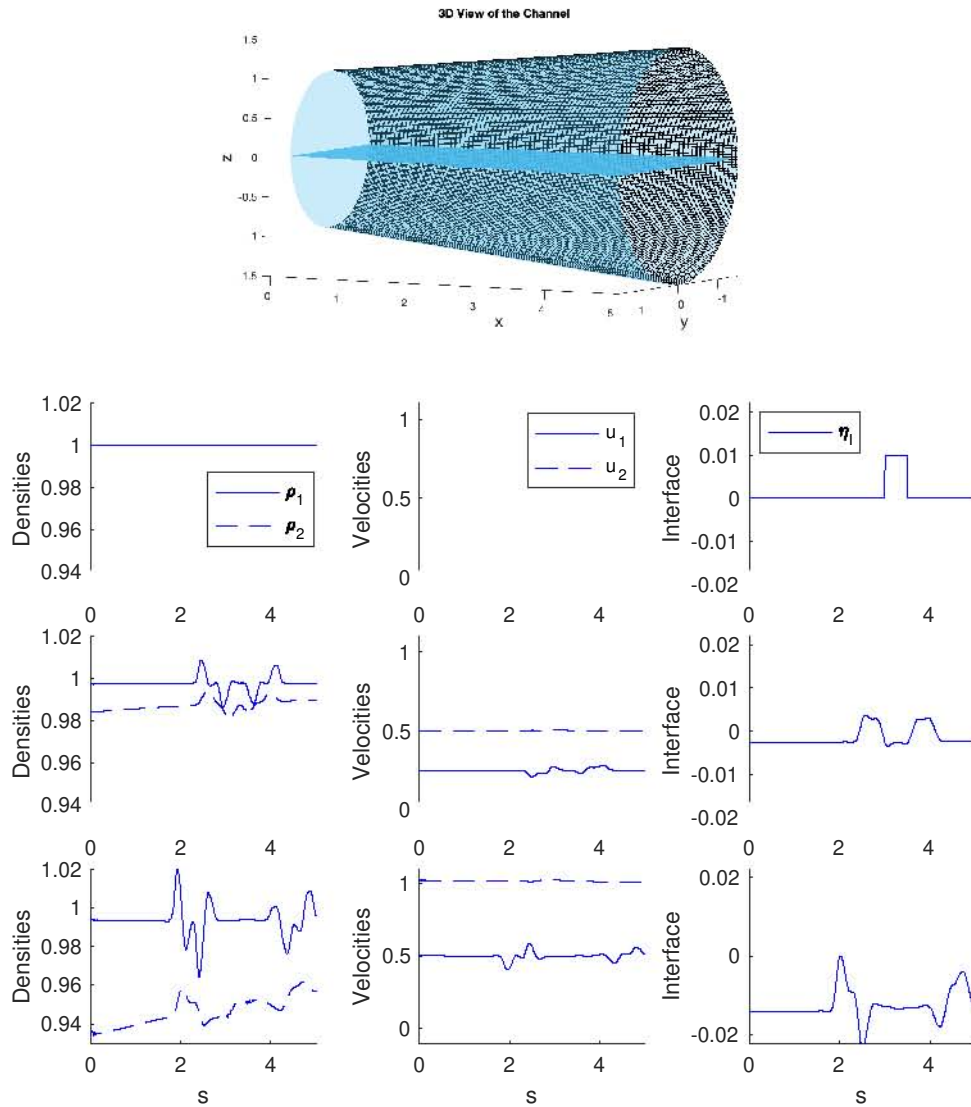


FIGURE 3.4: Top panel: 3D view of the pipe, showing the interface in blue at time $t = 0.5$ for the initial conditions (3.27). Left panels: densities of lower (solid line) and upper (dashed lines) layers. Middle panels: Corresponding velocities. Right panels: interface. The solutions are plotted at times $t = 0, 0.25, 0.5$ in descending order.

denoted with solid lines while the top one for gas is denoted with a dashed line. The changes in density are clearly identified. Due to the perturbation in the interface and the geometry of the pipe, a fluid displacement to the right is observed.

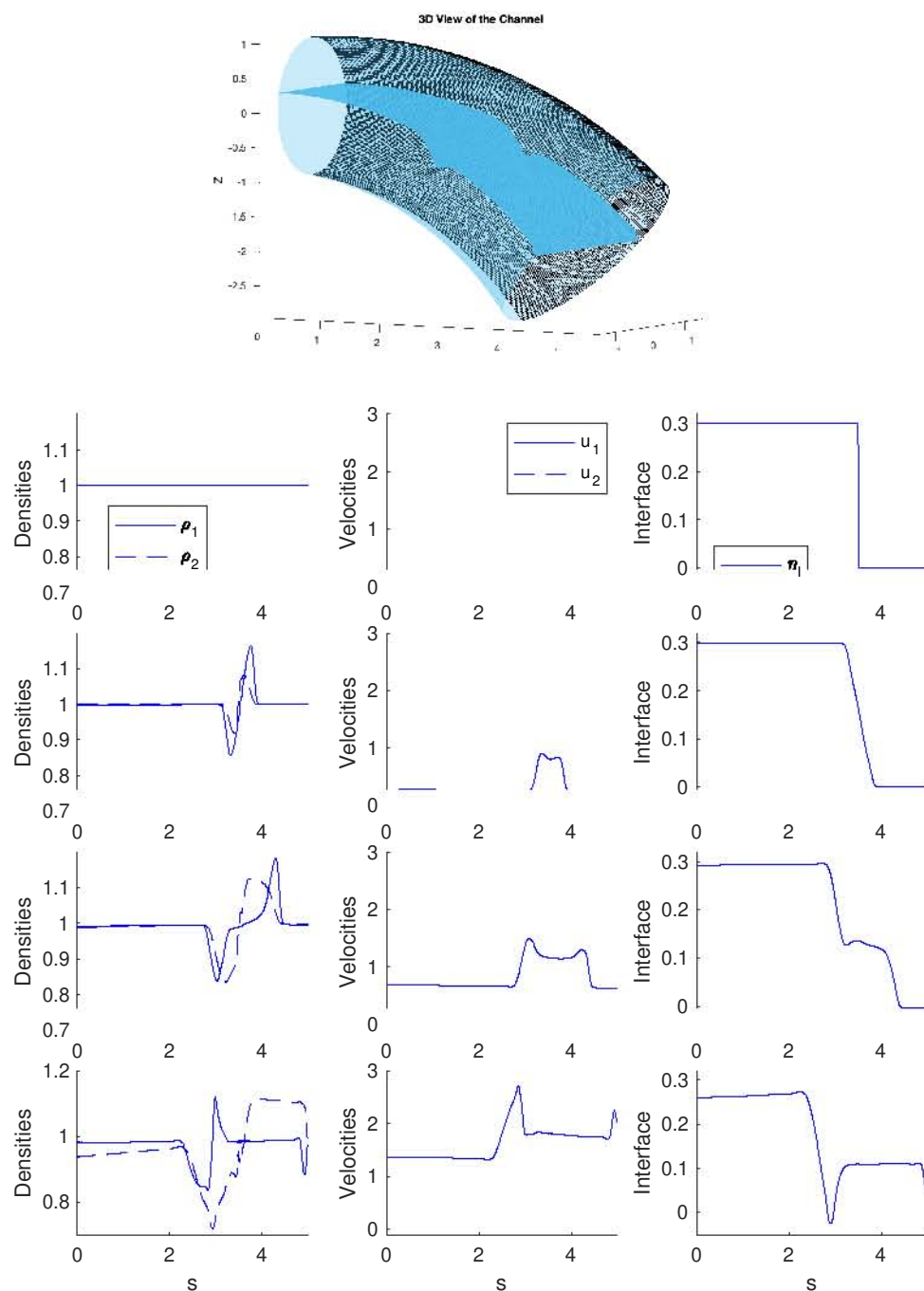


FIGURE 3.5: Top panel: 3D view of the pipe, showing the interface in blue at time $t = 0.5$ for the initial conditions (3.28). Left panels: densities of lower (solid line) and upper (dashed lines) layers. Middle panels: Corresponding velocities. Right panels: interface. The solutions are plotted at times $t = 0, 0.1, 0.25, 0.5$ in descending order.

3.5.3 Hydraulic jump 1

This numerical test considers a hydraulic jump. The pipe has radius

$$R(\theta, s) = 1 + 0.1 s,$$

so it opens up in the axial direction. Furthermore, it turns down with angle

$$\alpha(s) = -0.1 s \frac{\pi}{2}.$$

In this numerical test, the pressure of the upper layer associated with gas has a lower pressure reference $P_{2,\text{ref}} = 0.1$, with density reference values $\rho_{1,\text{ref}} = \rho_{2,\text{ref}} = 1$. A momentum exchange is given by $D_{s,1} = 1$, $D_{s,2} = -1$, and $\mu = 10$.

The initial conditions are given by

$$\rho_1 = \rho_2 = 1, V_{s,1} = V_{s,2} = 0, \eta_I = \begin{cases} 0.3 & \text{if } s \leq 3.5 \\ 0 & \text{otherwise.} \end{cases} \quad (3.28)$$

The time evolution is shown in Figure 3.5. As one can see, the interface has an initial jump, like in a Riemann problem. In its initial evolution, a rarefaction wave seems to show up. However, an intermediate state develops later on. Of course, here we have a varying geometry and other parameters involved, which makes this numerical test more complicated than a regular Riemann problem. The velocity of the liquid phase in the lower layer is greater than that of the top one. This indicates that the flow is dominated by the liquid layer.

3.5.4 Hydraulic jump 2

In this last numerical test, we have now increased the complexity of the flow. Initially, the left side of the pipe is filled mostly with liquid, while the opposite occurs on the right side. We use the same parameters as in the previous test. The initial conditions are given

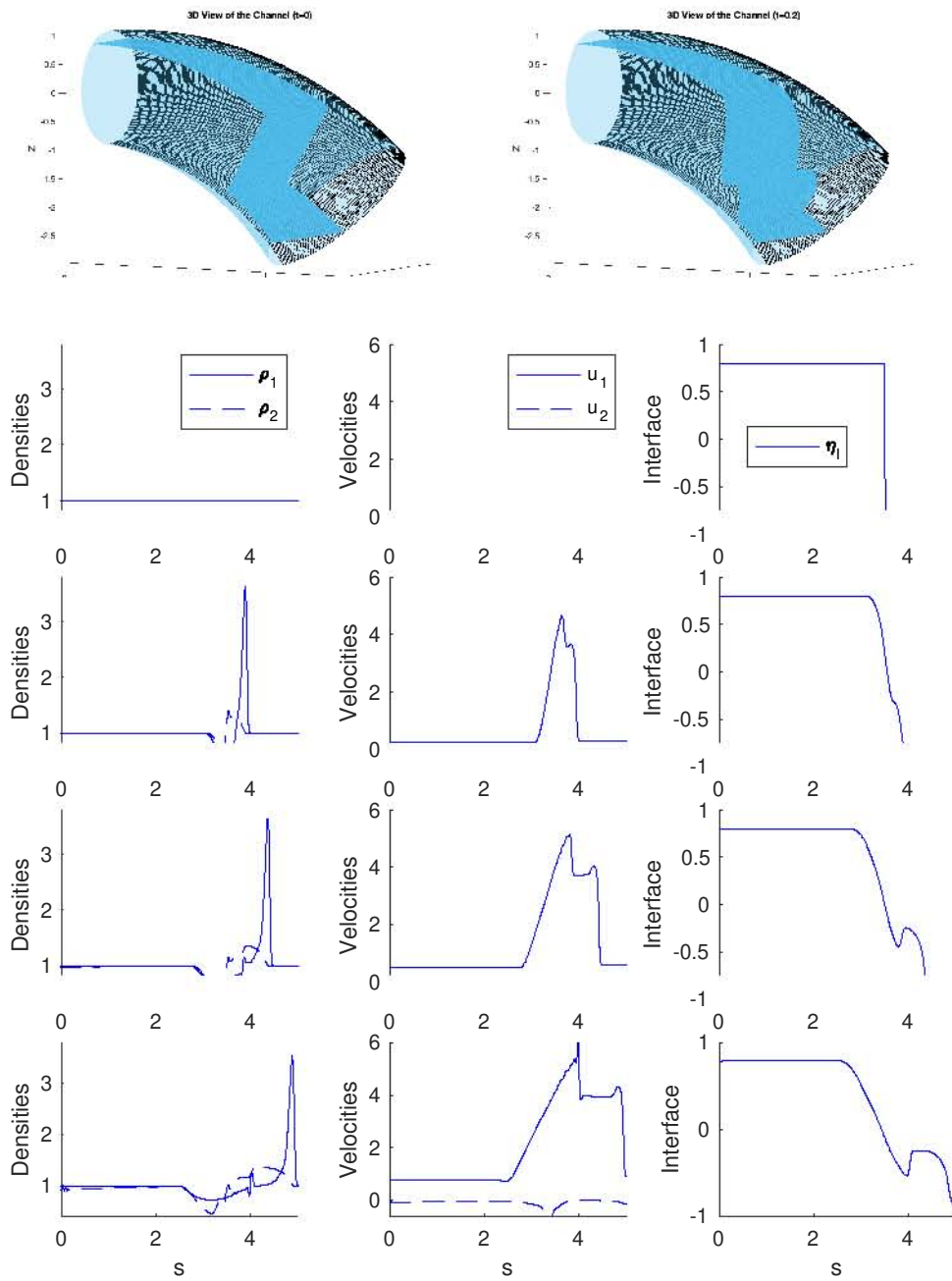


FIGURE 3.6: Top panel: 3D view of the pipe, showing the interface in blue at time $t = 0.5$ for the initial conditions (3.29). Left panels: densities of lower (solid line) and upper (dashed lines) layers. Middle panels: Corresponding velocities. Right panels: interface. The solutions are plotted at times $t = 0, 0.25, 0.5$ in descending order.

by

$$\rho_1 = \rho_2 = 1, V_{s,1} = V_{s,2} = 0, \eta_I = \begin{cases} -0.9 & \text{if } s \leq 3.5 \\ 0.9 & \text{otherwise.} \end{cases} \quad (3.29)$$

The time evolution is shown in Figure 3.6. Due to gravity, the flow starts moving to the right. A shockwave forms and starts propagating towards the right boundary. In this case, the velocity of the liquid phase is much stronger than that of the previous test, which could be caused by the higher jump and the higher pressure inside the pipe.

Chapter 4

Conclusions

4.1 Conclusions

As we mentioned at the beginning of this thesis, the Euler Equations are a valuable tool that can be adapted for understanding and modeling gas and air flow through ducts. The cylindrical coordinates played an important role for the description of the geometry of the pipe and the variables involved. Thanks to this, we were able to transform the Cartesian system of equations into a cylindrical-type system. In the new coordinates, the variables are described by the pipe's axial position, the distance from the wall to the cylindrical center in the corresponding cross section, and the angle of a point at the wall with a reference vector. The resulting equations may seem complicated, but can be greatly simplified by making the assumption that $V_r, V_\theta \ll V_s$, obtaining a reduced model.

Reynold's Theorem [1.4](#) had an important role in this work. Thanks to this theorem, the integration of the model was able to be developed and lead to the final expressions. Here, the cross sectional averaging process was crucial. The resulting integrals were not trivial or easily to solve analytically, so the analysis of the numerical approach to them is an important result of this work as well as the numerical method that we implemented.

Despite the complexity of the final model, the numerical approach had some interesting results. The central-upwind numerical scheme implemented for solving the final model allowed us to apply the model to different scenarios. For instance, we studied perturbations to steady state at rest. We observed the variations on the densities ρ_1, ρ_2 , the pressures $P_1(\rho_1), P(\rho_2)$ and how the velocities and interface evolve in time. It is important to recall that we studied water and gas flow interactions through pipes, like it occurs in home and city pipes that are used to supply water to citizens. However, the applications of this model are not just limited to that. The model was described for general cross sections, which can be applied to many realistic problems.

Bibliography

- [1] Elena Vázquez-Cendón, Arturo Hidalgo, Pilar Garcia Navarro, and Luis Cea. *Numerical methods for hyperbolic equations*. CRC Press, 2012.
- [2] Elewterio F Toro. *Godunov methods: Theory and applications*. Springer Science & Business Media, 2012.
- [3] Randall J LeVeque and Randall J Leveque. *Numerical methods for conservation laws*, volume 214. Springer, 1992.
- [4] Randall J. LeVeque. *Finite volume methods for hyperbolic problems*. Cambridge Texts in Applied Mathematics. Cambridge University Press, Cambridge, 2002. ISBN 0-521-81087-6; 0-521-00924-3. doi: 10.1017/CBO9780511791253. URL <https://doi.org/10.1017/CBO9780511791253>.
- [5] Alexander Kurganov, Sebastian Noelle, and Guergana Petrova. Semidiscrete central-upwind schemes for hyperbolic conservation laws and Hamilton-Jacobi equations. *SIAM J. Sci. Comput.*, 23(3):707–740 (electronic), 2001. ISSN 1064-8275. doi: 10.1137/S1064827500373413. URL <http://dx.doi.org/10.1137/S1064827500373413>.
- [6] Charles Demay and Jean-Marc Hérard. A compressible two-layer model for transient gas–liquid flows in pipes. *Continuum Mechanics and Thermodynamics*, 29(2):385–410, 2017.
- [7] Jorge Macías, Carlos Pares, and Manuel J Castro. Improvement and generalization of a finite element shallow-water solver to multi-layer systems. *International journal for numerical methods in fluids*, 31(7):1037–1059, 1999.

-
- [8] François Bouchut and Tomás Morales de Luna. An entropy satisfying scheme for two-layer shallow water equations with uncoupled treatment. *ESAIM: Mathematical Modelling and Numerical Analysis*, 42(4):683 – 698, 2008. doi: 10.1051/m2an:2008019.
- [9] A. Kurganov and E. Tadmor. New high-resolution central schemes for nonlinear conservation laws and convection-diffusion equations. *Journal of Computational Physics*, 160(1):241–282, 2000. ISSN 0021-9991.
- [10] Amiram Harten, Peter D. Lax, and Bram van Leer. On upstream differencing and Godunov-type schemes for hyperbolic conservation laws. *SIAM Rev.*, 25(1):35–61, 1983. ISSN 0036-1445. doi: 10.1137/1025002. URL <https://doi.org/10.1137/1025002>.
- [11] A. Kurganov and D. Levy. Central-upwind schemes for the Saint-Venant system. *M2AN. Mathematical Modelling and Numerical Analysis*, 36(3):397–425, 2002. ISSN 0764-583X. doi: 10.1051/m2an:2002019. URL <http://dx.doi.org/10.1051/m2an:2002019>.
- [12] A. Kurganov and G. Petrova. A second-order well-balanced positivity preserving central-upwind scheme for the Saint-Venant system. *Commun. Math. Sci.*, 5(1):133–160, 2007. ISSN 1539-6746. URL <http://projecteuclid.org/getRecord?id=euclid.cms/1175797625>.
- [13] J. Balbás and S. Karni. A central scheme for shallow water flows along channels with irregular geometry. *M2AN. Mathematical Modelling and Numerical Analysis*, 43(2):333–351, 2009. ISSN 0764-583X. doi: 10.1051/m2an:2008050. URL <http://dx.doi.org/10.1051/m2an:2008050>.
- [14] Alina Chertock, Shumo Cui, Alexander Kurganov, and Tong Wu. Well-balanced positivity preserving central-upwind scheme for the shallow water system with friction terms. *International Journal for numerical methods in fluids*, 78(6):355–383, 2015.
- [15] B. van Leer. Towards the ultimate conservative difference scheme. V. A second-order sequel to Godunov’s method [J. Comput. Phys. **32** (1979), no. 1, 101–136]. *Journal of Computational Physics*, 135(2):227–248, 1997. ISSN 0021-9991.

-
- [16] S. Gottlieb, C.-W. Shu, and E. Tadmor. Strong stability-preserving high-order time discretization methods. *SIAM Rev.*, 43(1):89–112 (electronic), 2001. ISSN 0036-1445. doi: 10.1137/S003614450036757X. URL <http://dx.doi.org/10.1137/S003614450036757X>.